CHRONIC MORPHINE TREATMENT-MODULATED TRAFFICKING OF AMPA RECEPTORS: A POTENTIAL MECHANISM FOR DRUG ADDICTION

A DISSERTATION
SUBMITTED TO THE FACULTY OF THE GRADUATE SCHOOL
OF THE UNIVERSITY OF MINNESOTA
BY

Yuet Fong KAM

IN PARTIAL FULFILLMENT OF THE REQUIREMENTS
FOR THE DEGREE OF
DOCTOR OF PHILOSOPHY

Ping-Yee Law, Ph.D., Advisor

August, 2012

ACKNOWLEDGMENTS

I am very grateful to my advisor, Dr. Ping Yee Law, for providing me an opportunity to conduct my PhD work at the University of Minnesota. Dr. Law offered me a lot of resources and support to pursue and develop my thesis work. I would like to thank my committee members, Drs. Paulo Kofuji, Dezhi Liao, Jonathan Marchant and Stanley Thayer for their valuable comments and suggestions on my research work. Further, I am indebted to Dr. Horace H. Loh who always supports my research work.

My thesis research would not be possible without the help from Drs. Horace H. Loh and Dezhi Liao who provided me important tools and resources in their laboratories. Moreover, I thank many people who have given their kind help to my work, especially Cherky Kibaly, Lei Zhang, Jinghua Xi and Hui Zheng.

My PhD study was funded through several grants from the National Institutes of Health to D.L., H.H.L. and P.Y.L., the University of Minnesota Medical School and Minnesota Medical Foundation (Milne Brandenberg Award), and the University of Minnesota Graduate School (Doctoral Dissertation Fellowship). I acknowledged the Department of Pharmacology, University of Minnesota, for providing me financial support to attend Neuroscience Meeting 2010 in San Diego, California.

Finally, I would like to thank my family members, especially my parents and sister Ida Kam, who provided a lot of support to me while I was conducting my study overseas, which is always challenging and difficult. Lastly, I am glad to go through much hardship during my PhD study while being supported by my husband, Martin Tsui, in Minnesota!

ABSTRACT

Morphine is the benchmark analgesic for treating chronic pain. However, its clinical uses are hindered by its highly addictive nature, as chronic treatment with the drug will produce physical and psychological dependence upon the cessation of use. Drug craving is the main driving force for relapse after prolonged periods of abstinence, and represents an enormous challenge for the treatment of drug addiction. Since addiction is a long-term behavioral alteration, it is believed that addictive drugs produce reorganization of specific neural circuits and adjustment of synaptic strength. The underlying mechanisms of these neural adaptations may represent a promising target for prevention and/or treatment of addiction, but the detailed mechanisms of these processes remain unclear. Therefore, the main goals of this work are to delineate signaling pathways controlling morphine-induced neural adaptations and investigate their functional role in opiate addictive behaviors.

α-amino-3-hydroxy-5-methyl-4-isoxazolepropionic acid (AMPA) receptors are postsynaptic glutamate receptors, and are responsible for mediating most excitatory synaptic transmission under normal conditions. More importantly, the dynamic localization of AMPA receptors plays a critical role for modifying synaptic strength and synaptic morphology. Here, I hypothesized that regulation of AMPA receptor trafficking by morphine treatment underlies the drug-induced neural modulation implicated in the addiction process. Hence, the first part of this dissertation research examined whether and how chronic exposure to morphine

modulates trafficking of surface GluR1 (a subunit of AMPA receptors) in primary hippocampal neurons. Using live-cell imaging techniques together with biochemical studies, I demonstrated that chronic exposure to morphine induced a significant loss of synaptic and extrasynaptic GluR1 by internalization. In mechanistic studies, I found that the GluR1 internalization was attributed to dephosphorylation of the receptor subunit at Ser^{845} following morphine treatment, but it did not result from altered neural network or NMDA receptor activation. Moreover, dephosphorylation of GluR1 at Ser^{845} was found to require morphine-evoked calcineurin activation. Therefore, calcineurin-dependent dephosphorylation of AMPA receptor and subsequent AMPA receptor internalization provides a novel mechanism for opioid-induced neural adaptations.

The second part of this dissertation research attempted to link morphine's effects on GluR1 phosphorylation and endocytosis to addictive behavior, especially formation of memory for the environmental context of the drug experience, because recall of this memory by encountering the drug-paired cues triggers relapse to drug seeking. In this approach, a mutant mouse line was used, in which GluR1 at Ser^{845} was mutated to Ala (S845A) leading to an absence of morphine-induced GluR1 endocytosis. A behavioral test, conditioned place preference (CPP), was carried out to assess the ability of morphine to produce a positive association with environmental cues. I found that S845A mice were significantly slower to acquire morphine-induced CPP when compared to

wild types (WT). This decreased sensitivity to morphine CPP in mutants was neither related to contextual memory deficits or abnormal locomotor activity, as there was no difference between WT and S845A mice in the contextual memory acquisition in the Morris water maze test or locomotion with or without morphine injection. To examine the persistence of morphine-associated contextual memory in the mutant mice, I also performed extinction tests on mice conditioned with 10 mg/kg morphine for four sessions, by which both WT and S845A mice exhibited similar CPP responses. Interestingly, a prolonged extinction was observed in S845A mutant mice, suggesting the S845A mutation either impaired the learning of the new conditioning or prolonged the retention of the old conditioning. Nevertheless, these results suggest that an alteration in GluR1 phosphorylation at Ser^{845} and subsequent receptor endocytosis/insertion are involved in acquisition and extinction of morphine CPP.

Altogether, the present findings indicate that calcineurin-mediated GluR1-S845 dephosphorylation is required for morphine-induced internalization of GluR1-containing AMPA receptors, providing a molecular basis for the drug-induced neural modulation. This work also suggests that this regulation of GluR1 phosphorylation and trafficking by morphine is involved in the modulation of the drug-associated contextual memory, which reflects the involvement of AMPA receptor trafficking in the mechanisms underlying opiate-seeking behaviors.

TABLE OF CONTENTS

LIST OF FIGURES

LIST OF ABBREVIATIONS

4.1N: Actin binding protein 4.1

ABP: AMPA receptor binding protein

AC: Adenylyl cyclase

AMPA: α-amino-3-hydroxy-5 methy-4-isoxazolepropionic acid

CaMKII: Ca^{2+}/calmodulin-dependent protein kinase

cAMP: Cyclic adenosine monophosphate

CPP: Conditioned place preference

CREB: cAMP-response element binding protein

C-terminus: Carboxyl-terminus

CTOP: D-Phe-Cys-Tyr-D-Trp-Orn-Thr-Pen-ThrNH_2

dbcAMP: dibutyryl-cAMP

DL-APV: DL-2-amino-5-phosphonovaleate

DRG: Dorsal root ganglion

G protein: Guanine nucleotide-binding protein

GABA: γ-aminobutyric acid

GluRs: Glutamate receptors

GRIP: Glutamate receptor interacting protein

LTD: Long-term depression

LTP: Long-term potentiation

MAPK: Mitogen-activated protein kinase

mEPSCs: Miniature excitatory postsynaptic currents

NMDA: N-methyl-D-aspartate

N-terminus: Amino-terminus

ORL_1: Opioid receptor-like

PAG: Periaqueductal gray

PICK1: Protein interacting with C kinase 1

PKA: Protein kinase A

SAPs: Synapse-associated proteins

TARPs: Transmembrane AMPA receptor regulatory proteins

TTX: Tetrodotoxin

VTA: Ventral tegmental area

CHAPTER 1

INTRODUCTION

1.1 An opiate analgesic: morphine

Opium has been widely used for both relieving pain and producing sedation since ancient times, and hence it is recognized as narcotic analgesic. It indeed is extracted from the dried latex of the seed pods of the opium poppy (*Papaver Somniferum*) (Kirby, 1967). A significant contribution to the opium processing occurred in the nineteenth century. The main constituents found in opium are a group of nitrogenous basic substances that are poorly soluble in water but readily dissolve in alcohol, named alkaloids (Kirby, 1967). Raw opium contains more than 20 alkaloids and the most abundant one, morphine, was firstly isolated by a German pharmacist, Friedrich Sertürner, in 1804 (Kirby, 1967; Luch, 2009). Later, morphine was discovered to be the most active component responsible for the opium's analgesic property. Nowadays, morphine is widely regarded as a benchmark of analgesics to treat both acute and chronic severe pain, such as labor pain, cancer pain, severe ulcerative colitis and hepatic cirrhosis (Foye 1989; Carr et al., 1994). Other alkaloids such as codeine, papaverine and noscapine with weak or no painkilling activities are prescribed for relieving mild pain, spasms of smooth muscles and cough (Eddy et al., 1968). Although thebaine has no therapeutic value, it is a key synthetic intermediate for the production of various compounds, such as oxycodone, etorphine, naloxone and naltrexone (Novak et al., 2000). All natural alkaloids in opium and any semi-synthetic derivatives of opium are termed as opiates, while opioid describes any natural, semi-synthetic or synthetic compounds with opiate-like activities.

1.2 Morphine addiction and other adverse effects

In comparison with other alkaloids from opium, morphine is a potent opiate analgesic but is also a highly addictive substance. Drug addiction is generally considered as the compulsive use of a drug, despite of any adverse physical and psychosocial consequences (Everitt et al., 2001). The underlying mechanism for this "abnormal" behavior involves the development of tolerance, physical dependence and psychological dependence upon repetitive exposure to the drug (Haefely, 1986). With chronic administration of morphine, tolerance is commonly encountered when the initial dose of the drug loses its efficacy over time and increasing doses are required for achieving the equivalent effect (Koob et al., 1988; Bhargava, 1991; Bodnar, 2011). The escalation of drug intake not only causes severe complications, but also has a higher potential leading to addiction. Meanwhile, body compensations or physiological adaptations to the morphine's action occur. Such body compensation will develop physical dependence that displays through the withdrawal symptoms once discontinuation of morphine use or exposure to antagonists, like naloxone (Nestler et al., 1993). The withdrawal symptoms include a variety of extremely unpleasant body reactions, including watery eyes, runny nose, sweating, nausea and vomiting, diarrhea, tremors, restlessness, irritability, yawning, insomnia, dysphoria, increased heart rate and blood pressure, as well as intense drug craving (Koob et al., 1992). Nevertheless, tolerance and physical dependence/withdrawal symptoms no longer last in detoxified drug addicts. Instead, psychological dependence like drug craving is still present (O'Brien et al., 1998). The addicts often suffer numerous psychological disorders, such as depression, anxiety, low self-esteem, confusion and paranoia (de Jong et al., 2006). As drug craving is a main driving force for ongoing drug use or relapse even after years of drug abstinence, it makes the biggest problem for the treatment of drug addiction and limits morphine's medical use. Apart from addictive nature, overdose of morphine and

other opiate drugs results in other complications as well. For instance, as they have a major influence on the smooth muscle and glandular secretions of the respiratory and gastrointestinal tracts, they will elicit respiratory depression and constipation. In addition, pupils will constrict that is one of the most recognized signs of opiate use (Goldfrank, 2006). All of the above physiological effects of opiate drugs are primarily mediated by specific opioid receptors (Harrison et al., 1998).

1.3 Opioid receptors

1.3.1 Opioid receptor classification

Opioid receptors belong to the superfamily of G protein-coupled receptors (GPCR), characterized by seven transmembrane helices and coupled with heterotrimeric guanine nucleotide-binding proteins (G proteins). The seven transmembrane domains of receptors are linked by three extracellular loops and three intracellular loops with an extracellular amino-terminus (N-terminus) and intracellular carboxyl-terminus (C-terminus). Based on previous studies examining their first ligand bindings and anatomical locations, they were classified into three main subtypes: μ (*m*orphine), κ (*k*etocyclazocine) and δ (vas *d*eferens) (Dhawan et al., 1996). Later, a cDNA of an orphan receptor bearing substantial homology to the classical opioid receptors was cloned and known as opioid receptor-like (ORL_1) receptor (Wick et al., 1994). To compare amino acid sequences of proteins, the three subtypes of opioid receptors are about 60% identical to each other, with the greatest homology found in the transmembrane (73-76%) and intracellular loops (86-100%) regions. The N-terminus (9-

10%), extracellular loops (14-72%) and the C-terminus (14-20%) are not well conserved among them (Chen et al., 1993).

1.3.2 μ-opioid receptor and its distribution

The μ-opioid receptor is the most important for at least two reasons. First, morphine predominantly binds to the μ-receptor subtype with an affinity of nanomolar K_i values, but has a low preference for δ- and κ-receptors in a submicromolar range (Raynor et al., 1994). In addition, μ-opioid receptors are required for both the wanted and unwanted effects of morphine on the central nervous system and certain visceral organs. For examples, studies on μ-opioid receptor deficient mice revealed that no analgesic response was observed in mutant animals subcutaneously injected with morphine at doses that classically produce a strong analgesia in wild types (up to 50 mg/kg) (Matthes et al., 1996; Sora et al., 1997 and Schuller et al., 1999). Roy et al. (1998) indicated that morphine at a dose inducing constipation in wild type mice had no influence on the gastrointestinal motility in μ-opioid receptor knockout mice. In fact, the localization of μ-opioid receptors can be inferred by the pharmacological actions of morphine, and vice versa. μ-Opioid receptors are distributed in several regions involved in nociceptive transmission, such as periaqueductal grey of the midbrain, the dorsal horn of the spinal cord and dorsal root ganglion (DRG) (Delfs et al., 1994; Zastawny et al., 1994). They are also found to locate throughout different brain regions such as amygdala, neocortex, thalamus, hypothalamus, caudate putamen of basal ganglia, hippocampus, ventral tegmental area (VTA) and nucleus accumbens (Mansour et al., 1995). Among them, amygdala, neocortex, thalamus and caudate putamen of basal

ganglia are associated with sensory-motor function and their signaling integration (Mircea et al., 1988; Mansour et al., 1994), while VTA and nucleus accumbens are a well-known reward circuitry area for addiction (Di Chiara and Imperato, 1988). Hippocampus, a vital area for contextual learning and memory consolidation, recently has been suggested to regulate the rewarding effects of abused drugs (Fan et al., 1999; Vorel et al., 2001). The distribution of the μ-opioid receptors in these brain regions hence confirms their importance for morphine-induced emotional tone, locomotion and addiction. Similarly, other undesirable effects of morphine such as nausea, respiratory depression, heart rate change and constipation arise from both central and peripheral sites of action, as the autonomic nervous system (e.g. area postrema, nucleus ambiguus, dorsal motor nucleus of vagus and nucleus of the solitary tract) and the gastrointestinal tract can express the μ-opioid receptors (Mansour et al., 1995, Holzer, 2009, Hassen et al., 1984).

1.3.3 μ-opioid receptor signaling

As mentioned above, opioid receptors are a member of GPCR superfamily and transduce cellular signals via coupling to inhibitory G_i/G_o proteins. Indeed, all G protein including $G_{i/o}$ will separate from the receptors upon stimulation and in turn dissociate into two functional units, Gα-GTP and Gβγ dimer. Both of these functional molecules are responsible for mediating activities of downstream effectors (Hepler and Gilman, 1992). Stimulation of μ-opioid receptors by morphine typically requires $G\alpha_{i/o}$ proteins to induce: (i) decrease in the activity of adenylyl cyclase (AC) and the level of cyclic adenosine monophosphate (cAMP); (ii) inhibition of voltage-gated Ca^{2+} channels, and (iii)

stimulation of K^+ channel (Sharma et al., 1977; Hescheler et al., 1987; North et al., 1987) (**Fig. 1.1**). However, ample evidence later have demonstrated that the μ-opioid receptor-coupled inhibitory AC and cAMP signaling were reversed to basal level upon persistent treatment with morphine and even up-regulated after the removal of morphine or the addition of antagonist. This dual regulation of AC signaling was hypothesized to correlate with opioid tolerance and dependence (Sharma et al., 1975, Collier and Francis, 1975; Ueda and Ueda, 2009). There are reports about mechanisms of the counterbalancing increase in cAMP level. For instance, chronic exposure to morphine led to phosphorylation of AC and Gβγ as well as membrane translocation of PKCγ (protein kinase C) (Chakrabarti and Gintzler, 2003; Mao et al., 1995). Moreover, the free Gβγ dimer from G_i proteins was found to induce not only stimulation of AC2 isoform (Shy et al., 2007), but also activation of cAMP-response element binding protein (CREB) via mitogen-activated protein kinase (MAPK) pathway (Shy et al., 2007; Xing et al., 1996; Tu et al., 2007). It should be noted that CREB is a transcription factor and can promote the gene expression of AC (Lane-Ladd et al., 1997). Apart from the typical signaling from $G_{i/o}$ protein, stimulation of the μ-opioid receptor is capable of regulating other multiplicity of transduction pathways such as activities of phospholipase C (Xie et al., 1999), PKC (Sanchez-Blazquez et al., 2010), Src kinase (Zhang et al., 2009), MAPK family and protein phosphatase (Gabra et al., 2007) in a variety of cells (Ortiz et al., 1995; Kam et al., 2004). Each of these is suggested to participate in mediating multiple physiological actions of opioid drugs including nociception, reward, tolerance and dependence (Pellegrini-Giampietro et al., 1988; Xie et al., 1999; Moncada et al., 2003; Gabra et al., 2007; Komatsu et al., 2009; Zhang et al., 2010; Sanchez-Blazquez et al., 2010; Rehni and Singh, 2011; Liu et al., 2011), implicating that there may be potential

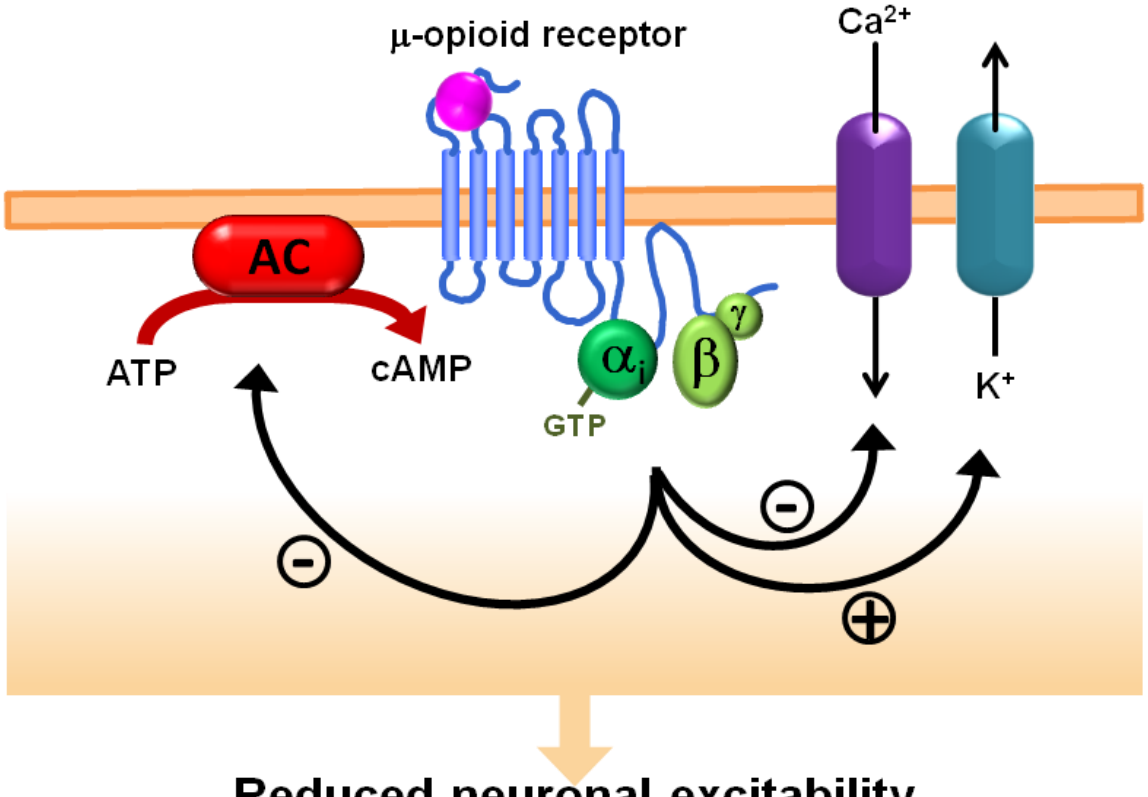

Figure 1.1. Typical signaling pathways regulated by μ-opioid receptors.

interactions between these intracellular effectors. However, it is still unclear which of these play a dominant role and how they coordinate to form distinct mechanism(s) for specific opioid actions.

1.4 Morphine-induced neuronal modulations: synaptic strength and organization

Classically, stimulation of μ-receptors with opioids can directly reduce the excitability of neurons by inhibiting AC activity; suppressing voltage-gated Ca^{2+} channels to prevent Ca^{2+} influx and activating K^+ channel to cause hyperpolarization as mentioned earlier (section 1.3.). The decreased neuronal excitability inhibits nerve impulse transmission and neurotransmitter release, thereby affecting the signal propagation in the entire neural circuit (**Fig.1.1**). Depending on the site, opioids regulate the release of excitatory or inhibitory neurotransmitters. Glutamate and substance P are examples of excitatory neurotransmitters. Primary afferent neurons of the DRG which express high density of the μ-opioid receptors (Delfs et al., 1994; Zastawny et al., 1994) are responsible for receiving and relaying pain signal. Pain generation is normally associated with excitation of primary afferent neurons, which in turn release glutamate and substance P in the dorsal horn of the spinal cord for forwarding the nociceptive information to the brain (**Fig. 1.2**). On the other hand, morphine acts on the μ-opioid receptors to deactivate the primary afferent neurons and inhibit the release of these two excitatory neurotransmitters at presynaptic terminals, so that it can produce analgesia (**Fig. 1.2**) (Piercey et al., 1979; Kondo et al., 2005). Another classical neural circuit mediated by morphine has been described in periaqueductal gray (PAG), VTA and

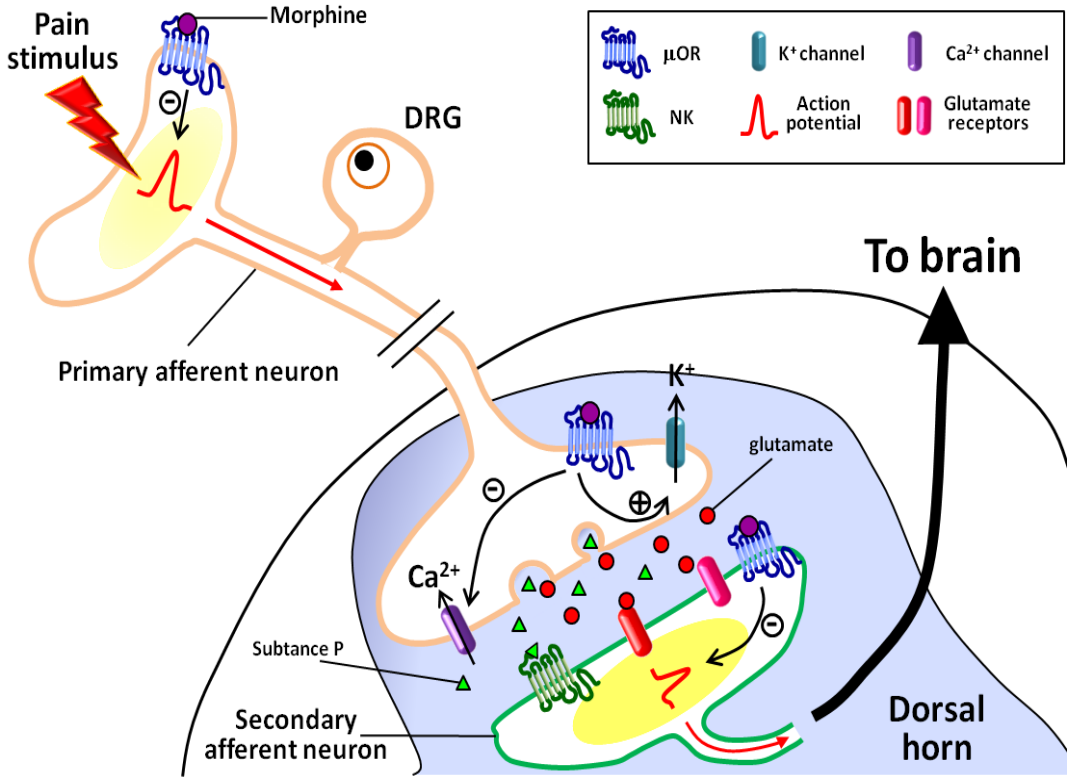

Figure 1.2. A schematic diagram illustrates the role of μ-opioid receptors for inducing analgesia in primary afferent neurons of the dorsal root ganglia.

The perception of pain is initiated by the activation of peripheral nociceptors to generate action potentials in primary afferent neurons of the dorsal root ganglia. The excited primary afferent neurons then release glutamate and substance P that in turn stimulate glutamate receptors and neurokinin (NK) receptors of secondary afferent neurons, respectively, for conveying pain signals to brain. Opiate agonists for example morphine primarily act on μ-opioid receptors (μOR) to inhibit the primary and secondary afferent neurons through suppression of Ca^{2+} channels and stimulation of K^+ channels. As a result, the release of glutamate and substance P decrease, nerve impulse generation in the secondary afferent neurons is blocked and so analgesia is caused.

hippocampus where morphine reduces the presynaptic release of γ-aminobutyric acid (GABA, an inhibitory neurotransmitter). As a result, the activities of adjacent PAG neurons, dopaminergic and pyramidal neurons are enhanced through a disinhibitory mechanism (Johnson and North, 1992; Zieglgansberger et al., 1979; Vaughan and Christie, 1997) (**Fig. 1.3**). Aside from the presynaptic action, recent studies on primary hippocampal neurons have suggested that morphine likely has a direct postsynaptic effect in mediating activity of excitatory synapses. Chronic treatment of hippocampal cultures with morphine led to a reduction of the amplitude, frequency, rise time and decay time of miniature excitatory postsynaptic currents (mEPSCs) only in dendritic spines that contained postsynaptic μ-opioid receptors (Liao et al., 2005; Liao et al., 2007). Collectively, these presynaptic and postsynaptic actions of morphine together with myriads of signaling transductions (described in section 1.3.3) cause alterations in synaptic strength (i.e. synaptic plasticity).

Changes in synaptic strength are often associated with changes in synaptic structure, such as size, density and shape of synapses, and they reciprocally affect each other for configuring a new synaptic connectivity. Therefore, it is not surprising that morphine and other opioid drugs have impact on synaptic organization. Mei et al (2009) demonstrated that the total length and branch number of dendrites as well as the density of spines were significantly reduced in pyramidal neurons of lateral secondary visual cortex of juvenile rats after prenatal morphine exposure, providing a potential mechanism by which infants of addicted mothers have deficits in brain development and psychological behaviors. Consistent observations occur in adult animals as well. Regardless of whether it is experimenter- or self-administration, chronic treatment of adult rats with morphine decreased density of spines in many brain areas, including

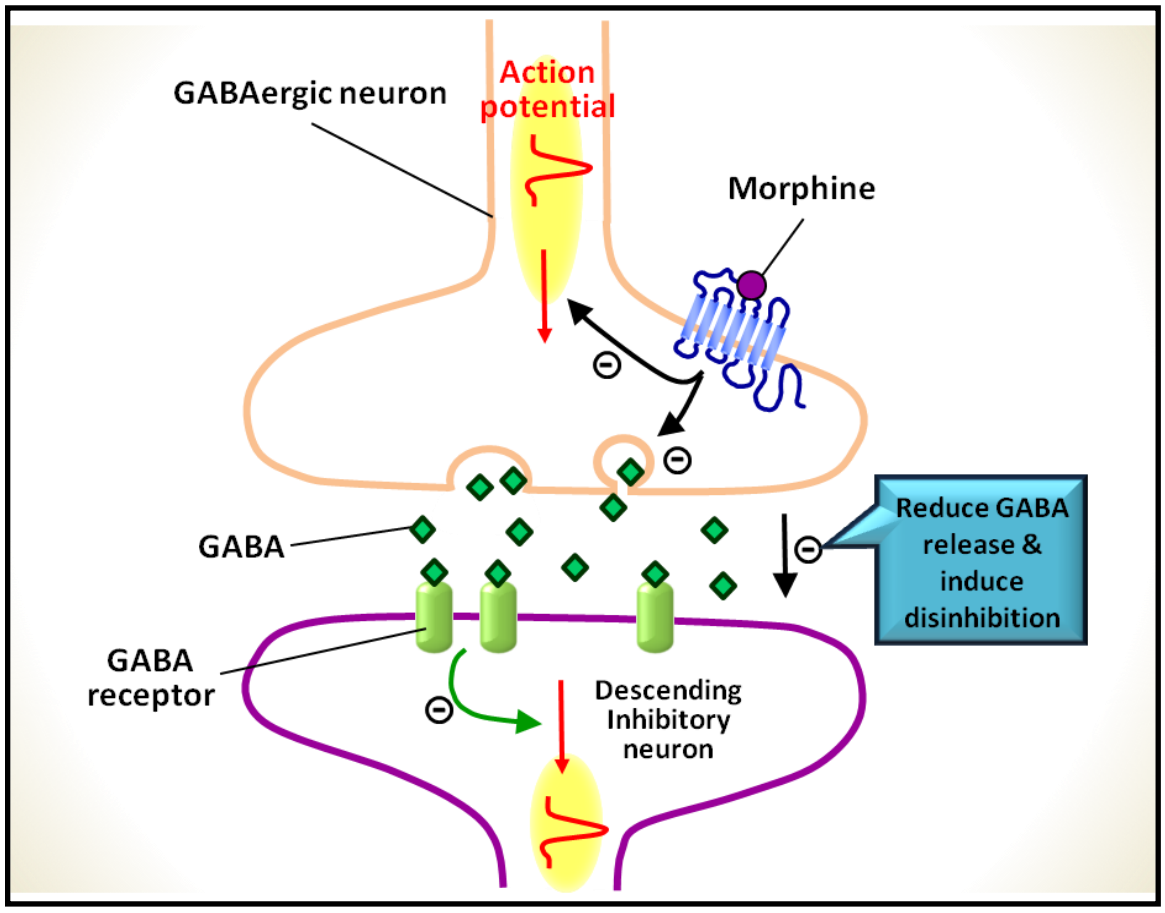

Figure 1.3. Morphine inhibition of GABA release from presynaptic terminals.

Morphine and other opioids induce hyperpolarization of various neurons such as GABAergic neurons and hippocampal interneurons, followed by inhibition of action potential-independent release of GABA. Therefore, postsynaptic inhibition is decreased (i.e. disinhibition).

frontal cortex, sensory cortex and nucleus accumbens. Interestingly, the decreased spine density in hippocampus only occurred in rats self-administrated morphine (Robinson and Kolb, 1999; Robinson et al., 2002). Altogether, the ability of morphine to remodel synaptic strength and morphology contributes to neural modulations in specific neural circuits that may account for opioids' physiological actions, especially addiction.

1.5 AMPA receptors are involved in synaptic plasticity

Synaptic plasticity results from not only changes in the amount of neurotransmitters released into a synapse, but also changes in the level of corresponding receptors on the synapse. It is well-known that this synaptic modification often involves two excitatory postsynaptic receptors, N-methyl-D-aspartate (NMDA) receptors and α-amino-3-hydroxy-5-methyl-4-isoxazole propionic acid (AMPA) receptors (Kandel and O'Dell, 1992). NMDA receptors and AMPA receptors are two principle ionotropic glutamate receptors (GluRs) to mediate the excitatory transmission in the mammalian CNS. Accumulating evidence indicates a remarkable difference in synaptic expression on both receptors. NMDA receptors are statically localized at postsynaptic membranes, whereas AMPA receptors undergo a dynamic exchange among intracellular pools, synaptic membrane and extrasynaptic membranes in response to actual neuronal activities (Liao et al., 1995; Lissin et al., 1999; Borgdorff and Choquet, 2002). Therefore, the number of surface-expressed AMPAR receptors at synapses in particular determines the strength of glutamatergic excitatory synapses (Liao et al., 1995; Luscher et al., 1999). At resting membrane potential, AMPA receptors but not NMDA receptors can open upon glutamate binding due to a voltage-dependent Mg^{2+}

blockage in the pores of NMDA receptors. Hence, AMPA receptors primarily control the strength of excitatory synapses under normal conditions (Mayer et al., 1984; Isaac et al., 1995) (**Fig. 1.4A**). Once depolarization is generated by sodium influx through AMPA receptors into postsynaptic cells, Mg^{2+} cations are expelled out into the extracellular space, and Na^{+} and Ca^{2+} cross NMDA receptors to the postsynaptic terminal (**Fig. 1.4B**). The entry of Ca^{2+} stimulates various protein kinases such as calcium/calmodulin-dependent protein kinase (CaMKII) and PKC and finally evokes synaptic insertion of AMPA receptors, which results in a long-lasting strengthening of synapses, called long-term potentiation (LTP) (Mayer et al., 1984; Pickard et al., 2001) (**Fig. 1.4C**). LTP, together with long-term depression (LTD, weakening of synapses), are well studied forms of synaptic plasticity (Bliss and Collingridge, 1993). Of note, LTD involves the removal of AMPA receptors from the postsynaptic sites (Shepherd and Huganir, 2007).

AMPA receptors are tetramers made up of different combinations of four subunits: GluR1, GluR2, GluR3 and GluR4. Each subunit comprises ~ 900 amino acids with a molecular weight of about 105 kDa. Subunit composition varies depending on the brain region and developmental stage, but at adult hippocampus two major populations of receptors are heterotetrameric GluR1/GluR2 and GluR2/GluR3 (Craig et al., 1993; Wenthold et al., 1996; Shi et al., 2001). GluR4 expression is mainly restricted to the early development (Zhu et al., 2000). Each subunit has a large extracellular N-terminus and four transmembrane domains displaying substantial homology among different subunits. Conversely, their cytoplasmic C-termini diversify to be either long (e.g. GluR1 and GluR4) or short (e.g. GluR2 and GluR3) (Kohler et al., 1994) that can determine their interactions with scaffolding proteins to regulate trafficking and stabilizing synaptic

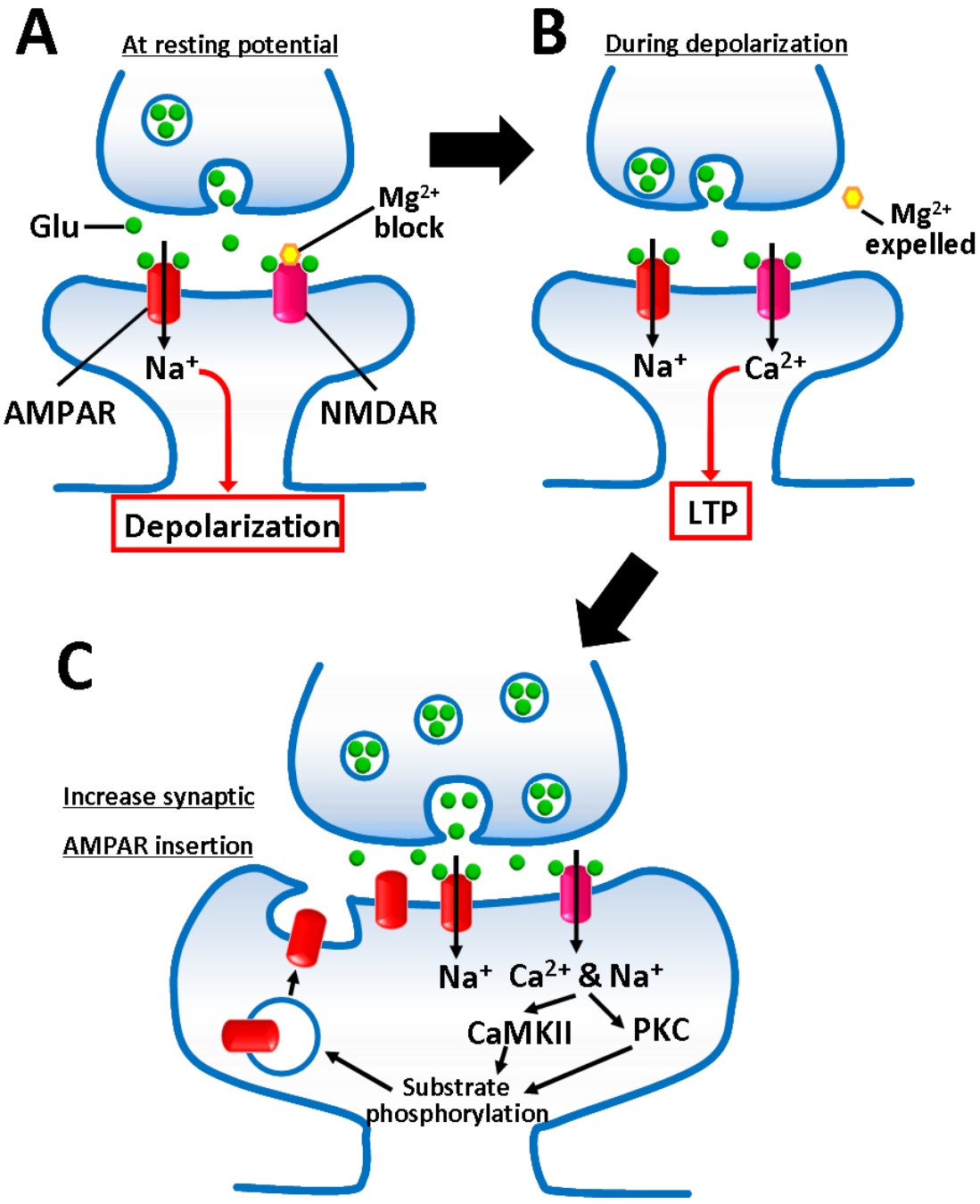

Figure 1.4. A putative mechanism underlies long-term potentiation.

AMPA receptors (Shi et al., 2001) (**Fig. 1.5**). Unlike NMDA receptors, the principal ions gated by AMPA receptors are Na^+ and K^+. The permeability of AMPA receptors to Ca^{2+} depends on the presence or absence of GluR2 subunits. The mRNA encoding for GluR2 undergoes a post-transcriptional editing by which an uncharged glutamate (Q) (within the second transmembrane) in the pore region is altered to positively charged arginine (R), thereby causing energetically unfavorable condition for Ca^{2+} to pass through (Sommer et al., 1991). In adult mammalian brains, the vast majority of GluR2 subunits are Q/R edited, and thus the presence of GluR2 in AMPA receptors makes the channel impermeable to Ca^{2+}. The prevention of Ca^{2+} entry into neurons is proposed as a mechanism against excitotoxicity (Kim et al., 2001). In contrast, if AMPA receptors lack GluR2 subunits, they become permeable to Ca^{2+}. The Ca^{2+} influx is associated with high channel conductance, accelerated kinetics and inward rectification (Swanson et al., 1997; Oh and Derkach, 2005). Therefore, the existence of GluR2 in AMPA receptors can control the receptor properties and so subsequent synaptic transmission (Derkach et al., 2007).

1.6 Molecular mechanisms for regulation of AMPA receptor trafficking and cellular distribution

1.6.1 Interactions between intracellular C-termini of AMPA receptors and scaffolding proteins

The C-terminal cytoplasmic tails of AMPA receptor subunits are diversified and can bind to a variety of regulatory proteins for mediating receptor assembly and

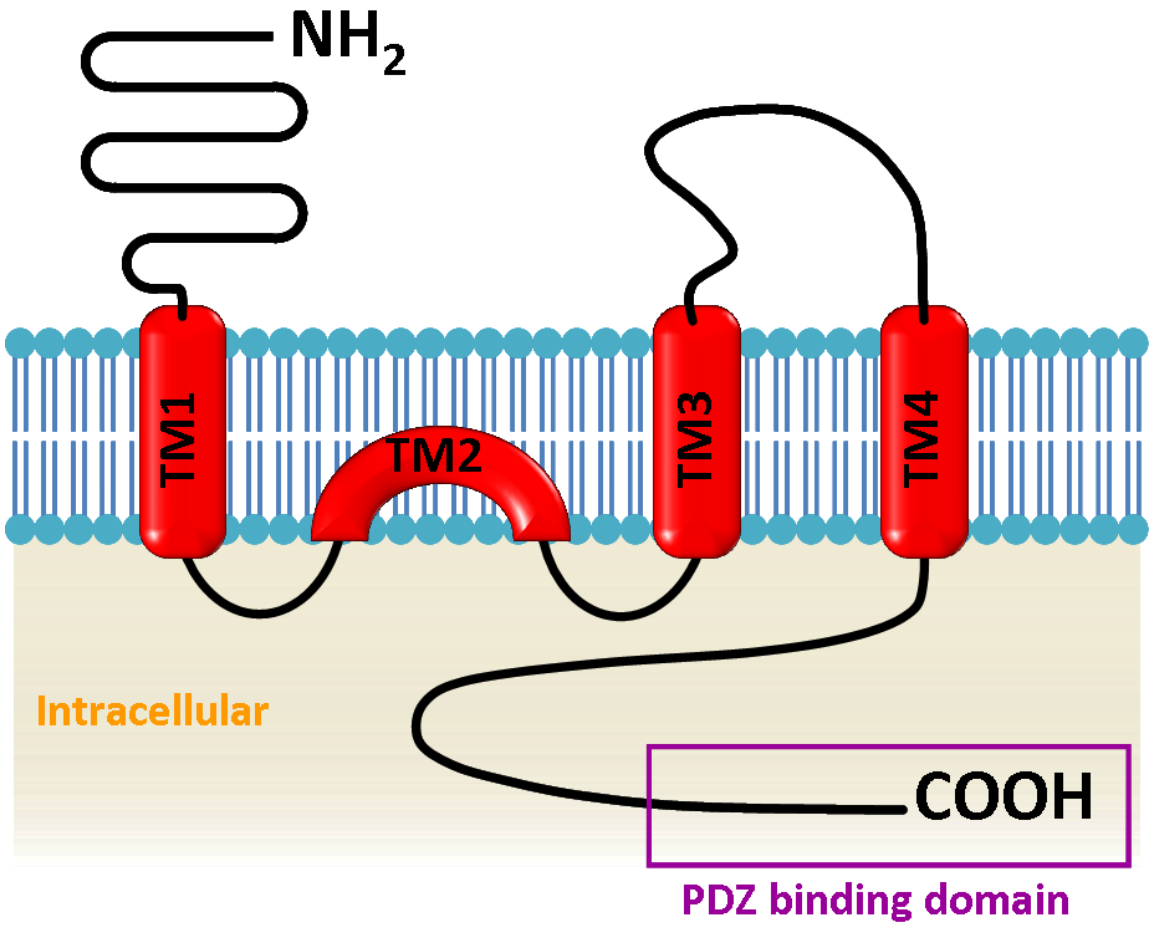

Figure 1.5. A diagram shows the structure of AMPA receptor subunits.

AMPA receptors are composed of different combinations of four subunits: GluR1-GluR4. Each subunit has an extracellular N-terminus, four transmembrane domains (TM1-4) and an intracellular C-terminus. They differ most in their C-termini, which determines their binding to various scaffolding proteins with or without PDZ domains.

trafficking (Borgdorff and Choquet, 2002). Numerous studies hence identify what proteins can bind to the regions and determine what specific roles the proteins play in the process. These interacting proteins basically can be divided into two categories: proteins that have PDZ domains and those that do not have.

The PDZ domain is an about 90 amino acid motif and is also known as the GLGF repeat, based on the presence of a Gly-Leu-Gly-Phe sequence. Most PDZ-mediated interactions occur via the recognition of short peptide sequences, which are located on the C-terminal tails of the binding proteins (Songyang et al., 1997). SAP90/PSD95 is the first identified PDZ-domain containing protein at vertebrate CNS synapses (Cho et al., 1992). Three additional isoforms, SAP97/hDlg, SAP102 and Chapsyn110/PSD93 were subsequently found (Garner and Kindler, 1996). This family of synapse-associated proteins (SAPs) is shown to preferentially express at the postsynaptic density of the glutamatergic synapses (Garner and Kindler, 1996). Currently, SAP97 is the exclusive PDZ protein known to interact directly with GluR1 and concentrates at synapses containing GluR1, but not necessarily GluR2 and GluR3 (Leonard et al., 1998; Valtschanoff et al., 2000), demonstrating a potential role for SAP97 in synaptic assembly of GluR1. Furthermore, a non-PDZ protein, actin binding protein 4.1 (4.1N), which is also enriched at synapses can form complexes with SAP97 and the homolog hDlg (Lin et al., 1997; Walensky et al., 1999). Hence, a putative mechanism for synaptic insertion of AMPA receptors indicates that the formation of SAP97 and 4.1N complex at synapses may serve as a platform for anchoring AMPA receptors via a mechanism involving autophosphorylated CaMKII by NMDA receptors (Leonard et al., 1998; Shen et al., 2000; Lisman and Zhabotinsky, 2001). During LTP induction, the transient Ca^{2+} entry through NMDA receptors leads to activation and persistent autophosphorylation of

CaMKII. The phosphorylated CaMKII then tightly bind to the NMDA receptors, where it may initiate a chain of protein-protein interactions including association with α-actinin and actin filaments. These actin filaments may provide a binding site for 4.1N that in turn forms a complex with SAP97. As 4.1N and SAP97 can interact with GluR1 subunits of AMPA receptors (Leonard et al., 1998; Walensky et al., 1999; Shen et al., 2000), the receptors anchor on this protein-complex platform at the synapses (Lisman and Zhabotinsky, 2001) (**Fig. 1.6**).

Despite of no direct interaction with AMPA receptors, PSD95 also affects their synaptic incorporation indirectly through a family of proteins called stargazin or transmembrane AMPA receptor regulatory proteins (TARPs). TARPs are recognized as key auxiliary subunits for AMPA receptors expressing on cell surface membrane, because several genetic studies have found that hippocampi of mice deficient in TARPs, especially TARPγ-8 isoform, had impairment in surface expression of AMPA receptors (Rouach et al., 2005). Importantly, another study demonstrated that TARPs could couple to AMPA receptors and PSD-95 at independent sites (Chen et al., 2000). This study also revealed that TARPs did not require PSD95 coupling to promote surface expression of AMPA receptors but relied on this interaction to cause clustering and retention of AMPA receptors at postsynaptic sites (Chen et al., 2000). In other words, TARPs may provide a link through which PSD-95 facilitates synaptic recruitment of AMPA receptors (**Fig. 1.7**). For GluR2 subunits, at least three PDZ-domain containing proteins are well-known to interact with their C-termini, including glutamate receptor interacting protein (GRIP), AMPA receptor binding protein (ABP) and protein interacting with C kinase 1 (PICK1) (Dong et al., 1997; Srivastava et al., 1998; Xia et al., 1999) (**Fig. 1.7**). These proteins are widely thought to mediate distinct steps in GluR2 trafficking. For example, GRIP and

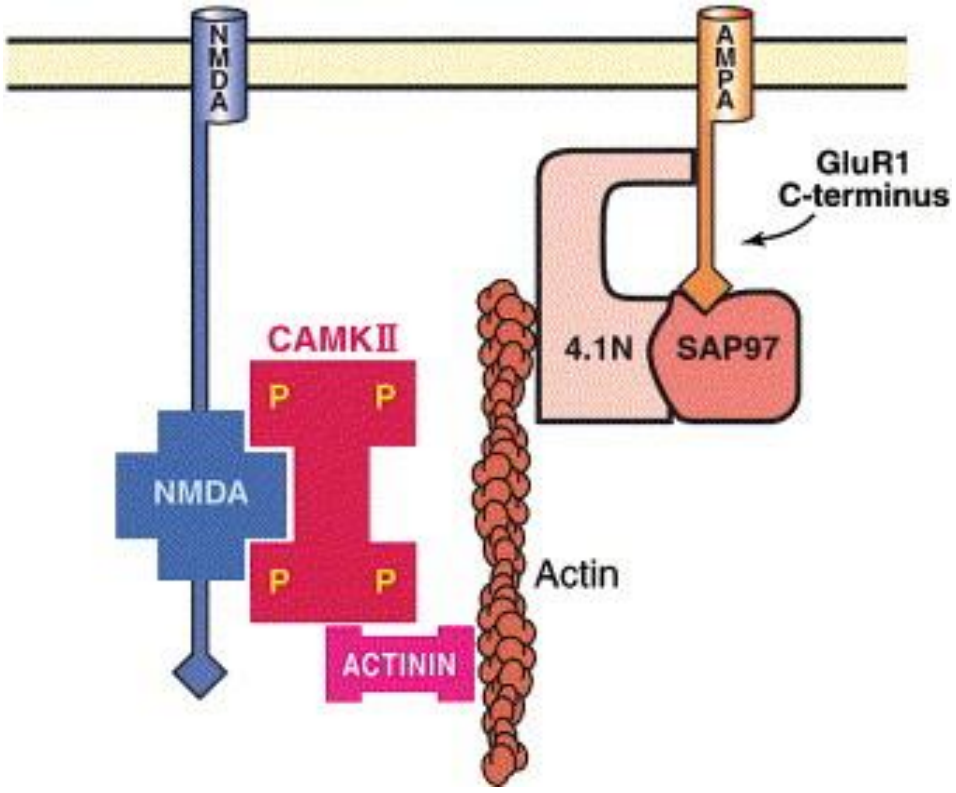

Figure 1.6. A cartoon revealing synaptic anchorage of AMPA receptors during NMDA receptor-dependent LTP.
(adapted from Lisman and Zhabotinsky, 2001)

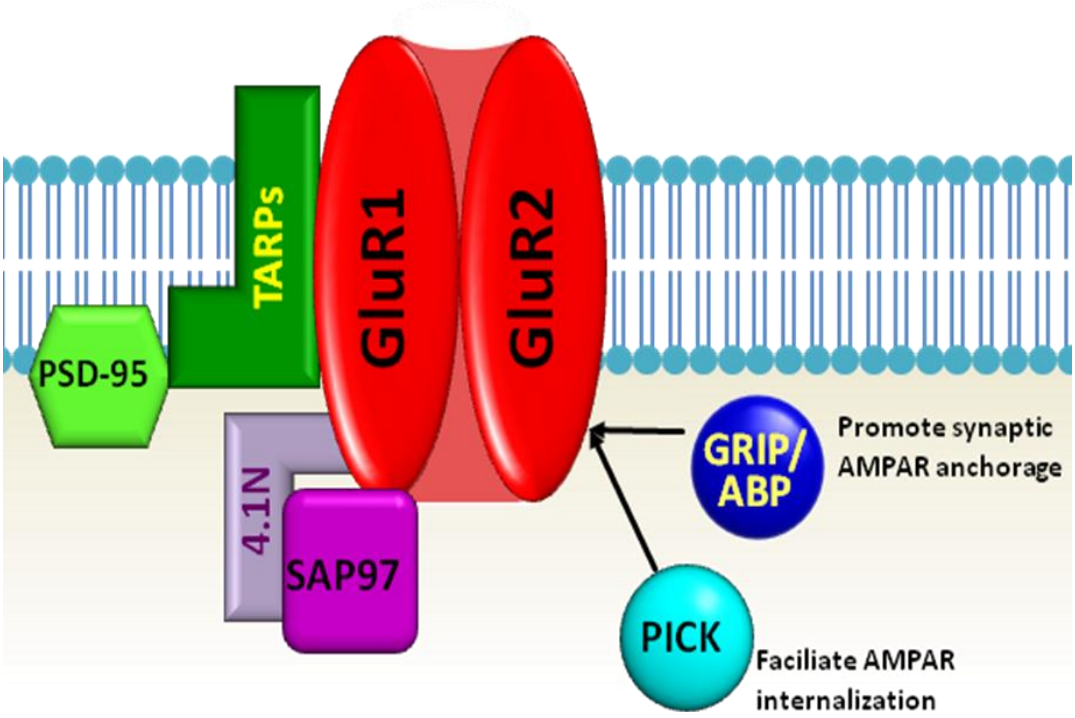

Figure 1.7. Interactions of AMPA receptors with various proteins for regulation of receptor trafficking and synaptic targeting.
GluR1 can interact with SAP97 and TARPs directly. TARPs binds to PSD-95, which is a core component of the postsynaptic density at the synapse where AMPA receptors can couple to other PDZ domain-containing proteins. For example, GRIP/ABP and PICK bind to GluR2. Also, cytoskeletal protein 4.1N can associate with C-terminus of GluR1 through non-PDZ domain interaction for anchoring AMPA receptors to the actin cytoskeleton and so stabilizing the receptors at cell surface. Notably, interactions of GluR2 with GRIP/ABP can promote synaptic insertion of AMPA receptors, whereas PICK binding to GluR2 facilitates endocytosis of AMPA receptors.

ABP serve as scaffolding proteins for anchoring GluR2 at postsynaptic sites (Dong et al., 1997). However, PKC or CaMKII-regulated interaction of PICK1 with GluR2 promotes internalization of the receptor subunit, followed by a decrease in surface GluR2 but not GluR1 at hippocampal CA1 synapses (**Fig. 1.7**). Therefore, these results suggest a specificity of internalization mechanism for different subunits of AMPA receptors (Terashima et al., 2004).

1.6.2 The role of AMPA receptor phosphorylation

All four subunits of AMPA receptors have several identified phosphorylation sites on their intracellular C-termini, and this receptor modification is another contributing factor for mediating receptor trafficking, localization and so synaptic plasticity (Song and Huganir, 2002). GluR1 subunits have at least two phosphorylation sites. Among them, serine 845 and serine 831 are the most extensively studied and are thought to participate in NMDA-dependent LTP and LTD (Song and Huganir, 2002). Serine 845 is a substrate for protein kinase A (PKA), while serine 831 can be phosphorylated by PKC and CaMKII during LTP (Roche et al., 1996; Mammen et al., 1997). It seems that phosphorylation of serine 845 by PKA facilitates GluR1 targeting at extrasynaptic sites only, but is insufficient to deliver AMPA receptors at synapses (Oh et al., 2006). Therefore, other signaling events such as phosphorylation of serine 831 and other residues on GluR1, as well as coupling to scaffolding proteins may be required (Hayashi et al., 2000; Esteban et al., 2003). On the other hand, induction of LTD involves protein phosphatase such as PP1/2A to dephosphorylate these two serine residues, which in

turn promotes internalization of cell surface GluR1 (Lee et al., 2003; Lee et al., 2004; Holman et al., 2007).

GluR2 have two common phosphorylation sites near its C-terminus, serine 880 and tyrosine 876 which are substrates for PKC and Src family tyrosine kinases, respectively (Seidenman et al., 2003; Hayashi and Huganir, 2004). Increased phosphorylation of both sites are found to be a critical step in the induction of cerebellar and hippocampal LTD (Seidenman et al., 2003; Chung et al., 2003; Hayashi and Huganir, 2004). In fact, phosphorylation of serine 880 and tyrosine 876 appears to destabilize the interaction of GluR2 with GRIP/ABP and allows recruitment of PICK1 to AMPARs, therefore facilitating the endocytosis of GluR2 (Seidenman et al., 2003; Hayashi and Huganir, 2004).

Taken together, there are at least two essential events for regulating AMPA receptor trafficking and localization, including interactions of receptors with synaptic scaffolding proteins and AMPA receptor phosphorylation. In fact, recent studies have proposed more complex scenario that involved some adhesion molecules and secreted factors binding to the extracellular domains of AMPA receptors (Passafaro et al., 2003; Saglietti et al., 2007).

1.7 Implications of AMPA receptor trafficking

A dynamic change in the level of synaptic AMPA receptors contributes to the generation of long-lasting synaptic plasticity – LTP and LTD, which may encode new information stored in the brain and thus modification of behaviors, especially learning

and memory. Therefore, regulation of AMPA receptor trafficking during synaptic plasticity is proposed to be one of the cellular mechanisms underlying the cognitive function. This notion is supported by findings of several elegant studies on mice with deficiency of GluR1 (and so GluR2/3 as predominant AMPA receptors) that was generated by Zamanillo and coworkers (Zamanillo et al., 1999). In comparison with wild type animals, the mutant mice had normal AMPA receptor- and NMDA receptor-mediated basal synaptic transmission, but exhibited impaired LTP (Andrasfalvy et al., 2003), revealing that synaptic delivery of GluR1-containing AMPA receptors is crucial for the induction of LTP. More importantly, the GluR1-lacking mice displayed deficit in hippocampus-dependent spatial working memory (Reisel et al., 2002; Schmitt et al., 2003) and one-trial spatial memory (Sanderson et al., 2007). Therefore, these results suggest that AMPA receptor trafficking was required for hippocampus-dependent learning and memory. As mentioned in section 1.6.2, trafficking of AMPA receptors depends on the receptors' phosphorylation status and hence mutation on these phosphorylation sites is also expected to affect synaptic plasticity and likely certain cognitive behaviors. For instance, NMDAR-dependent LTD was absent in transgenic mice lacking both PKA and CaMKII phosphorylation sites on GluR1 (S845A and S831A), which had normal Morris water maze learning but was impaired in rapid acquisition of new platform location (Lee et al., 2003) as well as incentive learning for food reinforcement (Crombag et al., 2008). These findings provide evidence that a particular form of LTD requiring GluR1 dephosphorylation underlies specific types of learning and memory.

1.8 Research goals

Opiate drugs including morphine are the most powerful analgesics known, but their clinical applications for the treatment of chronic pain are impeded by the development of drug addiction. Drug addiction indeed is related to experience-based behaviors such as the pursuit of rewards and cues linking drugs. Hence, it is considered a pathological form of learning and memory (Kelley, 2004; Hyman, 2005), which involves reorganization and/or strengthening of synaptic connections in specific neural circuits. Consistently, previous reports demonstrated that chronic morphine exposure not only reduces dendritic branching and spine density in different brain regions, but also alters both basic synaptic transmission and synaptic plasticity in hippocampus (Robinson and Kolb, 1999; Liao et al., 2005; Pu et al., 2002). Therefore, study on how chronic morphine treatment induces such long-lasting neural modulations is required to advance our understanding of addiction development, but the detailed molecular mechanism still remains unclear. As described earlier (section 1.5), dynamic trafficking of AMPA receptors plays a crucial role in the expression of synaptic plasticity (Malinow and Malenka, 2002) and also contributes to mediating spine growth and stability (Kopec et al., 2007). Importantly, immunostaining studies in hippocampal and cortical neurons revealed μ-opioid receptors forming clusters in spines that are co-localized with AMPA receptors (Liao et al., 2005). Thus, we hypothesize that morphine treatment can alter the dynamic localization of AMPA receptors, which is a key factor for the drug-induced neuronal modulations. In this dissertation research, the main goal is to investigate the molecular mechanisms underlying morphine-induced neuronal modulations or synaptic impairments, which can be associated with opiate addiction. To achieve this goal, we have three specific objectives:

1) To examine the dynamic trafficking of AMPA receptors following morphine application in cultured neurons of hippocampus, a brain area related to addiction;

2) To delineate the signaling pathways that govern morphine-regulated AMPA receptor trafficking, and;

3) To investigate the physiological role of the regulated AMPA receptor trafficking *in vivo*, especially morphine's reinforcing and seeking behavior.

In the classic model of addiction, the dopaminergic system, including VTA and nucleus accumbens, is a well-known reward circuitry important for addiction (Di Chiara and Imperato, 1988). However, the hippocampus, a vital brain region for contextual learning and memory consolidation, has recently been found to regulate the rewarding effects of abused drug (Fan et al., 1999; Vorel et al., 2001). Furthermore, hippocampal glutamatergic neurons directly project to the nucleus accumbens (Floresco et al., 2001) and can modulate many activities of dopaminergic neurons in the VTA (Legault et al., 2000). Hence, the hippocampus is believed to play an important role in drug addiction, and the exploration of hippocampal neuromodulation induced by addictive drugs will be critical in our understanding of the mechanisms for addiction (Koob and Volkow, 2010; Morón and Green, 2010). In this study, we therefore used cultured hippocampal neurons as a cellular model.

CHAPTER 2

MATERIALS AND METHODS

2.1 Materials

2.1.1 cDNA and Animals

For cDNA, a plasmid encoding superecliptic pHluorin in pCI-neo was kindly provided by Dr. Gero Miesenböck (University of Oxford, UK). For animals, a line of heterozygous mice harboring a mutation on GluR1-S845 on a C57BL/6J genetic background was a generous gift from Dr. Richard L. Huganir (Johns Hopkins School of Medicine, Baltimore, MD, US) and pregnant Sprague-Dawley rats were purchased from Harlan Laboratories.

2.2.2 Drugs, Reagents and Softwares

Drugs and reagents purchased from Sigma-Aldrich (St. Louis, MO) include: D(-)-2-amino-5-phosphonovaleric acid (D-APV), dibutyryl cyclic-AMP (dbcAMP), tetrodotoxin (TTX), 5'Fluoro-2'-deoxy-uridine (FUDR), uridine, poly-L-lysine, L-cystine, bovine serum albumin (BSA), ovornucoid, glutathione, iodoacetamide, regulatory subunit of type II cAMP-dependent protein kinase, Protein kinase A (PKA) catalytic subunit, protein A-Sepharose, l-cysteine, Earle's Balanced Salt Solution (EBSS), deoxyribonuclease (DNase). Other reagents are obtained from different manufacturers such as streptavidin-agarose beads and sulfo-NHS-SS-biotin from Pierce (Rockford, IL), papain from Worthington (Lakewood, NJ), FK506 from Calbiochem (La Jolla, CA) and Effentene transfection reagent (Qiagen, CA). Sep-Pak C_{18} chromatography column was from Millipore (Billerica, MA). Life technologies (Gaithersburg, MD) provided various media and reagents for cell cultures including NeuroBasal media, Minimum Essential Media (MEM), heat-inactivated fetal bovine serum, heat-inactivated horse serum, sodium

pyruvate, penicillin, streptomycin, L-glutamine and B27 supplement. Furthermore, antibodies against GluR1 and phospho-GluR1-S845 were from Chemicon (Temecula, CA), while anti-PSD-95 antibody was purchased from Santa Cruz Biotechnology (Santa Cruz, CA). For software programs, ImageJ, IPLab4 and ANY-maze^{TM} Video Tracking system were available from National Institutes of Health (Bethesda, MD), BD Biosciences (San Jose, CA) and Stoelting (Wood Dale, IL), respectively.

2.2 Construction of recombinant receptors and site directed mutagenesis

The coding sequence of superecliptic pHluorin was amplified by PCR (QuikChange protocol; Stratagene, La Jolla, CA) and inserted into the N-terminus of rat GluR1 after a signal peptide in pRK5 vector. The tagging position with pHluorin in GluR1 was exactly the same as that with enhanced GFP, which has been shown to have no effect on the receptor function (Shi et al., 1999; Lin e al., 2004). A point mutation of GluR1 at Ser^{845} was generated by site-directed mutagenesis using PCR according to the guidelines in QuikChange® manual. The pairs of mutagenic primers are indicated as below.

For mutating GluR1 at Ser^{845} to **alanine**:

5’-CCCTCCCCCGGAAC**GCT**GGGGCAGGAGCCAGCGG-3’ (sense)

5’-CCGCTGGCTCCTGCCCC**AGC**GTTCCGGGGGAGGG-3’ (anti-sense)

For mutating GluR1 at Ser^{845} to **aspartic acid**:

5’-CCCTCCCCCGGAAC**GAT**GGGGCAGGAGCCAGCGG-3’ (sense)

5’-CCGCTGGCTCCTGCCCC**ATC**GTTCCGGGGGAGGG-3’ (anti-sense)

2.3 Cell cultures

2.3.1 Primary Hippocampal Culture

Dissociated neuronal cultures were prepared from hippocampi of Sprague-Dawley rats or C57BL/6J mice at postnatal days 1 and 2 (Liao et al., 1999). In brief, isolated hippocampi were incubated in Digestion Solution [0.5 mM EDTA, 15 mg papain and 4 mg l-cysteine in Earle’s Balanced Salt Solution (EBSS)] for 30 minutes at 37 °C, swirling occasionally. The digestion solution was removed and Inhibition Solution (1 mg/ml BSA, 1 mg/ml ovornucoid, 0.001% DNase in EBSS) was added. The brain tissue was triturated with a 10-ml pipette until most chunks disappeared. The chunks of undissociated tissue were allowed to settle for 3 minutes. The supernantant was then carefully collected and centrifuged at 2000 rpm for 10 minutes at 4 °C. The cell pellet was resuspended in Plating Media (10% heat-inactivated fetal bovine serum, 5% heat-inactivated horse serum, 200 mM L-cystine, 10 mM sodium pyruvate, 50 units/ml penicillin, 50 μg/ml streptomycin, L-glutamine). For live-cell imaging experiments, neurons were plated at a density of 1×10^6 cells per dish onto a 35-mm glass-bottom petri dish coated with poly-L-lysine (thickness of glass coverslip = 0.08 mm; Lin et al., 2004). For all other biochemical studies, 3×10^6 cells were plated onto a poly-L-lysine-treated 60-mm petri dish. After removing the plating medium, hippocampal cultures were maintained in Neuron Feeding Media [NFM; 25% NeuroBasal media, 2% heat-

inactivated horse serum, 2% B-27, 10 mM sodium pyruvate, 0.016 mg/ml 5'Fluoro-2'-deoxy-uridine (FUDR), 0.032 mg/ml uridine, penicillin, streptomycin, L-glutamine in Minimum Essential Media (MEM)] and were kept at 37 °C in humidified air with 5% CO_2 (Ghosh and Greenberg, 1995; Liao et al., 1999). One week after plating, and every week thereafter, the cultures were fed with one-fourth volume of conditioned media from glial cells (section 2.3.2 Glial Culture). From the day of plating, cultured neurons were counted as DIV1 (day 1 *in vitro*). Neurons at DIV18-24 were used for imaging and biochemical experiments.

2.3.2 Glial Culture

To prepare a culture of glial cells, a total of 4 x 10^6 dissociated hippocampal cells (as described in section 2.3.1 Primary Hippocampal Culture) was plated onto a 150-mm culture plate. Glial Feeding medium (5% heat-inactivated horse serum, 10 mM sodium pyruvate, 50 units/ml penicillin, 50 μg/ml streptomycin, L-glutamine in MEM) was used for maintaining glial cell growth. In order to obtain glial conditioning media, the glial feeding medium was changed out for fresh NFM one week after plating. Two days later, the conditioned NFM from the glial culture was collected, followed by addition of 1X FUDR. The entire conditioned medium was eventually sterile-filtered (0.2 μm).

2.3.3 Clonal Cell Culture

For clonal cell line, Human Embryonal Kidney 293 (HEK293) cells were cultured in MEM, supplemented with 10% fetal bovine serum, 50 units/ml penicillin and 50 μg/ml

streptomycin at 37 °C in humidified air with 5% CO_2. Cells were fed every 3-4 days with fresh media until about 90% confluent in 100 mm tissue culture dishes. After removing the medium and washing with 5 ml 1X PBS, HEK293 cells were rinsed with 1 ml of 1X trypsin-EDTA solution for 3 minutes and resuspended in 9 ml of fresh medium. 1 ml of cell suspension was dispensed onto one dish for subculturing or diluted at a density of 4 x 10^5 cells/ml and seeded onto 6-well plates for transfection.

2.4 Transfection

Primary hippocampal neurons at DIV5-9 were transfected with various plasmids by standard calcium phosphate co-precipitation method (Ghosh and Greenberg, 1995). The Neuron Feeding Medium from primary cultures was collected, and about 300 μl glial conditional medium (section 2.3.2 Glial Culture) containing D(-)-2-amino-5-phosphonovaleric acid (D-APV) was added for covering each glass coverslip, which cells grown on. To prepare a precipitate for one coverslip, sterile H_2O, 1.5 μl $CaCl_2$ and 6 μg plasmid DNA in a final volume of 30 μl were mixed together in order. The $CaCl_2$/DNA dropwise was added to 15 μl of 2X HEPES-buffered saline (274 mM NaCl, 9.5 mM KCl, 0.38 mM $Na_2HPO_4.7H_2O$, 15 mM D-glucose and 42 mM HEPES in H_2O, pH 7.1-7.15) while swirling. After incubation of the precipitate solution for 30 minutes at room temperature, the entire solution was added onto the center of the coverslip. Then, the hippocampal culture was incubated for 5 h at 37 °C in a CO_2 incubator. The transfection medium was aspirated and 2 ml of the original medium supplemented with the glial conditional medium was added. To transfect HEK293 cells, Effectene transfection was conducted according to the manufacturer's instructions.

2.5 Live-cell confocal imaging and data analysis

Images were acquired by a 63× oil immersion objective of a Leica DMIRE2 fluorescence microscope, connected to a BD CARVII ™ confocal imager and a Hamamatsu EM CCD camera (Joiner et al., 2009). To maintain neuronal viability during image capturing, transfected hippocampal cultures were placed in a temperature-controlled chamber installed on the microscope (heated at 37°C) with continuous 5% CO_2 infusion (Leica Microsystems). Cells were then immediately returned to a humidified 5% CO_2 incubator at 37°C for prolonged drug treatment. All transfected cells, except those with abnormal morphologies, were randomly photographed. The X-Y coordinates of individual neurons on the stage fitted with X-Y translation were recorded by the IPLab4 software program, so that the same neuron could be located and imaged at different time points during the drug treatment.

All confocal images were taken as stacks (≤ 25 z-planes) at 0.4 μm intervals and then merged into one single image before further analysis with IPLab4 software as described (Joiner et al., 2009). The averaged pHluorin-GluR1 fluorescence of the cells was based on the quantification of the pHluorin-GluR1 intensity of each individual neuron in the field of view. To obtain this data, total area of the cell from the entire image was selected by an “autosegmentation” function in the IPLab4 program.

In the case of measuring fluorescence intensities (including pHluorin-GluR1 and DsRed) on specific regions such as spines and dendrites, the Region of Interest (ROI) was manually highlighted with “Segment Tools”. All fluorescence measurements represented raw data with background subtractions of the averaged blank field intensities. Dendritic spine was defined as a dendritic protrusion containing a rounded

head (Murai et al., 2003; Liao et al., 2005). Spine density was calculated by the number of spines normalized against the dendritic length (100 μm) in DsRed images.

2.6 Western blotting analysis

After drug treatments, cells were washed one time with Phosphate buffered saline (PBS) at 4°C, then immediately solubilized in extraction buffer [50 mM Tris, pH 7.4, 150 mM NaCl, 1 mM EDTA, 1% Triton X-100, 0.5% sodium deoxycholate, 30 mM NaF, 1 mM sodium orthovanadate, 1 mM dithiothreitol (DTT) and Complete protease inhibitor mixture (Roche, Basel, Switzerland)]. Supernatants of the lysates were collected after centrifugation at 13,000 × *g* for 5 min. A protein concentration in each sample was determined by a BCA assay (Pierce, IL) according to instructions supplied. About 0.8-1 mg proteins of each sample were used for either immunoprecipitation or biotinylation as described in section 2.7 and 2.8, respectively. The samples were then subjected to 10% Sodium Dodecyl Sulfate Polyacrylamide Gel Electrophoresis (SDS-PAGE) to separate proteins depending on their charge and molecular weight. After electrophoresis, electroblotting was performed for transferring the separated proteins onto a polyvinylidene difluoride membrane. In order to prevent non-specific background binding of antibodies to the membrane, it was firstly agitated in a blocking solution for at least 1 h at room temperature. The blocking solution is made of 5% w/v nonfat dry milk in Tris Buffered Saline with Tween-20 (TBST; 50 mM Tris-HCl, pH 7.4, 150 mM NaCl and 0.1% Tween 20). About 15 ml of the blocking solution containing a primary antibody, such as antiserum against GluR1 was incubated with the blocked membrane at 4 °C overnight. Later, the membrane was washed twice with TBST for 15 minutes each,

followed by incubation with the blocking solution containing alkaline phosphatase-conjugated secondary antibody for at least 1 h at room temperature. TBST was used again for washing the membrane three times for 15 minutes each. Then, the immunoblot was incubated with a ECF substrate (GE Healthcare, Buckinghamshire, UK) for 6 minutes to yield a highly fluorescent product, which can be detected by STORM 860 Analysers. The fluorescence intensity of each protein band was quantified using ImageJ.

2.7 Immunoprecipitation

After drug treatments, cells in 60-mm dishes were then lysed in 1 ml extraction buffer (as shown in 2.6 Western blotting analysis), followed by a centrifugation at 13,000 × *g* for 5 min. The pellets were discarded, whereas the supernatants of cell lysates were collected for BCA assay. 50 μl aliquot of the cell extracts was saved prior to immunoprecipitation for determining total level of AMPA receptor. About 0.8-1 mg total proteins were immunoprecipitated with 2 μg anti-GluR1 antibody at 4°C overnight under agitation. After a 3 h-incubation with protein A-Sepharose (50-60 μl), the pull-down complexes were washed three times with the extraction buffer without sodium deoxycholate. The GluR1 protein complexes finally were eluted by 2× Laemmli buffer, followed by SDS-PAGE and Western blotting analysis. The amounts of proteins in the receptor complexes were detected with antibodies against phospho-GluR1-S845, GluR1 and PSD-95.

2.8 Biotinylation

To label all surface proteins, after washing with ice-cold PBS/Ca^{2+}/Mg^{2+} (10 mM phosphate buffer, 2.7 mM KCl, 137 mM NaCl, 1 mM $CaCl_2$, 0.5 mM $MgCl_2$, pH 7.4), 3 week-old hippocampal neurons in 60-mm dishes were incubated with sulfo-NHS-SS-biotin (300 μg/ml) for 30 min at 4°C to biotinylate cell surface proteins as described previously (Mammen et al., 1997; Lin et al., 2000). The unbound biotin was washed away by PBS/Ca^{2+}/Mg^{2+} containing 0.1% BSA at 4ºC. The biotinylated cells were then incubated with the original growth media with or without 10 μM morphine (in the presence or absence of inhibitors if necessary) and returned to the 5% CO_2 incubator at 37°C for various time periods for receptor internalization. Receptor trafficking was stopped by rapidly cooling the cells at 4°C. Biotinylated proteins remaining on the cell surface were stripped by glutathione (150 mM glutathione, 150 mM NaCl, pH 8.75), but internalized receptors were protected and would still contain biotin. Subsequently, 50 mM iodoacetamide in PBS/Ca^{2+}/Mg^{2+} was used to neutralize glutathione. Cells were then immediately solubilized in the extraction buffer (as shown in section 2.6 Western Blotting Analysis) lacking DTT. After centrifugation at 13,000 × *g* for 5 min, 50 μl supernatants were aliquoted for determining total amount of AMPA receptors in each sample, while about 0.8-1 mg cell extracts were agitated with streptavidin-agarose beads at 4°C overnight. Lastly, the biotinylated receptors in the pull-down complexes, which should represent internalized receptors, were eluted by 2× Laemmli buffer and resolved by SDS-PAGE. Antibodies against GluR1 and GluR2 were used to detect internalized AMPA receptors in the pull-down complexes and total receptor expressions in cell extracts.

2.9 *In vitro* phosphatase assay

To measure phosphatase activity of calcineurin, ^{32}P-labeled RII peptide substrate corresponding to 19 residues in the regulatory subunit of type II cAMP-dependent protein kinase or Protein Kinase A (PKA) was prepared as described (Fruman et al., 1996). The serine phosphorylation of RII peptide substrate with [γ-^{32}P]ATP was carried out by a PKA catalytic subunit. The kinase reaction contained the following concentrations: 500 μl of 2X Buffer A (40 mM MES buffer, pH 6.5, 4 mM $MgCl_2$, 0.1 mM $CaCl_2$, 0.4 mM EDTA, 0.8 mM EGTA, 1 mM DTT, 0.1 mg/ml BSA), 6 μl 50 mM ATP, 60 μCi [γ-^{32}P]ATP and 45 μl 3.3 mM RII peptide in a final volume of 900 μl. The phosphorylation of the peptides was initiated by the addition of 100 μl of PKA catalytic subunit with 250 units of activity at 30 °C for 1h. Then the labeled peptides and unincorporated ATP were separated by Sep-Pak C_{18} chromatography column. The column was firstly equilibrated by using a syringe to apply 3 ml of 30% acetonitrile in 0.1% trifluoroacetic acid (TFA), followed by 5 ml of 0.1% TFA. After loading the entire kinase reaction to the column, the column was washed with 75 ml 0.1% TFA to remove the free ATP. Lastly, the radioactive peptides were eluted with 2 ml of 50% acetonitrile in 0.1% TFA, and subsequently lyophilized and resuspended in 1 ml buffer B (50 mM Tris, pH 7.5, 100 mM NaCl, 0.5 mM DTT, 100 mg/ml BSA) to obtain an approximate concentration of 150 μM.

After drug treatments, hippocampal neurons were lysed in hypotonic lysis buffer (50 mM Tris, pH 7.5; 1 mM EDTA; 0.1 mM EGTA; 0.5 mM DTT; 50 μg/ml PMSF; 10 μg/ml leupeptin and 10 μg/ml aprotinin). 6-8 μg of cell extracts were used for the phosphatase assay. Okadaic acid (OA) was added to the assay buffer (50 mM Tris, pH 7.5, 100 mM

NaCl, 0.5 mM DTT, 100 μg/ml BSA, 0.1 mM $CaCl_2$) in all experiments. Since OA can inhibit the activities of Ca^{2+}-independent phosphatases including phosphatase 1 and 2A by more than 90%, but has no significant effect on calcineurin, calcineurin activity can be measured clearly under the assay condition containing OA (Fruman et al., 1996). Reaction mixtures for the phosphatase assay contained 20 μl of cell lysates, 20 μl of assay buffer, 100 nM OA and 20 μl of 15μM ^{32}P-labeled RII peptide substrate. The mixtures were incubated at 30 °C for 10 min. Then, the reactions were terminated by adding 20 μl 50% trichloroacetic acid and 80 μl BSA (6 mg/ml). The samples were incubated on ice for 10 min, followed by centrifuging at 13,000 × *g* for further 10 min at 4 °C. The amount of $^{32}P_i$ released from RII peptide in the supernatant was measured by liquid scintillation. Blank samples containing only assay buffer were used. To determine the specific activity of the substrate, cpm in 20 μl of 15 μM substrate was measured. Net cpm for samples was calculated by substracting cpm measured in the blanks. The amount of $^{32}P_i$ released (pmol) in each sample was calculated by dividing the net cpm for the sample by the specific activity of the substrate. Final phosphatase activity was expressed as percentage of the control without drug treatment.

2.10 Animal behavioral studies

2.10.1 Mouse Line

Wild type and GluR1-S845A homozygous mice on a C57BL/6 genetic background are generated through mating of heterozygous mutant mice. All animals were housed in a group of four per cage and maintained on a 12-h day/night light cycle

in animal facilities, which are accredited by the Institutional Animal Care and Use Committees (IACUC) of the University of Minnesota. Food and water were present *ad libitum*. For all behavorial studies, 10- to 14-week-old male mice of both wild types and homozygous mutants were used and each mouse was utilized only once for each experiment. Mice were acclimatized to the laboratory environment for one week before starting the study. During this period mice were handled and weighed. If necessary, they were even habituated to the drug administration procedure by receiving at least two subcutaneous (s.c.) injections of saline. All protocols were approved by the IACUC by which all possible measures were conducted to minimize the number of mice used and suffering of animals.

2.10.2 Conditioned Place Preference (CPP) and locomotion

An experimental apparatus for CPP procedure is a three-compartment polyvinyl chloride box (**Fig. 2.1**). Two large side compartments provide different visual and tactile cues, such as black dotted or gray striped wall and smooth or rough floors respectively, and they are connected by a center transparent chamber. Removable guillotine doors are used to partition them. The CPP procedure consisted of three phases: i) habituation and preconditioning test, ii) conditioning as well as iii) CPP test. All experiments were conducted during the dark phase in dim light environment with a continuous masking noise. Moreover, animals' location and locomotion in the apparatus were tracked and measured by using ANY-maze^{TM} Video Tracking system and conventional cameras. The procedure began with habituation for three days. Each mouse was placed separately

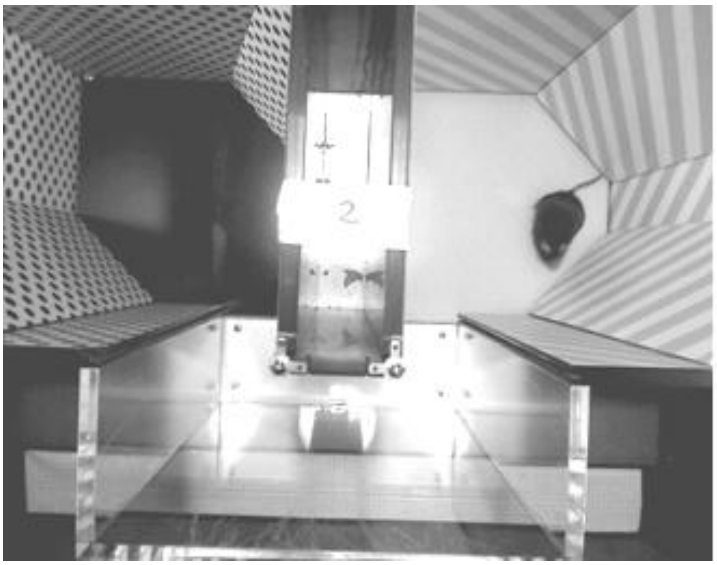

Figure 2.1. Conditioned place apparatus.
It is divided into three compartments. Left compartment has black dot wall with a black and smooth floor, while right compartment has pale-gray stripe wall with a gray and rough floor. The bottom is a transparent small compartment.

into the apparatus without any guillotine door for 15 minutes, so that they could explore the entire apparatus freely. On day 3, a preconditioning test was performed, in which the time spent in each compartment was recorded to determine any innate preference for either of the two large compartments. Animals showing a strong preference to any chamber (>60% of total time) were discarded, while others were grouped randomly: saline and morphine. The conditioning phase comprised two sessions per day (i.e. morning and afternoon session) for two to four consecutive days. All mice were injected with saline (0.9% NaCl, 1 ml/kg, s.c.) in the morning session and immediately confined to the assigned chambers for 40 minutes with using the guillotine doors. The ANY-maze^{TM} Video Tracking system was used to measure their basal locomotor activity. The afternoon session began after at least 4 h, in which they were administrated with either saline or morphine (5 mg/kg or 10 mg/kg, s.c.) right before confinement to the alternative chambers. Similarly, their locmotor activity in response to morphine injection was determined as well. On the day of CPP test, the guillotine doors between compartments were removed and mice in a drug-free state were given free access to the whole apparatus for 15 minutes. The time spent in each chamber was recorded again. The CPP score (in sec.) was defined as the time spent in the morphine-paired chamber during CPP test minus that spent in the preconditioning test. If the score was higher than 60 seconds, animals were recognized to have a preference for the morphine-paired chambers and so they were subjected to the subsequent extinction tests. Extinction test was the same as the CPP test (i.e. 15 minutes per session) and the test score was calculated by the time spent in the morphine-paired chamber during the extinction test minus that spent in the preconditioning test. Furthermore, it was carried out every two days until the drug preference response was extinct (i.e. test score <60 seconds) for three consecutive sessions.

2.10.3 Morris Water Maze

Morris water maze was used for testing hippocampus-dependent spatial memory of mice and performed during the day phase of the light cycle with a circular swimming tank (120 cm in diameter, Fig. 2). ANY-maze^{TM} Video Tracking system was employed again to measure mice activity and position. The swimming tank was filled with opaque water and surrounded by white curtains that had simple distinct signs for providing spatial cues. One day before training, each mouse was habituated to the water tank once for 1 minute. The training involved a hidden platform paradigm, by which an escape platform (with 11 cm diameter) was placed 0.5 to 1 cm beneath the water surface in the center of a quadrant of the tank. Mice received four trials of training with 1-min interval per day for six consecutive days. In each trial, they were placed into the tank randomly from four different designated start points and allowed to navigate for up to 60 seconds until they landed on the platform. If mice failed to find the platform within 60 seconds, they were manually guided to the position. The time each mouse spent to find the platform was scored as escape latency, and the score on each trial was averaged for a single day.

2.11 Statistics

All data are expressed as mean ± s.e.m. of the indicated number of experiments. Statistical significance was determined using *t*-test for a comparison between two groups and one-way or two-way ANOVA for a comparison between multiple groups (SPSS 13.0, Chicago, IL); a value of $p < 0.05$ was considered statistically significant.

CHAPTER 3

RESULTS

3.1 The effect of morphine on AMPA receptor trafficking

3.1.1 Expression of pHluorin-GluR1 can track dynamic location of AMPA receptors

Prolonged treatment with morphine not only induced collapse of dendritic spines *in vivo* and *in vitro*, but also diminished frequency and amplitude of mEPSCs at hippocampal neurons, indicating a reduction of the postsynaptic AMPA receptors (Robinson et al., 2002; Liao et al., 2005). However, no study has shown the temporal dynamics of AMPA receptor trafficking in response to morphine. To do this, we will use the latest approach that employs pH-sensitive GFP (super-ecliptic pHluorin) to visualize surface-expressed AMPA receptors at individual synapse in real time, due to its character of a reversible excitation ratio changes between pH 7.5 and 5.5 (Ashby et al., 2004). The pHluorin was introduced into the extracellular N-terminus of GluR1 (pHluorin-GluR1) (**Fig. 3.1A**), a subunit of AMPA receptors widely expressed in adult hippocampal neurons (Wenthold et al., 1996). The experimental principle is that pHluorin faced to the extracellular environment (about pH 7.4) can display a bright fluorescence, if pHluorin-GluRl locates at cellular surface. However, if the recombinant receptor undergoes internalization, pHluorin becomes stop to fluoresce because of exposing to the acidic lumens of endocytic and secretory vesicles (about pH 5.6) (**Fig. 3.1B**). To ensure the validity of the recombinant receptors, HEK293 cells were firstly transfected with either empty vector (Mock) or a plasmid encoding pHluorin-GluR1. Cell lysates then were immunoblotted with antibodies against GluR1 and green fluorescent protein (GFP) (**Fig. 3.2A**). Both antibodies could recognize a protein band with about 130 kDa in cells transfected with pHluorin-GluR1 but not control vector, and the molecular weight was corresponding to

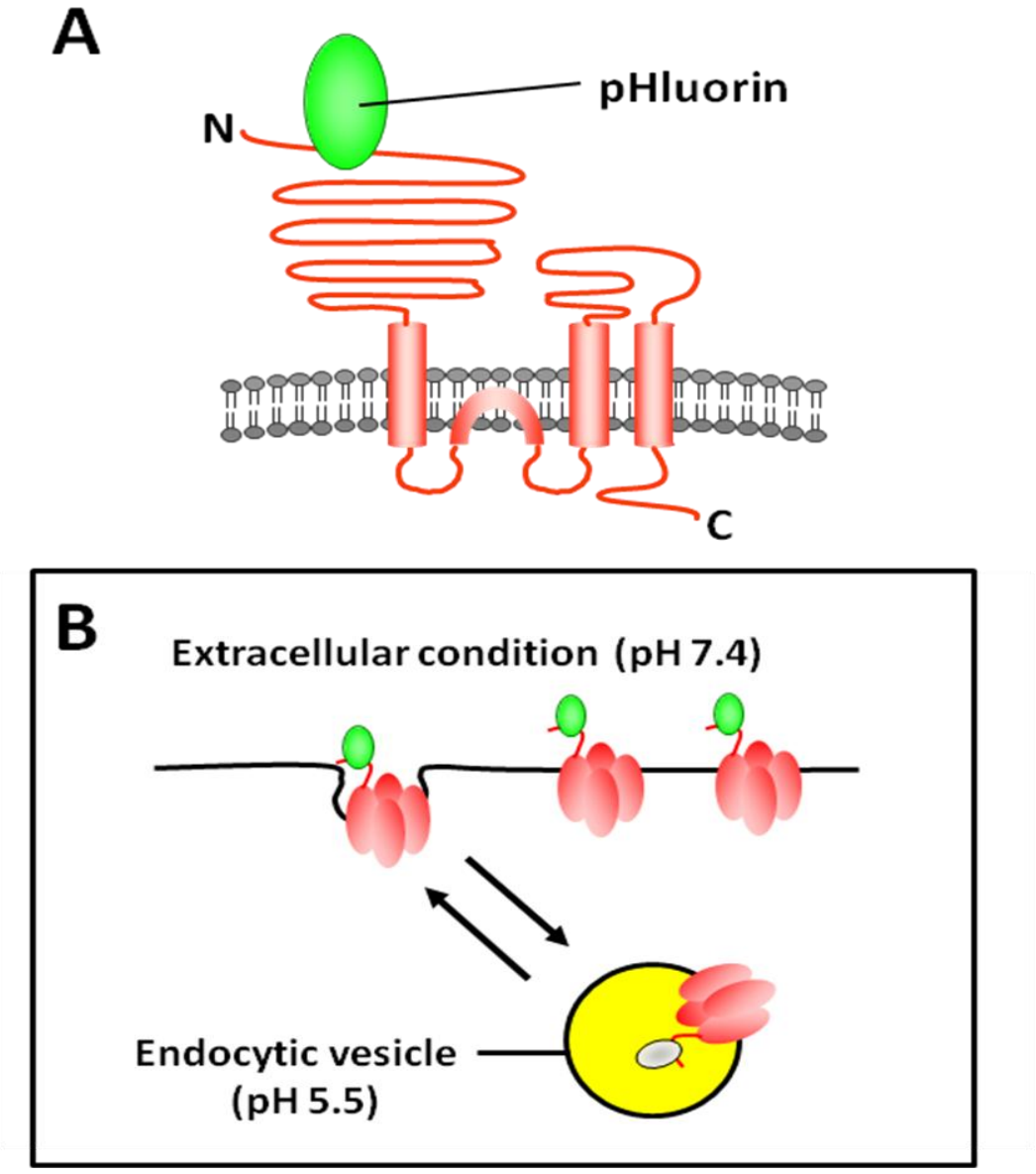

Figure 3.1. Super-ecliptic pHluorin-tagged GluR1. A, A schematic diagram illustrates the extracellular N-terminus of GluR1 tagged with pHluorin. **B**, A cartoon shows that surface-expressed pHlurin-GluR1 gives a strong fluorescence, but internalized receptor stops to fluoresce.

the size of the recombinant receptor. This result so confirmed intact receptors to be expressed (**Fig. 3.2A**). The membranes were re-probed with an anti-F-actin antibody to show equal protein loading in each sample (**Fig. 3.2A**).

To observe the distribution pattern of the recombinant AMPA receptor on neuronal cells, rat hippocampal cultures at DIV5-DIV9 were transfected with the plasmid of pHluorin-GluR1 by calcium phosphate co-precipitation method (Ghosh and Greenberg, 1995; section 2.4). At DIV18-24, images of transfected neurons were taken by a live-imaging system. **Figure 3.2B (i)** showed confocal fluorescence images on live neurons in pH 7.4 buffer that pHluorin-GluR1 effectively expressed in cells where they clustered in a punctate pattern on dendritic spines. We next determined whether the fluorescence came from the surface-expressed receptors. Thus cells were incubated in pH 6.0 buffer to quench the extracellular fluorescence (**Fig. 3.2B, ii**). The low pH buffer dramatically reduced dendritic fluorescence and completely removed that of spines (**Fig. 3.2B, ii**), indicating that most of the fluorescence was attributable to the surface-expressed receptors. Importantly, this reduced fluorescent signals could be reversed by replacement with pH 7.4 buffer again (**Fig. 3.2B, iii**), validating the pH sensitivity of pHluorin.

3.1.2 Morphine elicited loss of surface-expressed GluR1 subunits

To measure the dynamics of morphine-regulated AMPA receptor trafficking, cultured hippocampal neurons were contransfected with plasmids encoding pHluorin-GluR1 and DsRed (a soluble red fluorescence protein), which were used to visualize surface-

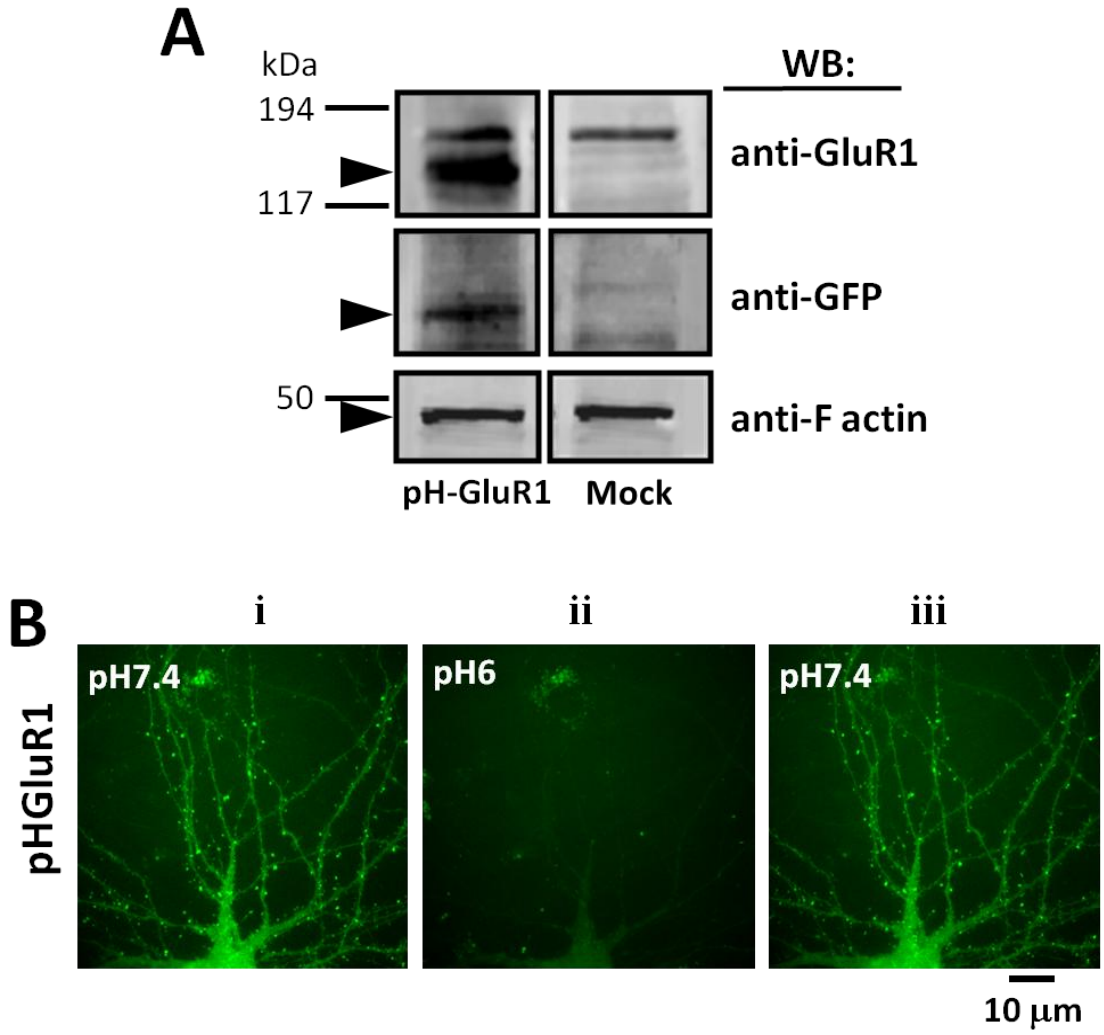

Figure 3.2. Visualization of surface AMPA receptors by pHluorin-tagged GluR1. **A**, HEK293 cells were transfected either with pHluorin-GluR1 (pH-GluR1) or vector (mock). Lysates were subjected to western blotting (WB) with the indicated antibodies. **B**, Hippocampal neurons (DIV6) grown on glass coverslips were transfected with pH-GluR1. About two weeks after transfection images of neurons were taken in pH 7.4 buffer (i), which was then removed by washing cells with pH 6 buffer (ii). Finally, the extracellular condition was returned to the normal pH (iii).

expressed AMPA receptors and to label dendritic spines, respectively. About two weeks after transfection (DIV18-24), same-labeled neurons were imaged before and after 10 μM morphine exposure at various time points (3h, 1d and 3d) (**Fig. 3.3**). Upon morphine exposure, a gradual decrease in fluorescence signal of the pHluorin-GluR1 was observed (**Fig. 3.3A**). The average fluorescence of pHluorin-GluR1 from the entire image of morphine-treated neurons significantly decreased by 12.8% for 3 h, 21.6% for 1 d, and 33.9% for 3 d after the drug application (relative to before morphine treatment) (**Fig. 3.3B**, *top*), implicating a loss of surface-expressed GluR1 by morphine. In contrast, the fluorescence intensity of pHluorin-GluR1 in untreated neurons remained constant or even slightly increased during the 3 d of observation, indicating that the decrease in green fluorescence by morphine was not due to photobleaching effect (**Fig. 3.3A, B**). Also, no significant change in overall protein expression of AMPA receptors was observed during drug treatment **(Fig. 3.4A)**. Interestingly, quantitative analysis on individual spines and the adjacent dendrites in **Figure 3.3B** (*middle* and *bottom*) showed that treatment with morphine for 3 h clearly diminished the surface fluorescence of pHluorin-GluR1 on spines but not at dendritic shafts. Therefore, the loss of synaptic GluR1 by morphine should occur before the loss of extra-synaptic GluR1. Consistent with our previous studies (Liao et al., 2005), the density of DsRed-labeled spines was substantially reduced after 1 and 3 d of morphine treatment (before, 63.4±4.47 spines/100 μm; 1 d, 43.3±4.02 spines/100 μm; 3 d, 37.2±3.28 spines/100 μm) (**Fig. 3.5**). These findings provide direct live imaging evidence that chronic treatment with morphine results in two distinct processes, including the loss of surface-expressed AMPA receptors and the loss of spines.

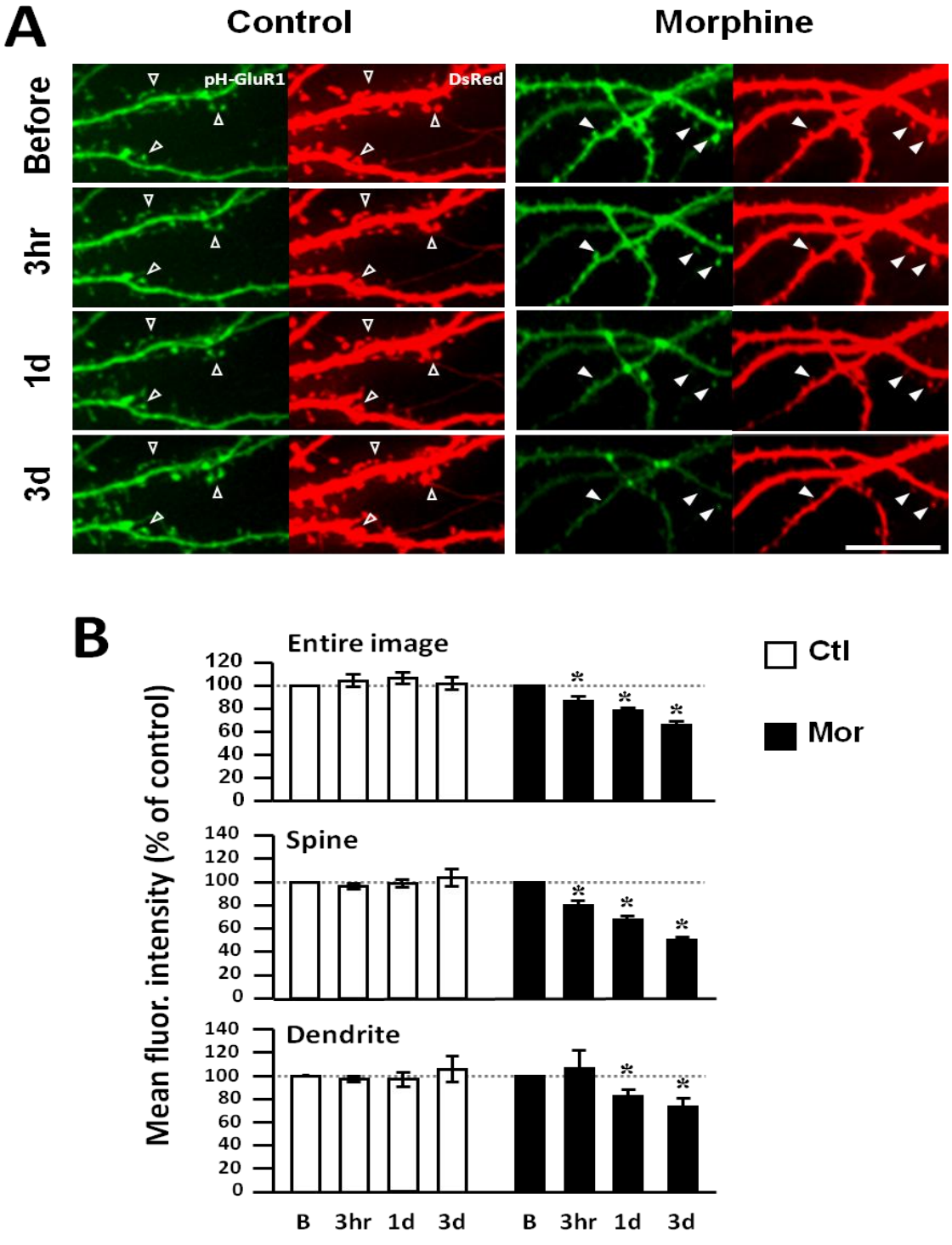

Figure 3.3 (con't)

Figure 3.3. Chronic treatment with morphine causes loss of synaptic and extra-synaptic surface pHluorin-GluR1 subunits.

A, Examples of confocal images of primary hippocampal neurons expressing pHluorin-GluR1 (pH-GluR1) and DsRed (*Left*, untreated control neurons; *right*, morphine-treated neurons). The transfected cells were imaged before (B) and after exposure to 10 μM morphine for various durations (3 h, 1 d and 3 d). Open arrowheads denote that both fluorescence intensities remained constant or even increased under untreated control conditions. Solid arrowheads denote that morphine progressively decreased the fluorescence intensity of pHluorin-GluR1 and the density of DsRed-labeled dendritic spines. *Scale bar*, 10 μm. **B**, Mean pHluorin-GluR1 fluorescence from different regions (the entire images, spines and dendrites) of untreated (Ctl; open bars; n = 16) or morphine-treated neurons (Mor; black bars; n = 16) were normalized with data before treatments and are shown as percentages. * denotes a significant decrease comparing with the value before treatment. In each group, a minimum of five dendrites from a single neuron were analyzed. Error bars represent ± SEM.

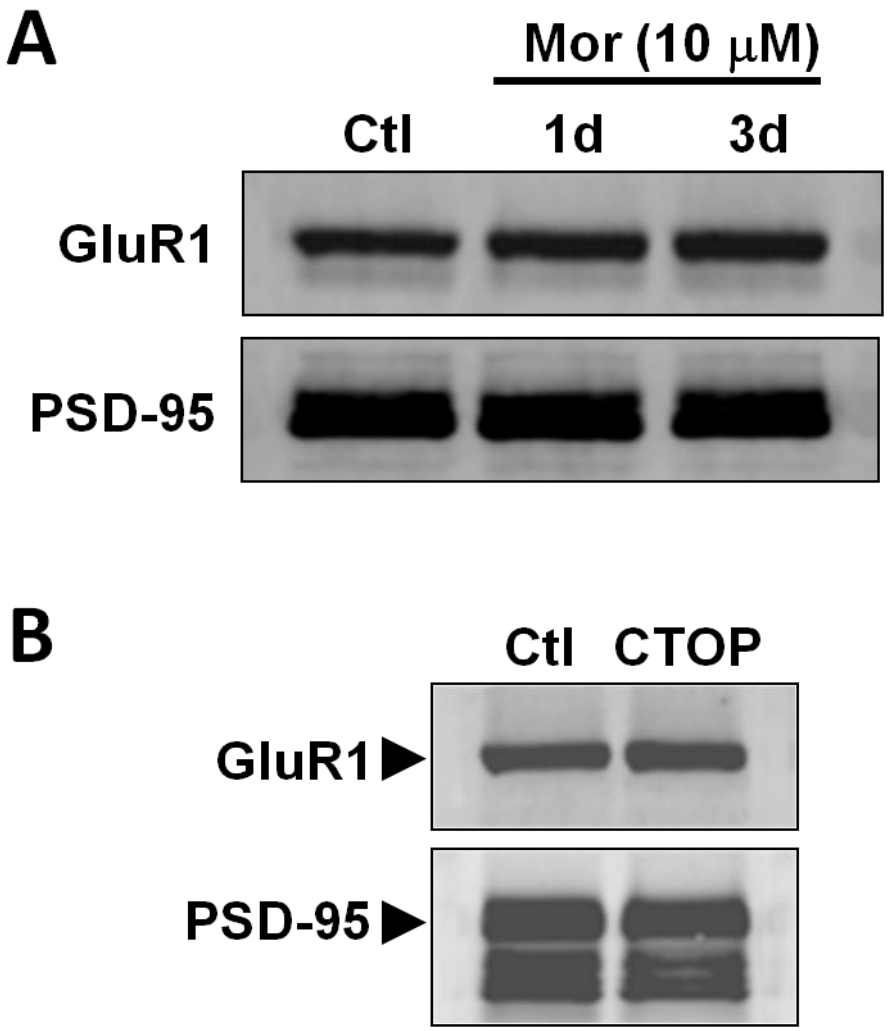

Figure 3.4. The effects of morphine and CTOP on the protein level of GluR1. **A,** Representative immunoblot shows hippocampal neurons treated with or without 10 μM morphine for 1 d and 3 d. **B**, Neurons were treated with or without CTOP for 1 d. Cells were lysed and the protein expressions of GluR1 and PSD-95 were determined by Western blots (**A**, *n*=3; **B**, *n*=3).

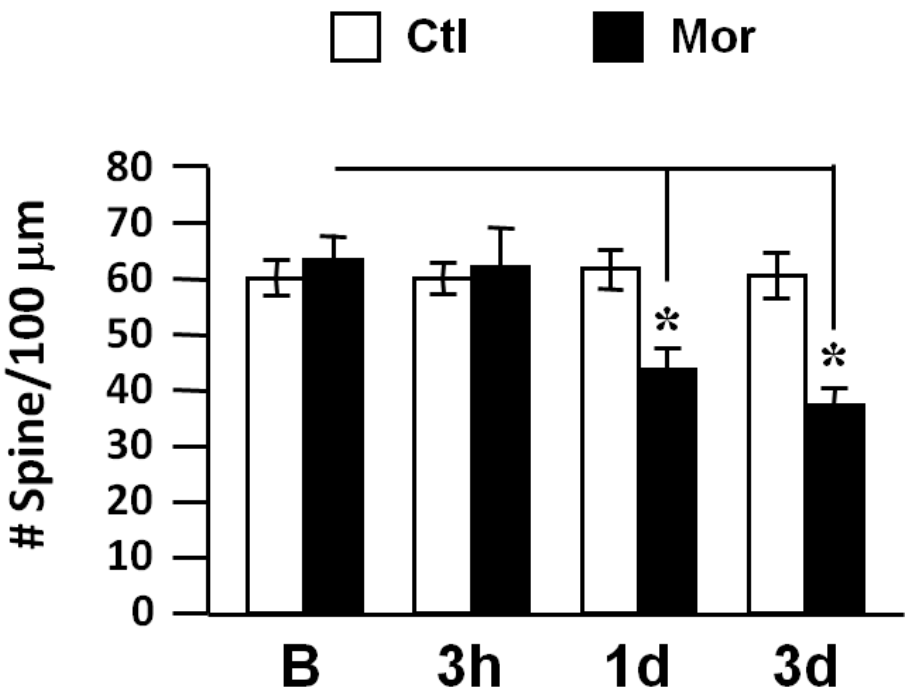

Figure 3.5. The effect of morphine treatment on the density of dendrtic spines.

The number of spines in control (Ctl; *open bars*) versus morphine-treated (Mor; *black bars*) neurons was determined from the DsRed images in Figure 3.3. Morphine significantly decreases the density of dendritic spines after 1-3 days of treatment. * denotes a significant decrease comparing with the value before treatment ($p < 0.05$; $n = 16$ in each group). Error bars represent ± SEM.

3.1.3 Morphine-induced removal of synaptic GluR1 preceded morphological shrinkage of dendritic spines

Which comes first, the loss of AMPA receptors or the loss of dendritic spines? To illustrate the temporal sequence of the above two processes, we compared the fluorescence intensities of pHluorin-GluR1 before and after the morphine treatment at 3 h, 1 d and 3 d on dendritic spines with those of DsRed (**Fig. 3.6**). In the untreated control, the fluorescence of neither pHluorin-GluR1 nor DsRed was significantly changed (**Fig. 3.6A**, *upper two panels*; **Fig. 3.6B**, *left*). On the other hand, chronic application of morphine reduced both fluorescence of pHluorin-GluR1 and DsRed on the same spines, but with different time kinetics. Upon 3 h of morphine exposure, pHluorin-GluR1 fluorescence on spines clearly decreased, whereas the DsRed signal on the spines remained unchanged (**Fig. 3.6A**, *lower two panels*; **Fig. 3.6B**, *right*). As mentioned the above, morphine has not yet caused any significant change in spine density after 3 h (**Fig. 3.5**), so the drug-induced loss of synaptic GluR1 happened before the spine shrinkage, suggesting that morphine-mediated loss of synaptic GluR1 was not a result of spine retraction, but rather a plausible cause for spine retraction.

3.1.4 Morphine triggered internalization of GluR1

The loss of the AMPA receptors on the cell surface could be a result of either an increase in receptor internalization or a decrease in surface recruitment of the receptor. To directly examine whether morphine exposure mediates endocytosis of the AMPA receptors, surface proteins including GluR1 in the live hippocampal cultures were

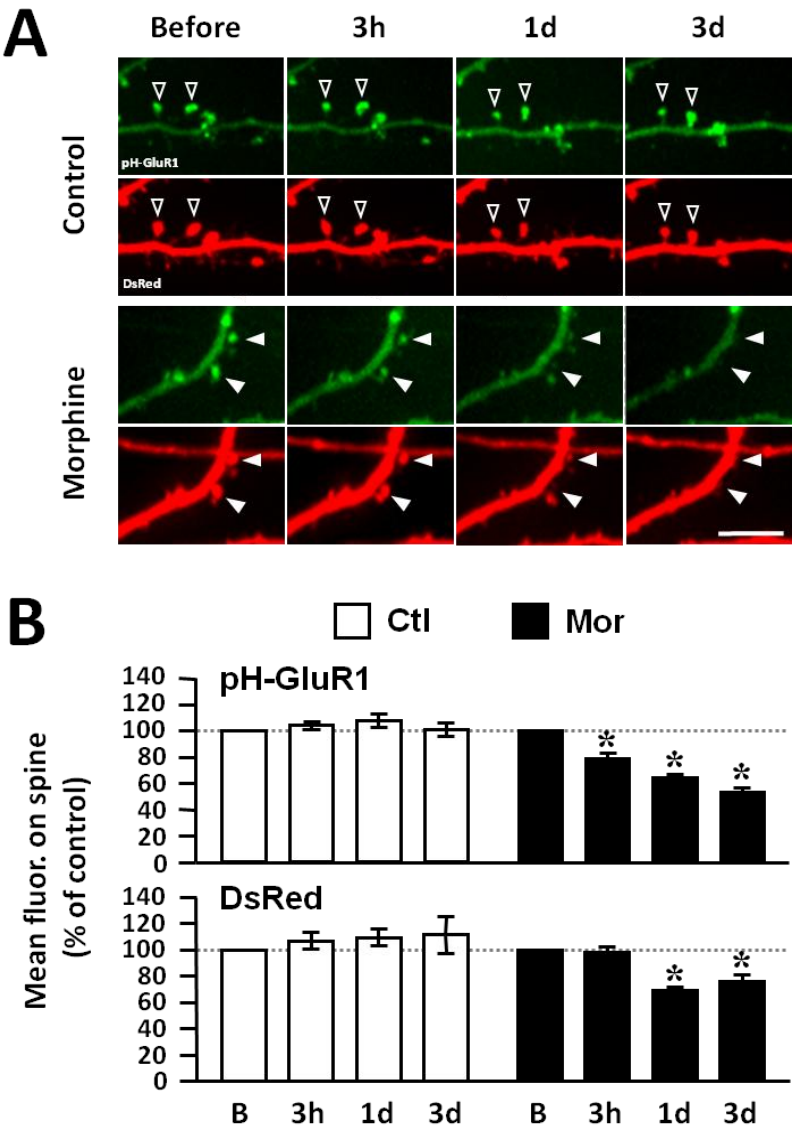

Figure 3.6. Time kinetics of the loss of synaptic GluR1 and the loss of spines as revealed by pHluorin-GluR1 and DsRed fluorescences.

Confocal images from Fig. 3.3 were further analyzed, in which hippocampal neurons overexpressing pHluorin-GluR1 and DsRed were imaged before and after treatment with no drug (control, ctl) or morphine (Mor) (10 μM). **A**, Representative confocal images show magnified images of neurons under different treatments. **B**, A graph shows mean fluorescent intensities of pHluorin-GluR1 and DsRed on spines only. Scale bar represents 5 μm. Values in the bar graph normalized to data before treatments are shown. * $p < 0.05$ compared with data before treatment; error bars represent ± SEM. In each treatment, a minimum of five dendrites from a single neuron were analyzed (n=16).

biotinylated prior to morphine treatment. After stripping, only internalized receptors would be protected and still contain biotin (see Materials and Methods, section 2.8). As shown in **Figure 3.7A**, upon application of morphine (10 μM), the amount of biotinylated GluR1 subunits progressively increased by twofold to threefold over the control (at 12-24 h), indicating a time-dependent increase in internalized GluR1 subunits. However, there was no significant difference in the amount of the internalized NMDA receptor between control and morphine-treated neurons (**Fig. 3.7B**), suggesting that morphine specifically affected trafficking of GluR1 subunits. Furthermore, intracellular actin could not be detected in the complex pulled down by strepavidin-agarose bead (**Fig. 3.7B***, left panel*), but was present in the total lysates (**Fig. 3.7B***, right panel*), confirming that only surface-expressed receptors can be biotinylated in our experimental model.

3.2 Delineation of signaling pathways involved in regulation of AMPA receptor trafficking by morphine treatment

3.2.1 The effect of morphine on AMPA receptor trafficking was mediated through μ-opioid receptor

To investigate the specificity of morphine's effect on AMPA receptor trafficking, hippocampal neurons overexpressing pHluorin-GluR1 and DsRed were incubated with a reduced dosage of morphine (1 μM) or co-treated with the selective μ-opioid receptor antagonist D-Phe-Cys-Tyr-D-Trp-Orn-Thr-Pen-ThrNH_2 (CTOP) for live-cell imaging experiments (**Fig. 3.8; Fig. 3.9**). In contrast to the higher concentration of morphine (10 μM), 1 μM morphine did not significantly reduce the fluorescence signal of synaptic

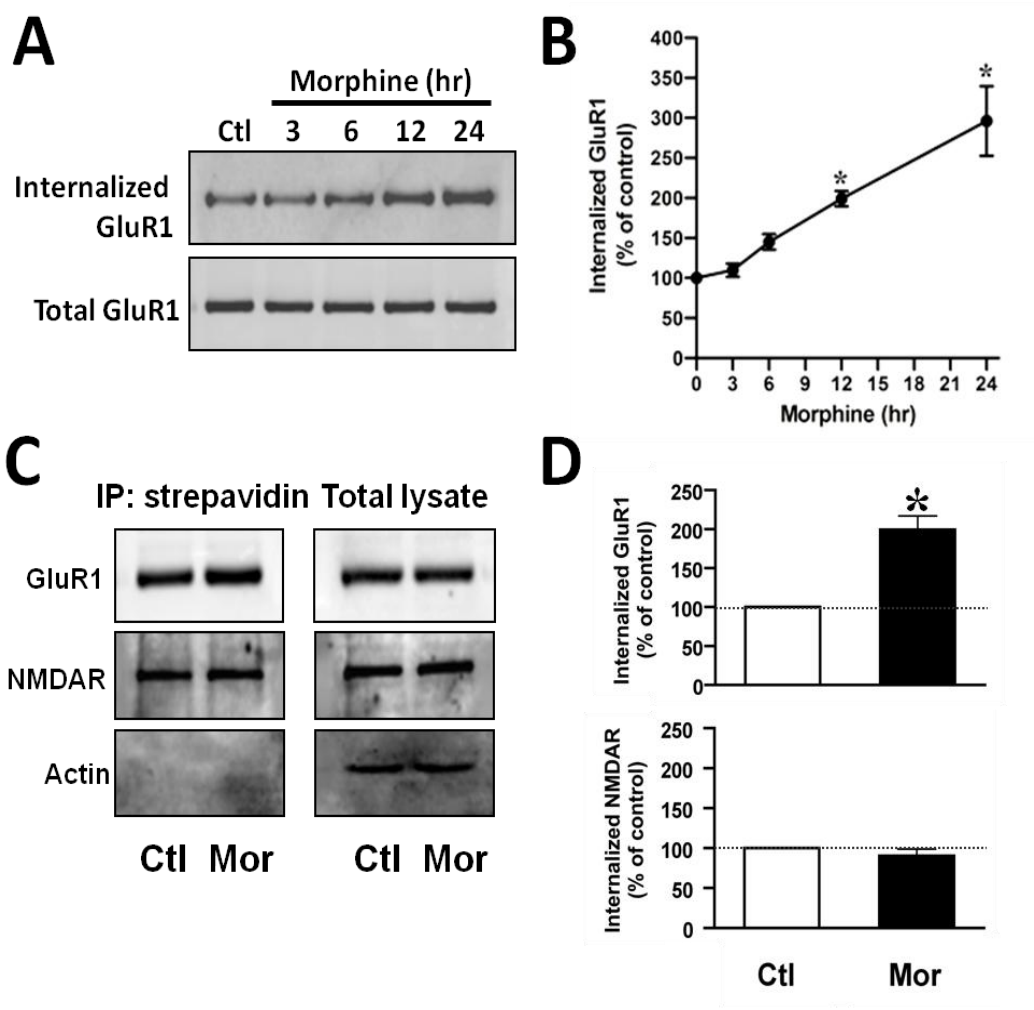

Figure 3.7. Surface biotinylation assay demonstrates a significant increase in GluR1 internalization upon morphine treatment.

A, Surface biotinylated hippocampal neurons were treated with no drug (Ctl) or 10 μM morphine for various durations (3, 6, 12 and 24 h). After cleavage of extracellular biotin, internalized GluR1 subunits were precipitated with immobilized steptavidin beads and detected with an anti-GluR1 antibody by western blotting (*top*). Total GluR1 subunits from whole-cell lysates were also detected for a comparison (*bottom*). **B**, Densitometric quantifications of western blots on internalized GluR1 (normalized to the untreated control level; $n = 4$). **C**, Surface biotinylated neurons were incubated with no drug (Ctl) or 10 μM morphine for 1 d. *Left*, internalized GluR1 and NMDA receptors were isolated by strepavidin precipitation and detected with anti-GluR1 and NMDA receptor antibodies (*top and middle*). No intracellular actin was found in the pull-down complex, indicating only surface proteins were biotinylated (*bottom*). *Right*, total GluR1, NMDA receptors and actin from whole cell lysates were detected for a comparison. **D,** Densitometric quantifications of western blots on the internalized GluR1 and NMDA receptors (normalized to the untreated control level; $n = 3$). * $p < 0.05$, comparing with the untreated control. Error bars represent ± SEM.

pHluorin-GluR1 at the 3 h time point (**Fig. 3.8**). Nevertheless, this lower concentration of morphine did induce a comparable reduction in fluorescence of the receptor at both spines and dendrites at longer time points (1 and 3 d) (**Fig. 3.8**). Hence, a higher concentration of morphine was likely to induce a more rapid loss of the synaptic AMPA receptors. More importantly, this down-regulated effect of morphine was attenuated by CTOP (10 μM), indicating the participation of μ-opioid receptor in morphine-modulated surface-expressed GluR1 (**Fig. 3.9**). It should be noted that both CTOP alone and CTOP with morphine enhanced the surface delivery of GluR1 at spines and dendrites due to increased fluorescence intensity in both regions (**Fig. 3.9**), but this did not alter the receptor protein expressions (**Fig. 3.4**). These results imply that the constitutive activity of μ-opioid receptor and/or endogenous opioids could regulate the distribution of AMPA receptors on cell surface. Consistently, biotinylation studies showed that the morphine-induced GluR1 internalization was also blocked in the presence of CTOP (10 μM) (**Fig. 3.10**). Collectively, these data indicate that morphine-induced GluR1 internalization is mediated by μ-opioid receptor.

3.2.2 Morphine-regulated GluR1 trafficking is not caused by alteration of neural circuitry

Opioid agonists have been shown to inhibit presynaptic release of transmitters such as GABA through activation of a voltage-dependent potassium channels. This results in a change in neural circuitry (Williams et al., 2001), which may indirectly contribute to the regulation of AMPA receptor trafficking. To test this possibility, a blockade of action potentials was achieved by using the sodium channel blocker Tetrodotoxin (TTX). As

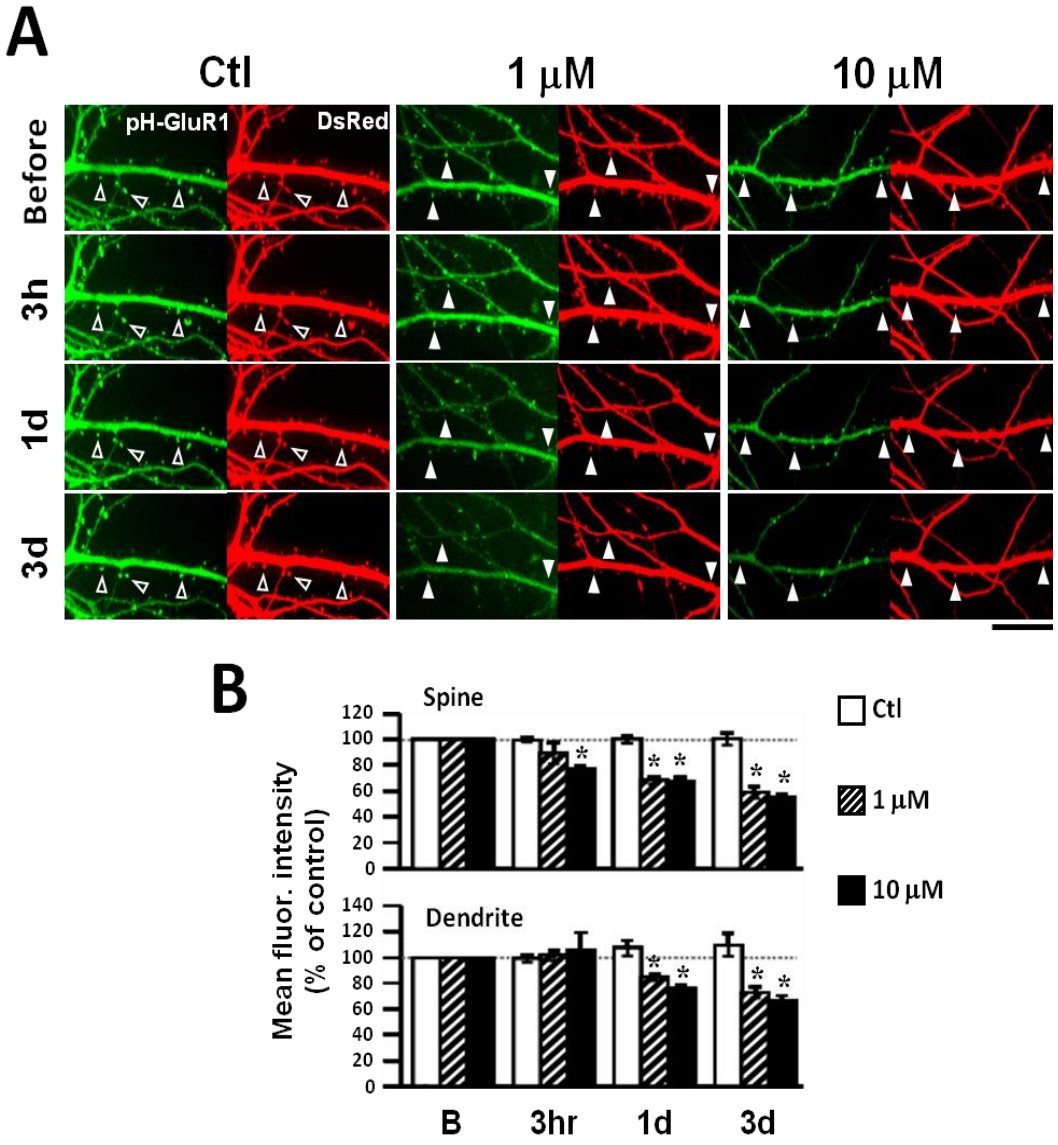

Figure 3.8. Reduction of surface-expressed GluR1 by a lower dose of morphine.
A, Time-lapse images were taken on neurons expressing pHluorin-GluR1 and DsRed before and after treatment with no drug (Ctl), 1 μM or 10 μM morphine for various times (3 h, 1 d and 3 d). Open arrowheads denote that both fluorescence intensities remained constant or even increased under untreated control conditions. Solid arrowheads denote that morphine progressively decreased the fluorescence intensity of pHluorin-GluR1 and the density of DsRed-labeled dendritic spines. Scale bar, 10 μm. **B**, Changes in averaged pHluorin-GluR1 fluorescence on spines (*top*) and dendrites (*bottom*) were normalized with data before treatments and are shown as percentages. * denotes a significant decrease comparing with the value before treatment ($p < 0.05$). In each group, a minimum of five dendrites from a single neuron were analyzed ($n = 10$ in each group). Error bars represent ± SEM.

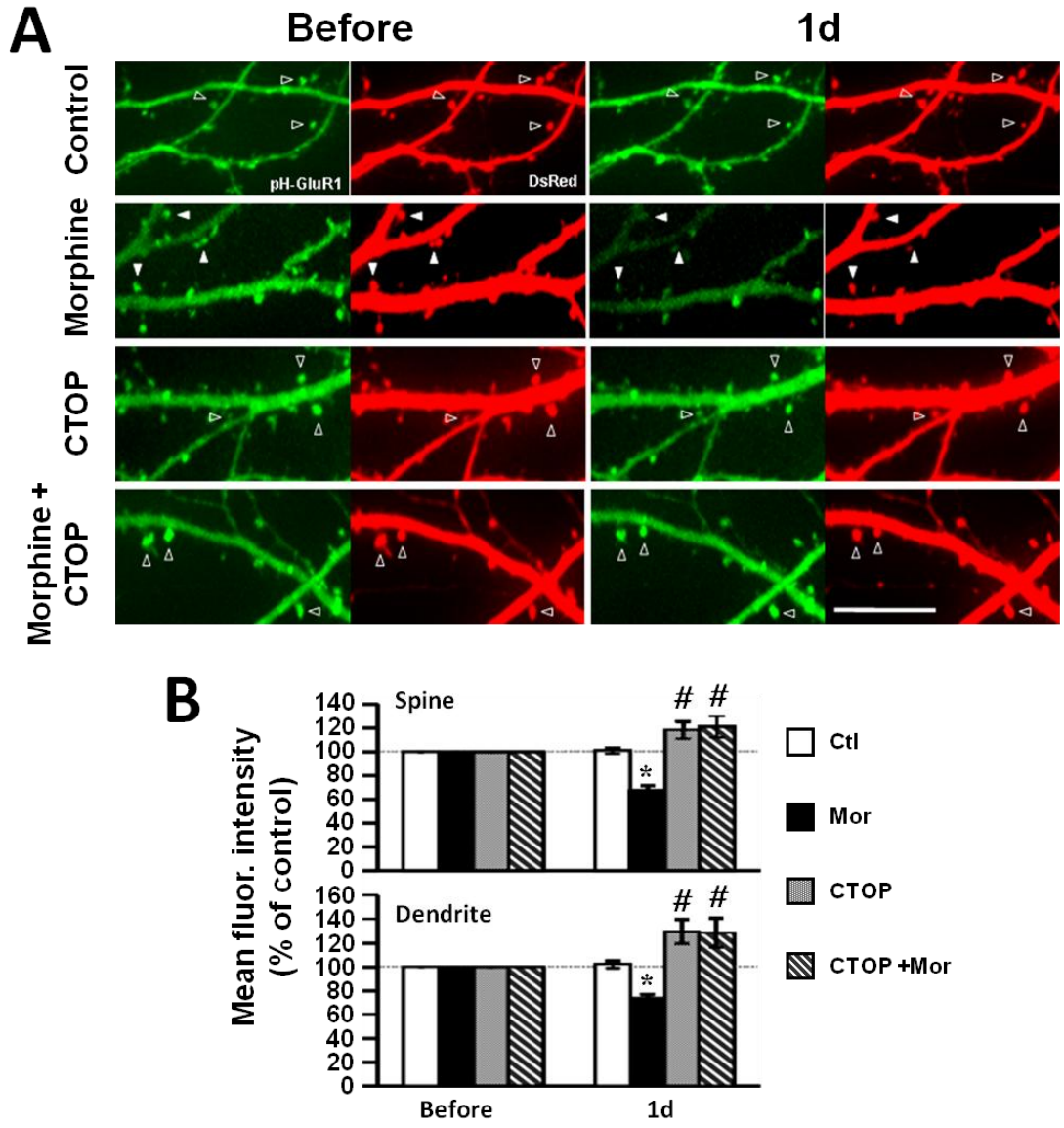

Figure 3.9. Morphine decreased surface-expressed GluR1 through μ-opioid receptors.
A, Hippocampal cultures were co-transfected with plasmids encoding pHluorin-GluR1 and DsRed. Time-lapse images were taken before and after treatment with no drug (control; Ctl) or morphine (Mor) (10 μM) in the absence or presence of CTOP (a μ-opioid receptor antagonist; 10 μM). Solid arrowheads denote that morphine progressively decreased the fluorescence intensity of pHluorin-GluR1 and the density of DsRed-labeled dendritic spines. **B**, A bar graph demonstrates mean pHluorin-GluR1 fluorescence from dendritic spines and shafts. Scale bar represents 10 μm. Values normalized to data before treatments are shown. * denotes a significant decrease comparing with the value before treatment, while # represents a significant increase ($p < 0.05$). Error bars represent ± SEM. For each condition, at least five dendrites of single neuron were analyzed (n=12).

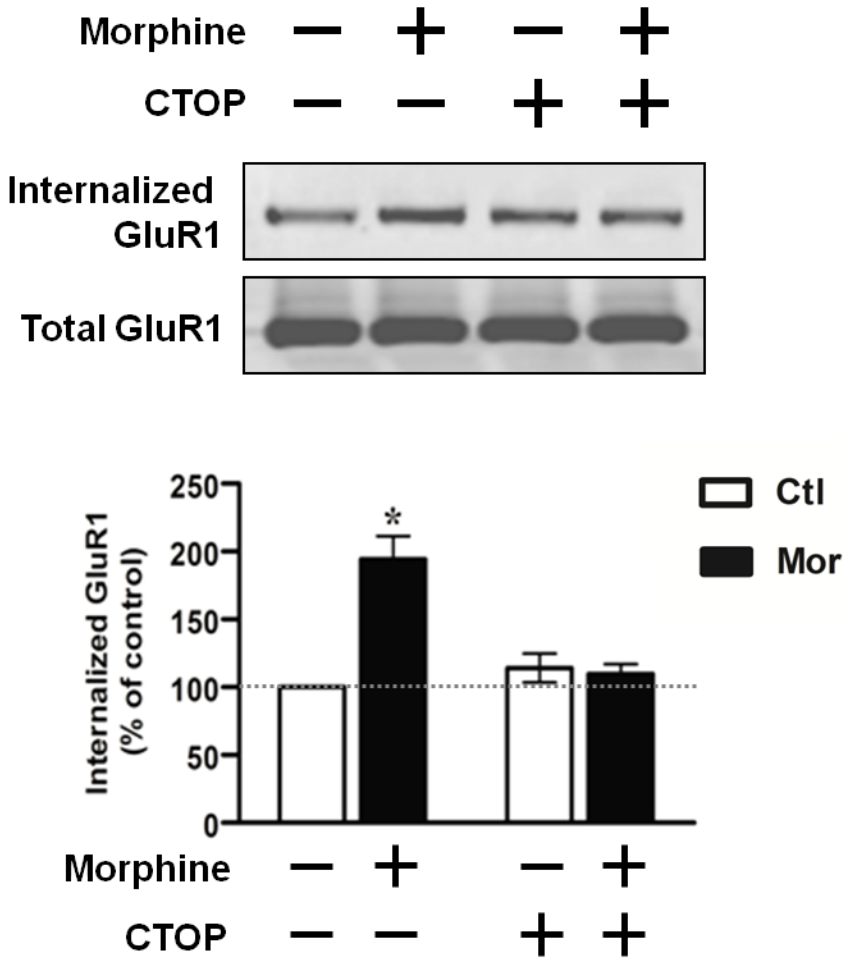

Figure 3.10. Surface biotinylation assay shows the requirement of μ-opioid receptors for morphine-induced GluR1 internalization.

Surface biotinylated hippocampal neurons were treated with no drug, 10 μM morphine, 10 μM CTOP or morphine with CTOP for 24 h. *Upper immunoblot*, internalized GluR1 subunits were isolated by using streptavidin precipitation. *Lower immunoblot*, total GluR1 subunits from whole cell lysates were loaded for comparison. A graph indicates the amount of internalized GluR1 subunits was normalized to the untreated control (n = 3). * $p < 0.05$, comparing with the untreated control. Error bars represent ± SEM.

shown in **Figure 3.11A**, hippocampal neurons expressing pHluorin-GluR1 and DsRed were imaged before and 1 day after the addition of 10 μM morphine, 1 μM TTX, TTX with morphine, or no drug (control). TTX was applied into cultured neurons 1 h before addition of morphine and was present during the course of experiment. Although incubation with TTX alone did not change fluorescence intensity of pHluorin-GluR1 from the entire images, the fluorescence intensity was significantly elevated at dendritic spines and diminished at dendritic shafts (entire, 107±6%; spine, 117±5%; dendrite, 88±5%) (**Fig. 3.11A, B**). This suggests that TTX can cause a translocation of GluR1 subunits from dendritic shafts to dendritic spines. Despite TTX-induced redistribution of GluR1 on surface membrane, application of both TTX and morphine resulted in a significant reduction on the fluorescence of pHluorin-GluR1 at spines and dendrites (entire, 76±3%; spine, 70±4%; dendrite, 60±4%) (**Fig. 3.11A, B**). In addition, biotinylation studies demonstrated that morphine still enhanced internalization of GluR1 even in the presence of TTX (**Fig 3.11C**). These findings indicate that morphine-evoked loss of synaptic and extra-synaptic GluR1 via the receptor internalization is not caused by indirect alteration in neural activity.

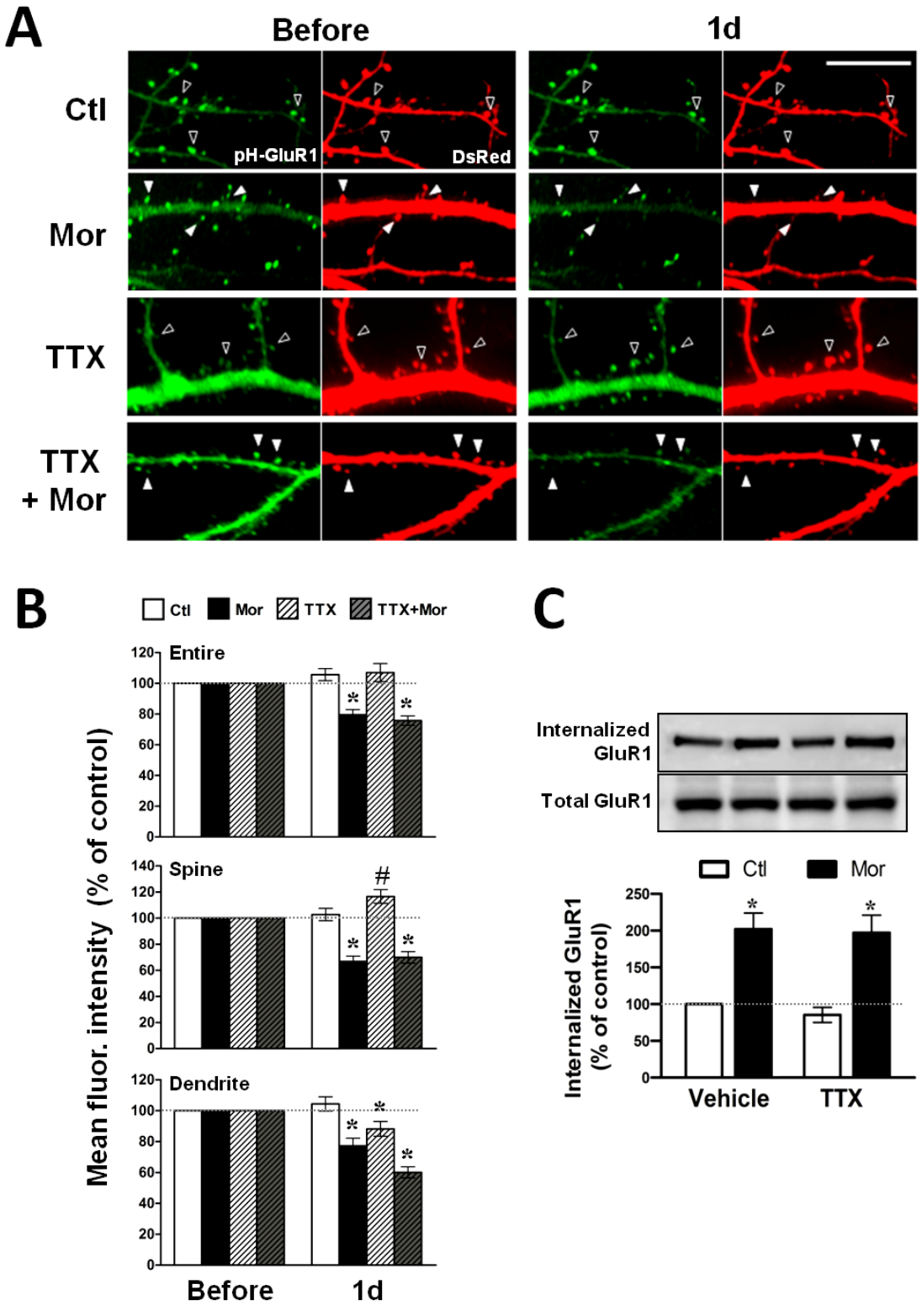

Figure 3.11. (con't)

Figure 3.11. Morphine-regulated GluR1 trafficking is not due to alterations of neural networks.

A, Time-lapse images were taken on hippocampal neurons co-expressing pHluorin-GluR1 (pH-GluR1) and DsRed before and 1 day after various treatments [untreated control (Ctl), 10 μM Morphine (Mor), 1 μM TTX, TTX with morphine]. Open arrowheads indicate that both fluorescence intensities remained constant or even increased under untreated control conditions. Solid arrowheads indicate that morphine progressively decreased the fluorescence intensity of pHluorin-GluR1 and the density of DsRed-labeled dendritic spines. Scale bar, 10 μM. **B**, Mean fluorescence intensities (fluor.) of pHluorin-GluR1 from different regions of neurons (entire images, spines and dendritic shafts) were normalized to data before treatments. *, Significant decrease comparing with the value before treatment; #, Significant increase ($p < 0.05$, $n = 15$ in each group). **C**, Surface biotinylated neurons were pre-incubated with no drug (vehicle) or 1 μM TTX for 1 h, and then were exposed to morphine (10 μM; 1 d). *Top immunoblots*, internalized GluR1 subunits were isolated by using streptavidin precipitation and detected with an anti-GluR1 antibody. *Bottom immunoblots*, total GluR1 subunits from whole-cell lysates were measured for comparison. Densitometric quantifications of Western blots on the internalized GluR1 are shown in the bottom (normalized to the control without any drug treatment; * $p< 0.05$; $n = 3$). Error bars represent ± SEM.

3.2.3 Morphine decreased phosphorylation of GluR1 at Ser^{845} and its interaction to PSD-95

AMPA receptor trafficking and synaptic plasticity can be mediated by receptor phosphorylation at cytoplasmic C termini (Malinow and Malenka, 2002). To further investigate the molecular mechanism by which morphine regulates GluR1 internalization, we hypothesized that morphine can affect the phosphorylation status of GluR1. Because activation of G_i-coupled MOR can inhibit adenylyl cyclase, decrease intracellular cAMP level and inactivate PKA (Duman et al., 1988; Ueda et al., 1988), we examined the effect of morphine on the phosphorylation status of GluR1 at Ser^{845} (S845), a substrate of PKA (Esteban et al., 2003). Cultured hippocampal neurons were incubated with 10 μM morphine in the absence or presence of 10 μM CTOP. The GluR1 complex was immunoprecipitated with an anti-GluR1 antibody followed by the western blotting detection with the phosphorylated GluR1-S845 and PSD-95 antibodies (**Fig. 3.12** and **Fig. 3.13**). The amount of GluR1 phosphorylation at S845 was significantly decreased along the duration of the morphine treatment from 3 h to 1 d, whereas the total amount of GluR1 was unchanged (**Fig. 3.12A, B**), indicating that morphine treatment either inhibited the phosphorylation of GluR1-S845 or enhanced the dephosphorylation of the receptor subunit. Meanwhile, the amount of PSD-95 in the receptor complex also gradually decreased when compared with the untreated neurons (**Fig. 3.12A, B**), suggesting the dissociation of GluR1 subunits from the PSD of dendritic spines and subsequent translocation. In contrast, co-treatment with CTOP reversed these effects (**Fig. 3.13A, B**, *right*), further confirming the important role of μ-opioid receptor in the effects of morphine. Altogether, the morphine-decreased phosphorylation of GluR1-S845 and morphine-induced dissociation from PSD-95 indicate a probable

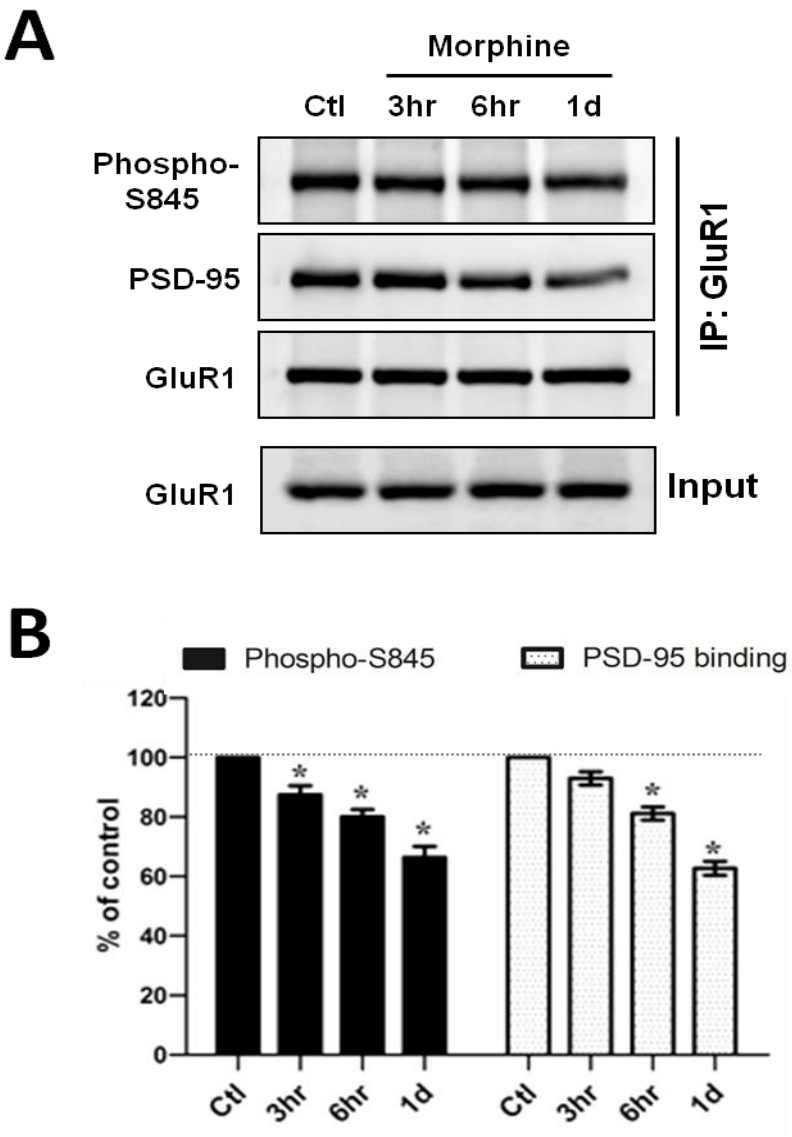

Figure 3.12. Morphine decreases the phosphorylation of GluR1 at Ser^{845} and inhibits the interaction between GluR1 and PSD-95.

A, Neurons were treated with no drug (Ctl) or 10 μM morphine for various durations (3 h, 6 h and 1 d). The cell lysates were immunoprecipitated with an anti-GluR1 antibody. The amount of phosphorylated GluR1 at Ser^{845} (Phospho-S845), PSD95, and total GluR1 subunits in the immunoprecipitation complex were detected with appropriate antibodies. Total GluR1 from whole-cell extracts (Input) was also determined. **B,** The western blots in **A** were quantified with densitometry and normalized to the untreated control (n = 5). Note that the amount of PSD95 immunoprecipitated by the anti-GluR1 antibody significantly decreases at 6 h and 1 d after addition of morphine, indicating a dissociation between the postsynaptic density and GluR1 subunits upon drug treatment. * $p < 0.05$ relative to the control. Error bars represent ± SEM.

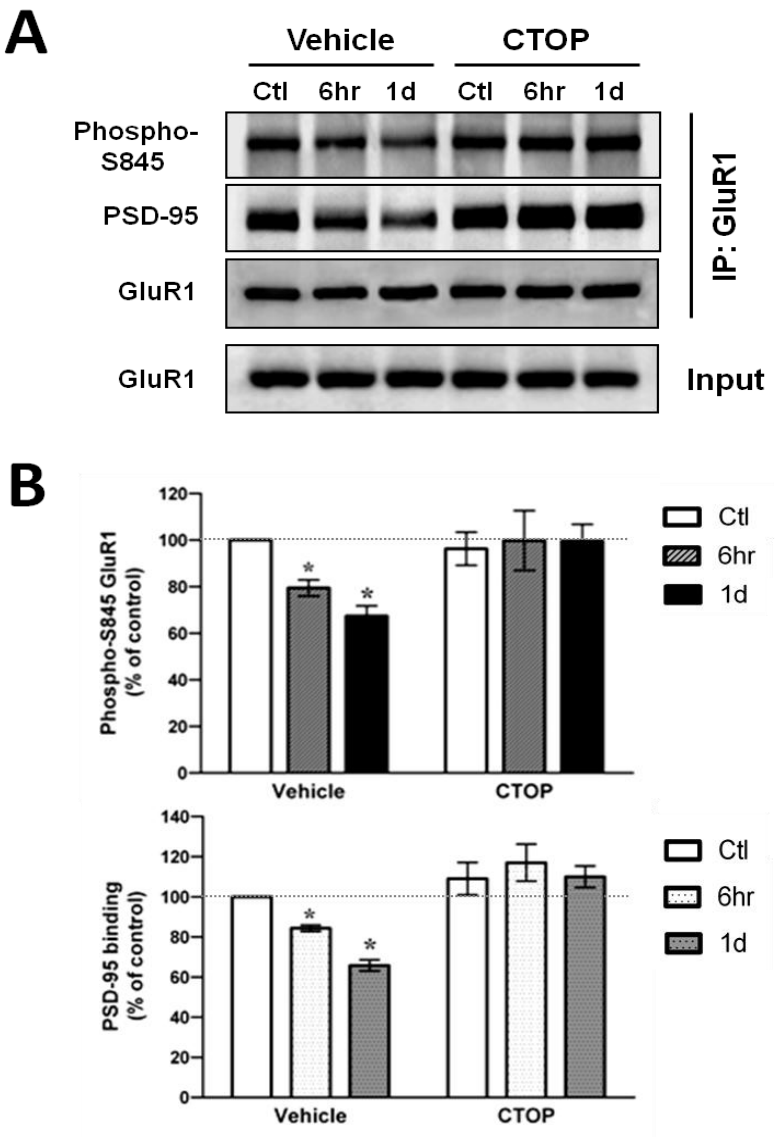

Figure 3.13. Morphine evoked GluR1-S845 dephosphorylation and PSD-95 dissociation from AMPA receptor complexes through μ-opioid receptors.

A, Neurons were treated with no drug (Ctl) or 10 μM morphine for 6 h and 1 d in the absence (vehicle) or presence of 10 μM CTOP. The cell lysates were immunoprecipitated with an anti-GluR1 antibody. The amount of GluR1-S845 phosphorylation (Phospho-S845), PSD95, and total GluR1 in the immunoprecipitation complex was detected. Total GluR1 subunits from whole cell lysates (Input) were also determined. **B,** show densitometric quantifications of western blots in **A** on the amount of phospho-S845 GluR1 and PSD-95 in the receptor complex (normalized to the untreated control; $n = 3$). * $p < 0.05$ relative to the control. Error bars represent ± SEM.

mechanism for the opioid agonist to regulate the AMPA receptor trafficking. Therefore, to detect obvious GluR1 dephosphorylation, hippocampal neurons were exposed to 10 μM morphine for 1 d in all subsequent experiments.

3.2.4 Morphine regulated GluR1 phosphorylation in a calcineurin-dependent manner

The phosphorylation status of GluR1-S845 depends on the balance between PKA and calcineurin/protein phosphatases 1 (Dell'Acqua et al., 2006). We therefore examined whether morphine-inhibited phosphorylation of GluR1-S845 was induced by suppressing the cAMP/PKA signaling pathway. Hippocampal neurons were pre-incubated with 10 μM morphine for 3 d, followed by stimulation with a PKA activator, dibutyryl-cAMP (dbcAMP) for 5 and 15 min (2 mM) (**Fig. 3.14A**). In response to dbcAMP, the phosphorylation of GluR1-S845 was significantly increased at 5 min and further elevated at 15 min, indicating that dbcAMP-induced PKA activation stimulated GluR1-S845 phosphorylation in a time-dependent manner (**Fig. 3.14**). However, pretreatment with morphine caused complete and partial inhibitions of GluR1-S845 phosphorylation induced by dbcAMP at 5 min and 15 min, respectively (**Fig. 3.14**). The complete inhibition on the effect of dbcAMP at 5 min suggests that, in the presence of morphine, the dephosphorylation exceeds the phosphorylation of GluR1 by PKA. The partial restoration by longer incubation with dbcAMP implicates that the phosphorylation of GluR1-S845 by PKA may overcome the phosphatase activity that morphine may regulate.

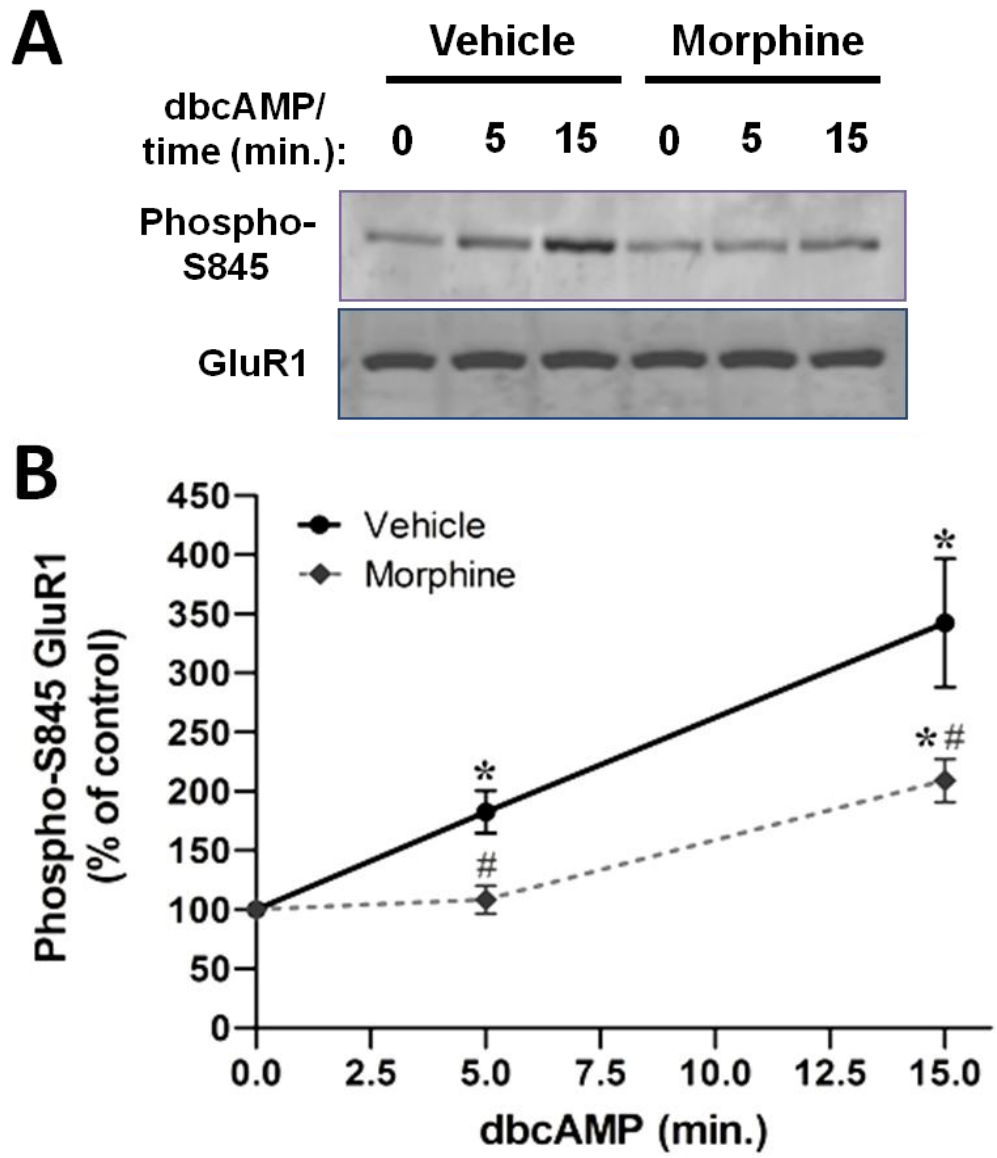

Figure 3.14. Morphine-induced PKA inhibition is not a dominant factor mediating GluR1-S845 dephosphorylation. A, Hippocampal neurons were pretreated with no drug (vehicle; left) or morphine at 10 μM (right) for 3 d, followed by stimulation with 2 mM dbcAMP for 0, 5 and 15 min. Cell lysates were immunoblotted using antibodies against phospho-GluR1-S845 (top) and GluR1 (bottom). **B,** Densitometric quantifications of Western blots in **A** on the level of phosphorylated GluR1-S845 (normalized to the controls without dbcAMP stimulation, 0 min). *, Significant increase in GluR1-S845 phosphorylation by dbcAMP. #, Significant decrease in the effect of dbcAMP by morphine pretreatment ($p < 0.05$; $n = 4$). Error bars represent ± SEM. Note that pretreatment with morphine elicits a clear but not complete reduction in the dbcAMP-induced GluR1-S845 phosphorylation.

Due to the kinetics of morphine's effect on the dbcAMP-induced GluR1-S845 phosphorylation, we hypothesized that morphine treatment might promote dephosphorylation of GluR1-S845 through the activation of phosphatases. Thus, we examined the role of calcineurin with its specific inhibitor FK506 (Lieberman and Mody, 1994). A concentration of FK506 at 1 μM was shown to have a significant inhibition on calcineurin in neuronal cells (Asai et al., 1999). **Figure 3.15**, A and B show the level of GluR1-S845 phosphorylation in untreated and morphine-treated hippocampal cultures with pretreatment of FK506 (1 μM; 45 min). Comparing with untreated control, exposure to morphine alone led to a significant decrease in GluR1-S845 phosphorylation (**Fig. 3.15A, B**, *left*). In contrast, the pretreatment with FK506 completely attenuated the effect of morphine (**Fig. 3.15A, B**, *right*), suggesting that morphine-mediated dephosphorylation of GluR1-S845 is dependent on calcineurin.

To further support this conclusion, we performed an *in vitro* phosphatase assay to determine whether morphine exposure can increase the activation of calcineurin. Hippocampal neurons were treated with 10 μM morphine for various durations before cell lysis (**Fig. 3.16**). To establish an assay condition in which the activity of calcineurin can be examined clearly, okadaic acid (100 nM), an inhibitor for phosphatase 1 and 2A, was included in all assay buffers (as described in Materials and Methods, section 2.9) (Fruman et al., 1996). As shown in **Figure 3.16**, phosphatase activity markedly increased 30 minutes after morphine application and persisted during 1 d of morphine treatment (30 min, 147 ± 11%; 1 h, 141 ± 9%; 3 h, 140 ± 5%; 6 h, 142 ± 3%; 1 d, 160 ± 14%) (**Fig. 3.16**). However, this effect of morphine was eliminated, when

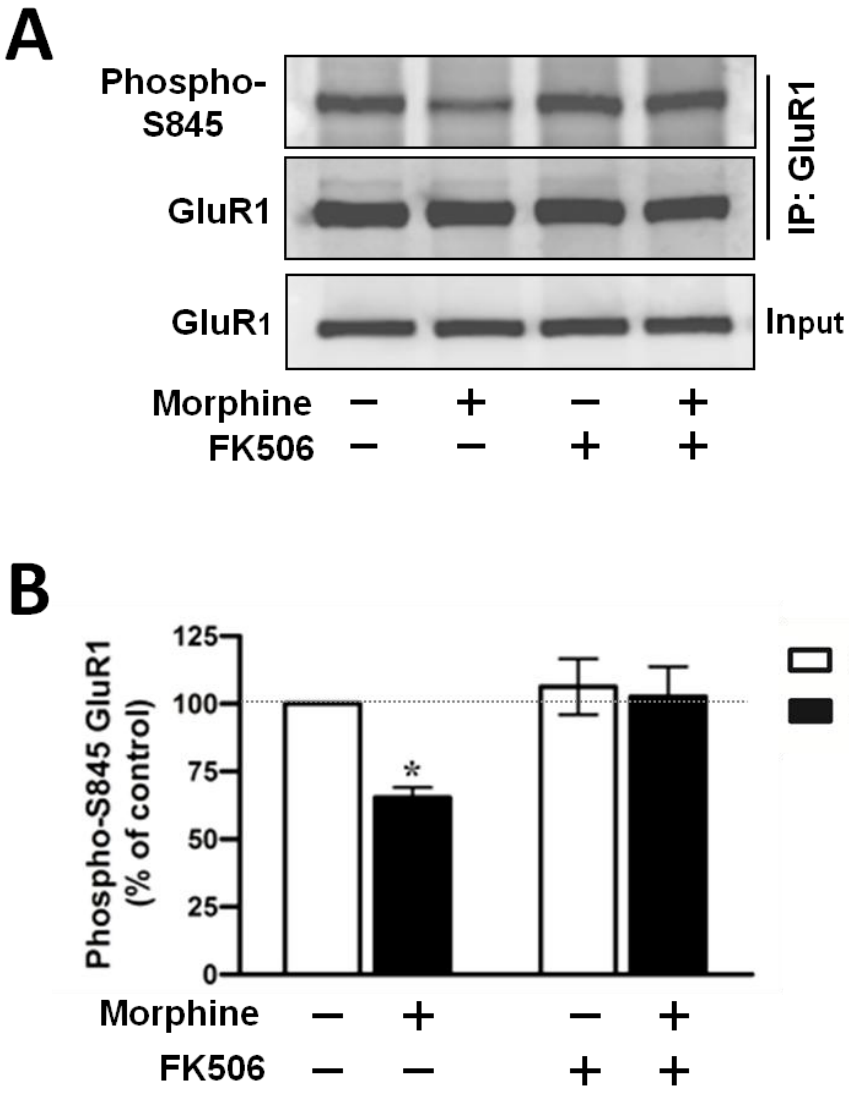

Figure 3.15. Calcineurin plays a crucial role in mediating morphine-induced GluR1-S845 dephosphorylation. **A**, A complete elimination of morphine-induced GluR1-S845 dephosphorylation by a calcineurin inhibitor FK506. Hippocampal neurons were incubated in the absence (*left*) or presence (*right*) of 1 μM FK506 for 45 min, followed by exposure to morphine (10 μM; 1 day). Cell lysates were immunoprecipiated by an anti-GluR1 antibody and the pull-down complexes were immunoblotted using antibodies against phospho-GluR1-S845 (*top*) and GluR1 (*bottom*). **B**, Densitometric quantifications of western blots in **A** on the level of phosphorylated GluR1-S845 (normalized to the control without any drug treatment). *, Significant decrease in GluR1-S845 phosphorylation upon morphine treatment ($p < 0.05$; $n = 5$). Error bars represent ± SEM.

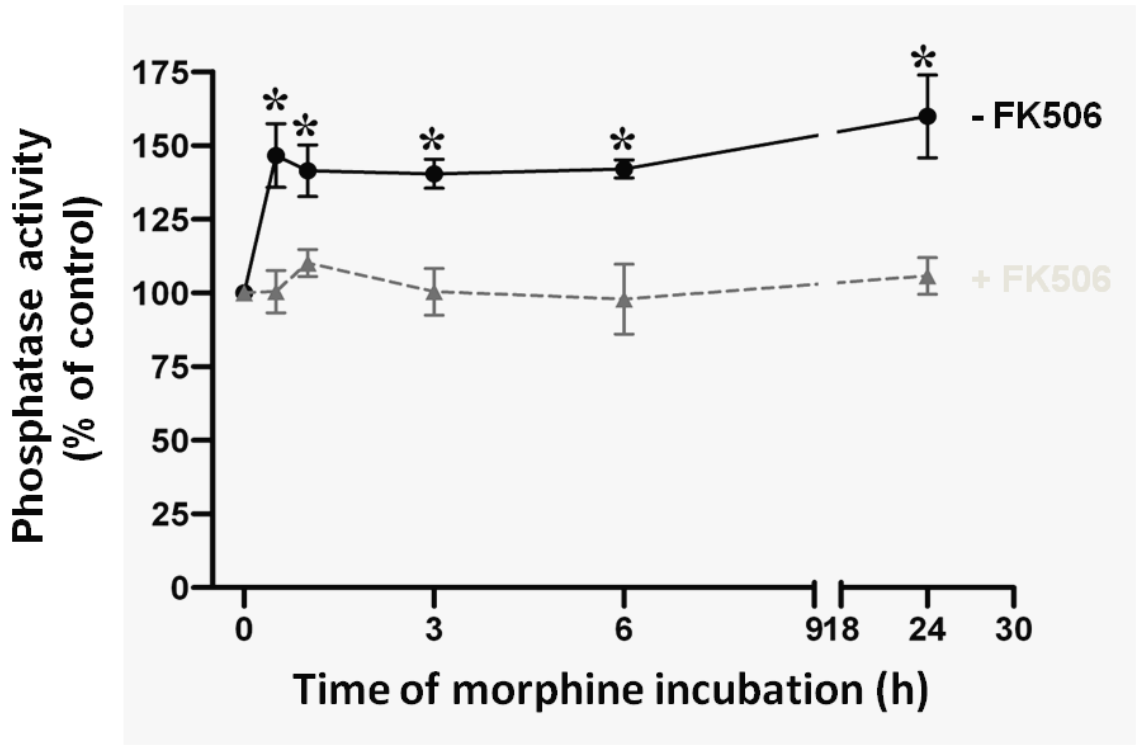

Figure 3.16. Calcineurin activity was increased after morphine application. Hippocampal neurons were treated with 10 μM morphine for various durations (0, 0.5, 1, 3, 6 and 24 h) and harvested for preparation of cell lysates. Phosphatase activity in each sample was measured in the absence (solid line) and presence (dotted line) of 1 μM FK506. The phosphatase activity was expressed as percentage of the control by dividing each value for the phosphatase activity (pmol/mg) of morphine-treated cells by that of untreated cells. Assays were performed in duplicate, and the data shown are means ± SEM from four independent experiments. *, Significant increase in phosphatase activity as compared to the control ($p < 0.05$).

FK506 (1 μM) was added to the assay buffers (30 min, 100 ± 7%; 1 h, 110 ± 5%; 3 h, 100 ± 8%; 6 h, 98 ± 12%; 1 d, 106 ± 6%) (**Fig. 3.16**), indicating that the increase in phosphatase activity due to morphine is primarily activation of calcineurin. This morphine-induced calcineurin activation was totally suppressed by co-treatment with CTOP as well (**Fig. 3.17**). Together, these results suggest that morphine acts through μ-opioid receptor to increase the activity of calcineurin, which in turn promotes dephosphorylation of GluR1-S845.

3.2.5 Morphine-induced calcineurin activation and GluR1-S845 dephosphorylation is independent of NMDA receptors

Calcineurin is a Ca^{2+}-dependent protein phosphatase (Klee et al., 1979), and has been shown to be activated by Ca^{2+} influx through NMDA receptors (Li et al., 2002). Because morphine is reported to alter protein expression and functional property of NMDA receptors *in vivo* (Inoue et al., 2003; Ma et al., 2007; Yang et al., 2000), which may change the intracellular concentration of Ca^{2+}, we evaluated the participation of NMDA receptor in morphine-regulated calcineurin activity and GluR1-S845 dephosphorylation. DL-APV (100 μM), a NMDA receptor antagonist, was applied 1 h before treatment with morphine. We found that morphine still increased calcineurin activity and decreased GluR1-S845 phosphorylation in neurons pretreated with DL-APV when compared with neurons without drug pretreatment (**Fig. 3.17** and **Fig. 3.18A**). Therefore, the contribution of NMDA receptors to the morphine's effect is excluded. In agreement with the data in **Figure 3.11**, application of TTX did not affect the morphine-induced calcineurin activation (**Fig. 3.17**) and GluR1-S845 dephosphorylation (**Fig. 3.18B**),

further verifying that the calcineurin-dependent GluR1-S845 dephosphorylation is not an indirect consequence of altered neural network by morphine.

3.2.6 Calcineurin plays an important role in morphine-regulated GluR1 trafficking

To explore the participation of calcineurin in morphine-regulated GluR1 endocytosis, surface-biotinylated hippocampal cultures were incubated with FK506 (1 μM) for 45 min prior to morphine exposure (10 μM; 1 day) (**Fig. 3.19**). Compared with the untreated control, the 2.5-fold increase of the GluR1 internalization by morphine was completely blocked in the presence of FK506 (**Fig. 3.19**), suggesting an essential role of calcineurin in morphine-induced GluR1 endocytosis. To verify the involvement of calcineurin in morphine-induced loss of surface-expressed GluR1, hippocampal neurons over-expressing pHluorin-GluR1 and DsRed were imaged before and after treatment with no drug (control), morphine, FK506 or FK506 with morphine (**Fig. 3.20**). Upon morphine treatment alone (10 μM for 1 day), the averaged fluorescence of pHluorin-GluR1 from the entire image, spines and dendrites was significantly reduced (**Fig. 3.20**), revealing the removal of synaptic and extra-synaptic GluR1. In contrast, pretreatment with FK506 (1 μM, 45 min) attenuated the morphine-induced decrease in pHluorin-GluR1 on spines and dendrites (**Fig. 3.20**). These data demonstrated that morphine regulates AMPA receptor trafficking primarily through a calcineurin-dependent pathway.

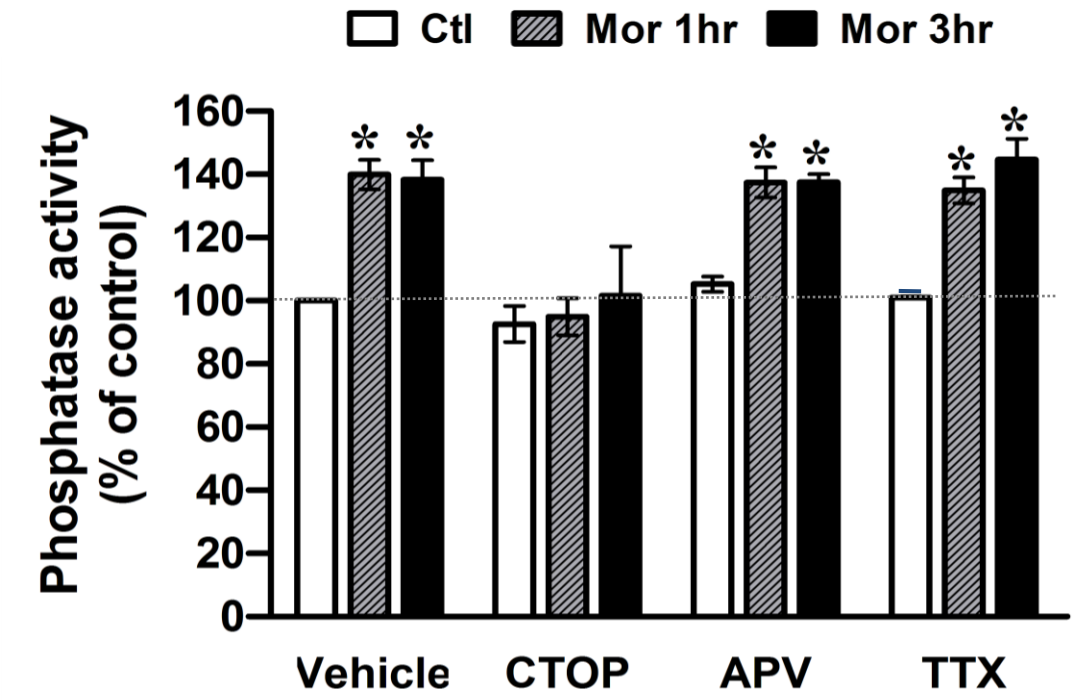

Figure 3.17. The effect of CTOP, DL-APV and Tetrodotoxin on morphine-induced calcineurin activation.

Hippocampal neurons were incubated with no drug (vehicle), CTOP (10 μM), DL-APV (100 μM) or TTX (1 μM) for 45 min, followed by exposure to 10 μM morphine for 1 and 3 h. Calcineurin activity in cell lysates was measured. Assays were performed in duplicate, and the data shown are means ± SEM from three to four independent experiments. * denotes a significant increase in phosphatase activity as compared to the control without any drug treatment ($p < 0.05$).

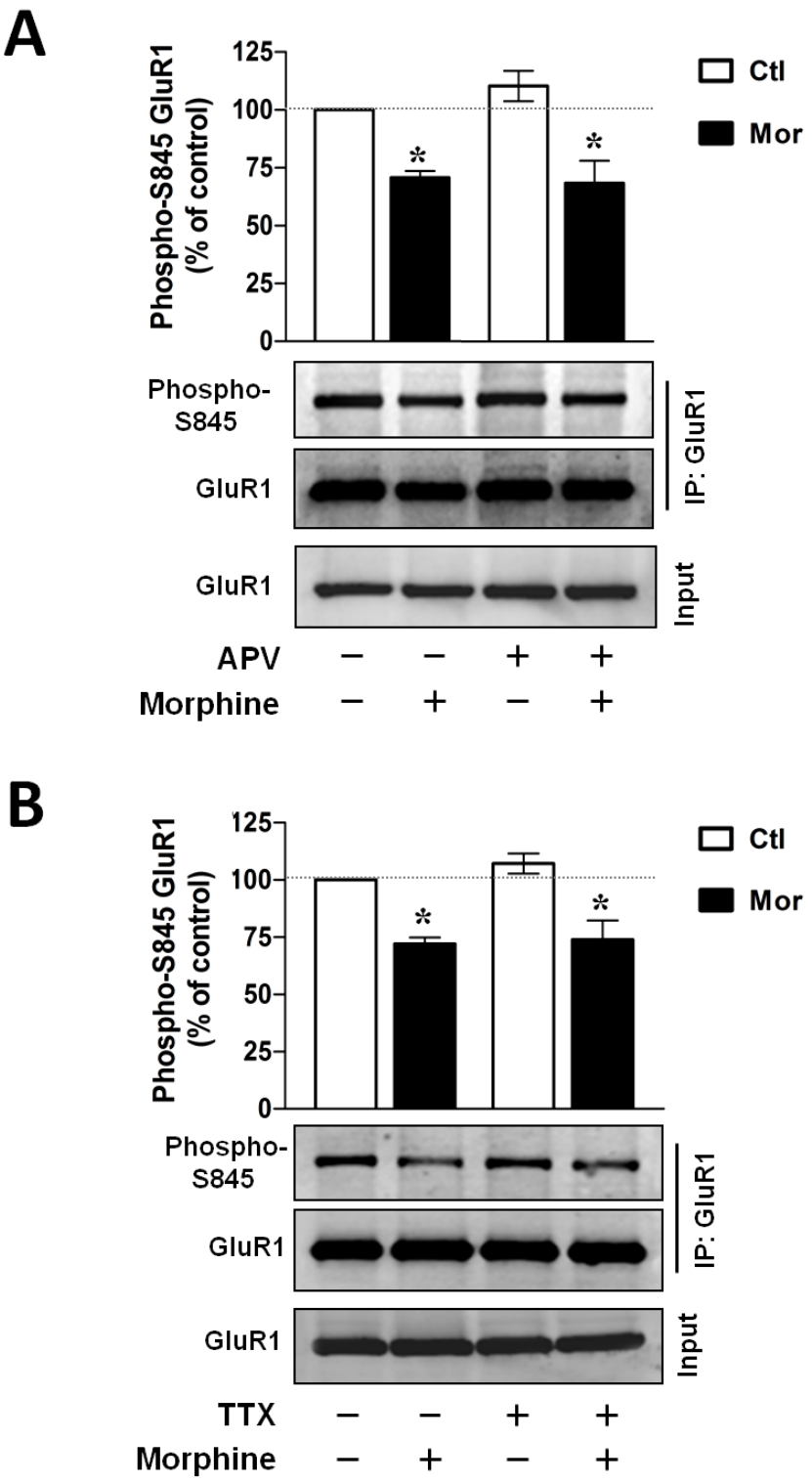

Figure 3.18. (con't)

Figure 3.18. There was no influence of DL-APV and Tetrodotoxin on morphine-induced GluR1-S845 dephosphorylation.

Hippocampal neurons were pretreated with no drug, 100 μM DL-APV (**A**) or 1 μM TTX (**B**) for 1 hour and then were exposed to morphine (10 μM) for 1 day. Cell lysates were immunoprecipiated by an anti-GluR1 antibody and the pull-down complexes were immunoblotted using antibodies against phospho-GluR1-S845 (*top*) and GluR1 (*middle*). Total GluR1 from whole cell extracts (Input) was also detected (*bottom*). Bar charts in show densitometric quantifications of western blots on the level of phosphorylated GluR1-S845 (normalized to the control without any drug treatment). * denotes a significant decrease in GluR1-S845 phosphorylation upon morphine treatment ($p < 0.05$; $n = 4$). Error bars represent ± SEM.

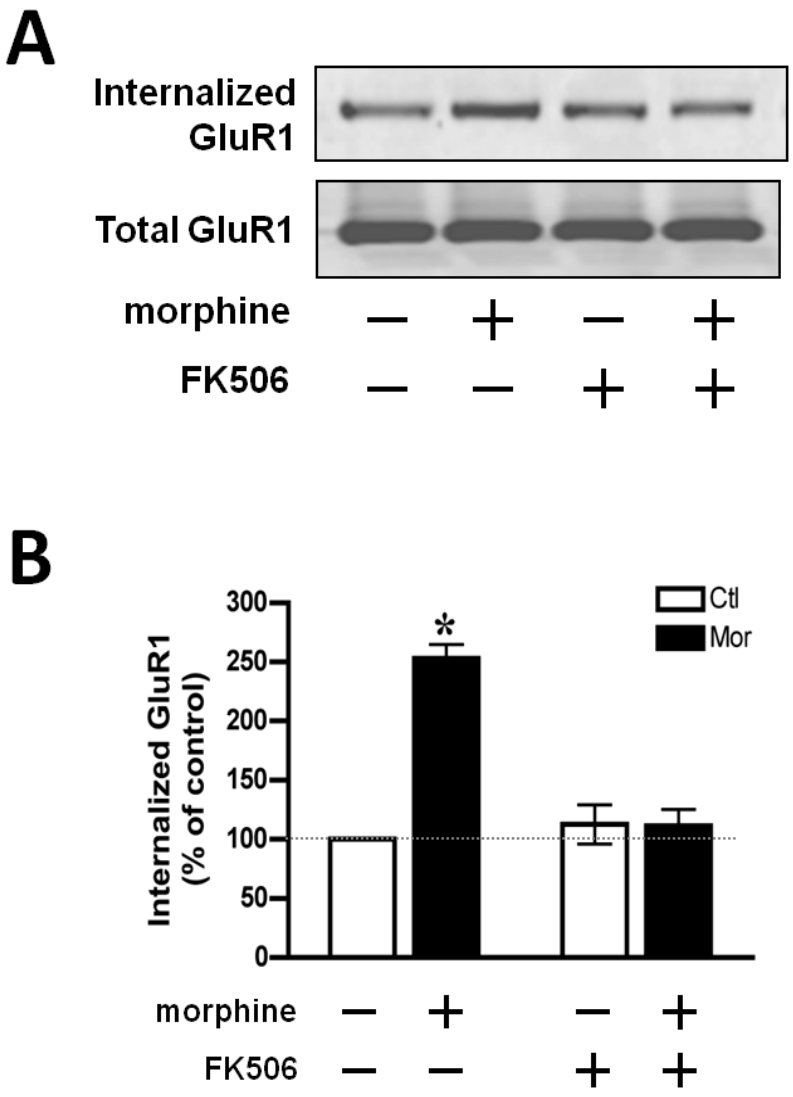

Figure 3.19. Inhibition of calcineurin blocks the morphine-regulated GluR1 internalization.

A, Surface biotinylated hippocampal neurons were incubated in the absence (*left*) or presence (*right*) of 1 μM FK506 for 45 min, followed by treatment with morphine (10 μM; 1 d). *Top*, The internalized GluR1 subunits were precipitated with immobilized streptavidin and detected with an anti-GluR1 antibody by Western blotting. *Bottom*, total GluR1 subunits from whole-cell lysates were detected for a comparison. **B,** Densitometric quantifications of Western blots in **A** on the internalized GluR1 (normalized to the control without any drug treatment; $p < 0.05$; $n = 3$). Error bars represent ± SEM.

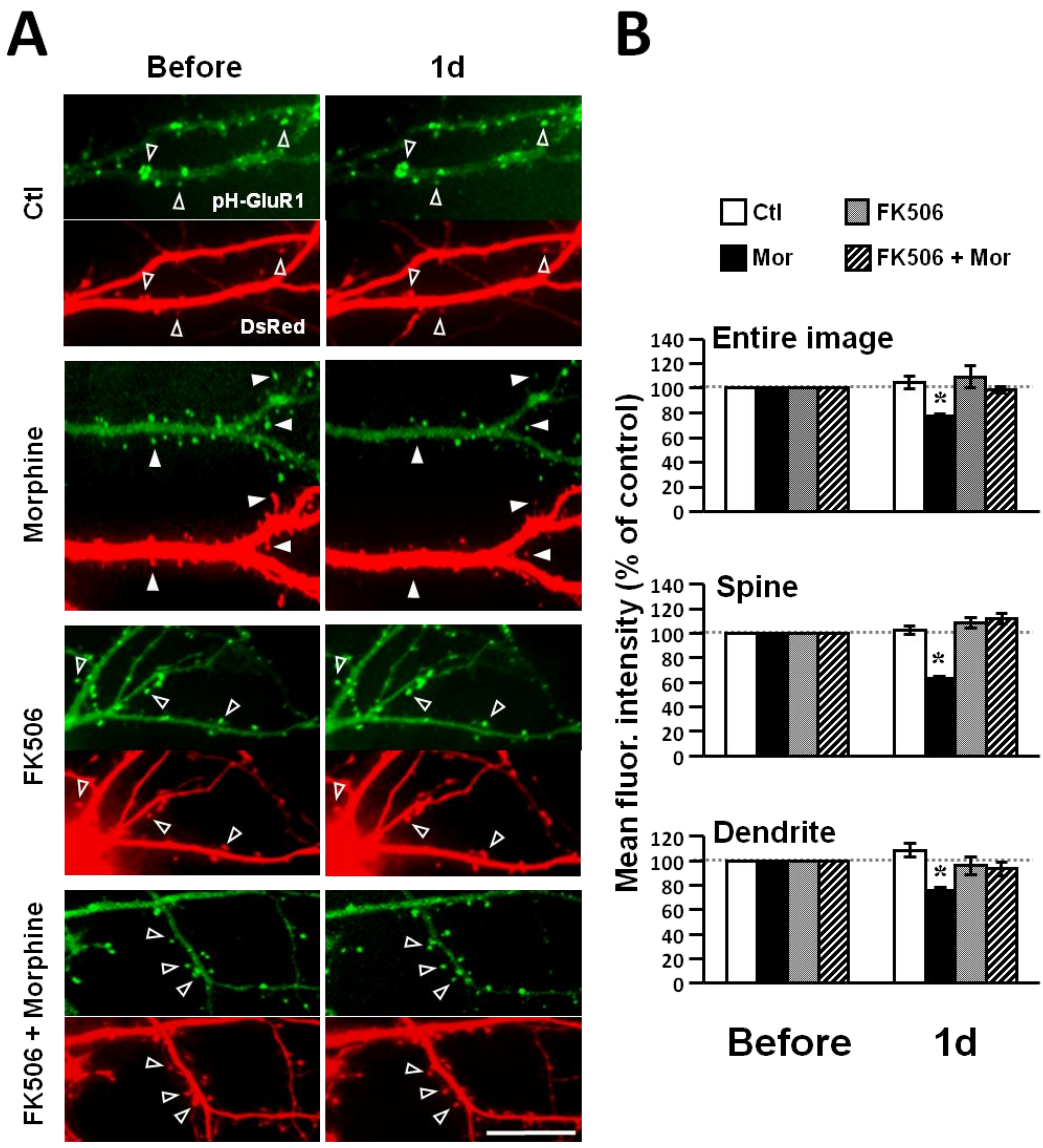

Figure 3.20. The effect of FK506 on the reduction of surface-expressed GluR1 by morphine.

A, Neurons co-expressing pHluorin-GluR1 and DsRed were imaged before (*left*) and 1 day (*right*) after treatment with no drug (Ctl), 10 μM morphine, 1 μM FK506 or FK506 with morphine. Open arrowheads denote no change in pHluorin-GluR1 fluorescence and spine morphology. Solid arrow heads denote a decrease in the pHluorin-GluR1 fluorescence and spine morphology by morphine. Scale bar, 10 μm. **B**, Mean fluorescence intensities of pHluorin-GluR1 from different regions of neurons (the entire image, spines and dendritic shafts) were normalized to data before treatments in the four groups of experiments (no drug, morphine, FK506 or FK506 with morphine). * $p < 0.05$, comparing with data before treatment. At least 5 dendrites of single neurons were analyzed (n = 15 in each group). Error bars represent ± SEM.

As mentioned in section 3.2.5, it seems that the activation of NMDA receptors is not essential for GluR1-S845 dephosphorylation by morphine (**Fig. 3.18A**). Thus, their involvement in the morphine-regulated GluR1 internalization is not expected, if dephosphorylation at Ser^{845} is associated with GluR1 internalization. To confirm this, DL-APV was applied before morphine treatment to inhibit NMDA receptors in experiments of live-cell imaging (**Fig. 3.21A, B**) and surface biotinylation (**Fig. 3.21C**). **Figure 3.21 A** and **B** shows that although DL-APV pretreatment (100 μM; 1h) slightly but not significantly facilitated redistribution of pHluorin-GluR1 from dendrites to spines, morphine still triggered a great removal of synaptic and extrasynaptic pHluorin-GluR1. Furthermore, DL-APV also had no influence on morphine-induced GluR1 endocytosis (**Fig. 3.21C**). All of these results suggest that morphine regulates GluR1 phosphorylation at Ser^{845} and trafficking in a NMDA receptor-independent manner.

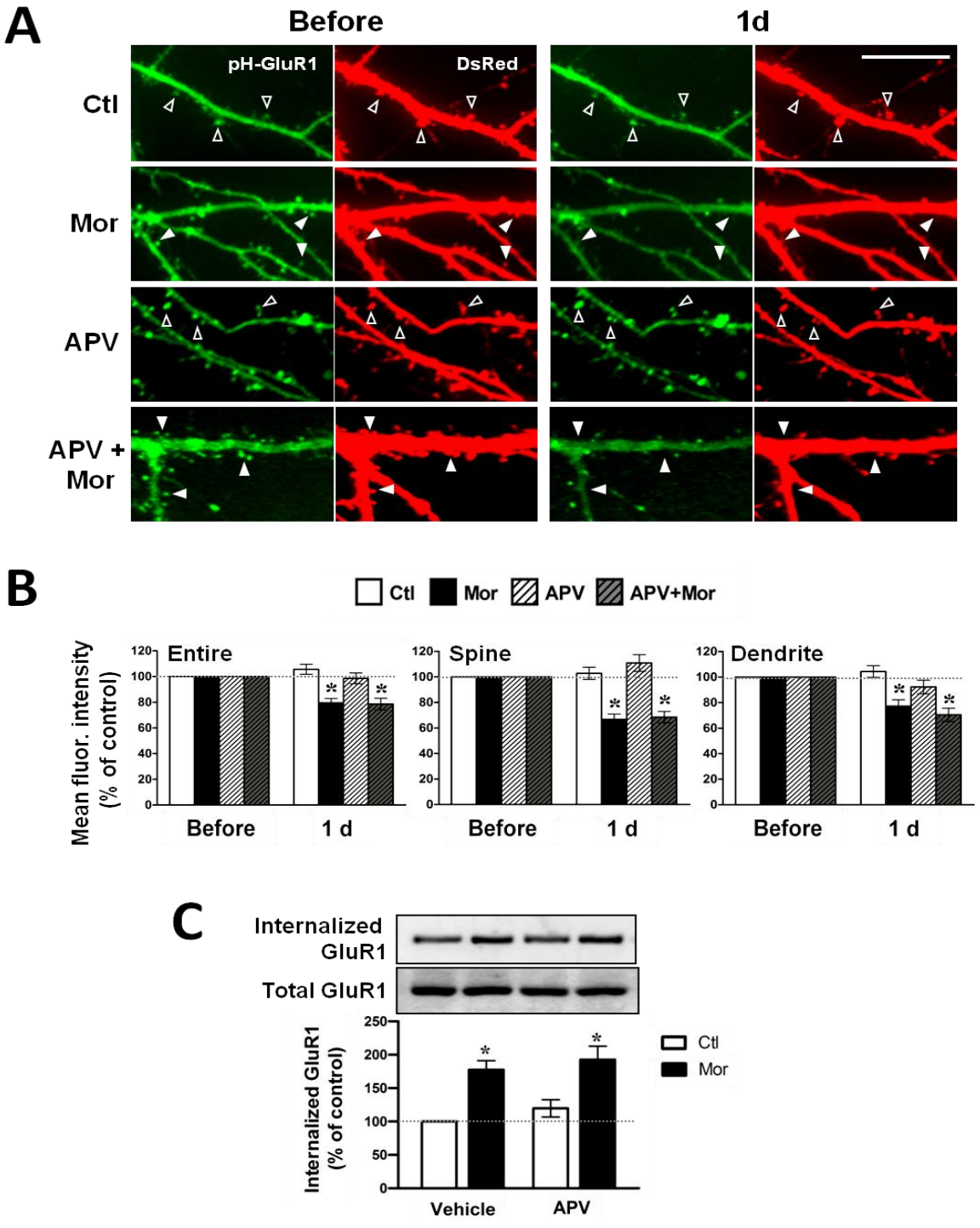

Figure 3.21. (con't)

Figure 3.21. DL-APV does not affect the morphine-regulated GluR1 trafficking.

A, Neurons co-expressing pHluorin-GluR1 and DsRed were imaged before (*left*) and 1 day (*right*) after treatment with no drug (Ctl), 10 μM morphine (Mor), 100 μM APV or APV with morphine. Open arrowheads denote no change in pHluorin-GluR1 fluorescence and spine morphology. Solid arrowheads denote a decrease in the pHluorin-GluR1 fluorescence and spine morphology by morphine. *Scale bar* , 10 μm. **B**, Averaged fluorescence of pHluorin-GluR1 from different regions of neurons (entire image, spines and dendritic shafts) were normalized to values before treatment in the four groups of experiments (no drug, morphine, APV, and APV with morphine). ***** $p < 0.05$, comparing with data before treatment. At least five dendrites of single neurons were analyzed ($n = 12$ in each group). (**C**) Surface biotinylated hippocampal neurons were pre-incubated with no drug (vehicle) or 100 μM DL-APV (*right*) for 1 h, and then exposed to morphine (10 μM; 1 day). Top immunoblot, The internalized GluR1 subunits were precipitated with streptavidin and detected with an anti-GluR1 antibody. Lower immunoblot, Total GluR1 subunits from whole-cell lysates were detected for comparison. A graph shows densitometric quantifications of western blots on the internalized GluR1 (normalized to the control without any drug treatment; * $p< 0.05$; $n = 3$). Error bars represent ± SEM.

3.2.7 Dephosphorylation of GluR1-S845 was essential for morphine-induced GluR1 internalization

To directly test the involvement of calcineurin-dependent GluR1-S845 dephosphorylation in the regulation of GluR1 trafficking by morphine, we generated a GluR1 mutant, in which the Ser^{845} residue was mutated to a negatively charged aspartic acid (S845D) to mimic continuous phosphorylation of AMPA receptors (Boehm et al., 2006). Hippocampal cultures over-expressing either GFP-GluR1 wild-type or GFP-GluR1-S845D mutant were subjected to biotinylation before morphine treatment (10 μM for 1 day) (**Fig. 3.22**). Internalized recombinant receptors (about 127 kDa) were detected by an anti-GFP antibody, and internalized endogenous GluR1 (about 100 kDa) was determined by an anti-GluR1 antibody (**Fig. 3.22A**, *top and middle immunoblots*). Equal protein amounts of both recombinant and endogenous receptors from each sample were also validated by the anti-GluR1 antibody (**Fig. 3.22A**, *bottom immunoblot*). Without drug treatment, we found a trend that the basal amount of internalized GFP-GluR1-S845D mutant was slightly less than that of internalized GFP-GluR1 wild-type, but this did not reach statistical significance (wild-type, 100%; S845D, 90±7.8%) (**Fig. 3.22B**, *left panel*). Morphine treatment enhanced internalization of GFP-GluR1 wild-type, but not the GFP-GluR1-S845D mutant (wild-type/morphine, 174±12.1%; S845D/morphine, 87±12.3%) (**Fig. 3.22A**, *top immunoblot*; **Fig. 3.22B**, *left panel*). This suggests that the dephosphorylation of GluR1-S845 is important for morphine to regulate the AMPA receptor endocytosis. The effect of morphine on endogenous GluR1 was used as a positive control, in which morphine was able to induce a significant internalization of endogenous GluR1 regardless of whether the cells were transfected with GFP-GluR1 wild-type or S845D mutant (**Fig. 3.22A**, *middle immunoblot*; **Fig. 3.22B**, *right panel*).

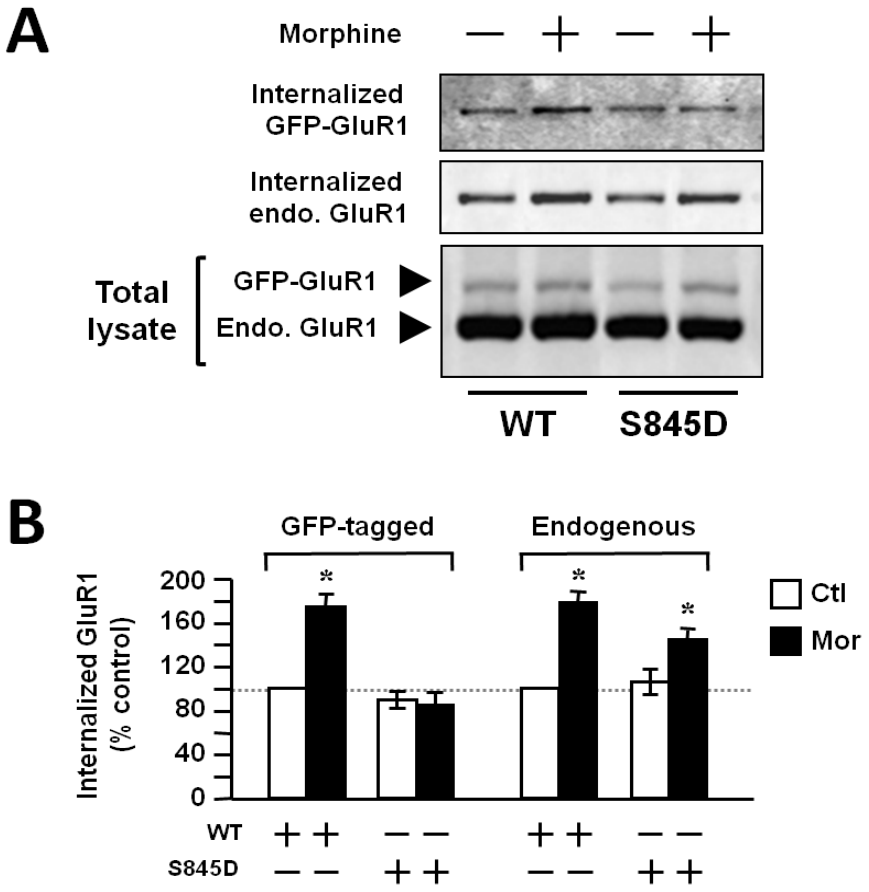

Figure 3.22. Morphine-induced GluR1 internalization requires dephosphorylation of the receptor at Ser^{845}. A, Hippocampal neurons were transfected with either GFP-GluR1 wild-type (WT; *left*) or GFP-GluR1-S845D (*right*). The transfected cells were subjected to surface biotinylation, followed by morphine treatment (10 μM for 1 day). All internalized receptors were isolated by streptavidin precipitation. *Top*, internalized exogenous GFP-GluR1 was detected with an anti-GFP antibody. *Middle*, internalized endogenous (endo.) GluR1 was detected with an anti-GluR1 antibody. *Bottom*, total protein expressions of exogenous and endogenous GluR1 subunits from whole-cell lysates were detected for comparison. In neurons expressing GFP-GluR1-WT (*left*), morphine induced internalization of both exogenous GFP-GluR1-WT and endogenous GluR1. In neurons expressing GFP-GluR1-S845D (*right*), morphine induced internalization of endogenous GluR1 but not exogenous GFP-GluR1 mutant. **B**, Quantification of western blots in **A** on the internalized receptor [normalized to the untreated control (Ctl); * $p < 0.05$; $n = 3$].

Nevertheless, in the presence of the receptor mutant, the endogenous GluR1 was internalized by morphine to a lesser extent than that in the presence of wild-type (from 178±10.2% to 144±10.3%) (**Fig. 3.22B**, *right panel*), implying that some endogenous GluR1 might form a functional receptor unit with the recombinant receptor.

To further confirm the above biochemical studies, live-cell imaging experiments were also carried out with employing both pHluorin-GluR1-S845D and pHluorin-GluR1-S845A. The pHluorin-GluR1-S845A is a phospho-blocking mutant carrying a substitution of Ser^{845} with neutral amino acid, alanine (S845A). It is expected that both mutants are unable to be further dephosphorylated (Man et al., 2007). Therefore, hippocampal neurons were co-transfected with DsRed and either pHluorin-GluR1 wild-type, pHluorin-GluR1-S845D or pHluorin-GluR1-S845A. The transfected cells subsequently were imaged before and 1 day after morphine treatment (10 μM) (**Fig. 3.23; Fig. 3.24**). No obvious morphological difference was observed among cells over-expressing wild-type and mutant receptors (**Fig. 3.23A**; **Fig. 3.24A**). This is similar to the findings of earlier studies that mimicking GluR1 phosphorylation or dephosphorylation at Ser^{845} does not significantly change surface or synaptic GluR1 levels (Kessels et al., 2009; Lee et al., 2003). In the pHluorin-GluR1 wild-type labeled cells, morphine significantly decreased the averaged green fluorescence from the entire images, spines and dendrites (**Fig. 3.23B**; **Fig. 3.24B**). In contrast, morphine did not alter the green fluorescence intensity when the cells were overexpressed with either pHluorin-GluR1-S845D or pHluorin-GluR1-S845A (**Fig. 3.23B**; **Fig. 3.24B**), demonstrating that morphine-induced AMPA receptor internalization can be blocked by both phospho-mimic S845D and S845A phospho-blocking mutants. Since both mutants can provide a constant phosphorylation status of GluR1 and they are effective in suppressing morphine-induced GluR1

trafficking, this suggests that a change in GluR1 phosphorylation by morphine is required for the regulation of receptor trafficking. It is possible that an induction of receptor dephosphorylation itself may send a downstream signal transduction to trigger or modulate AMPA receptor internalization.

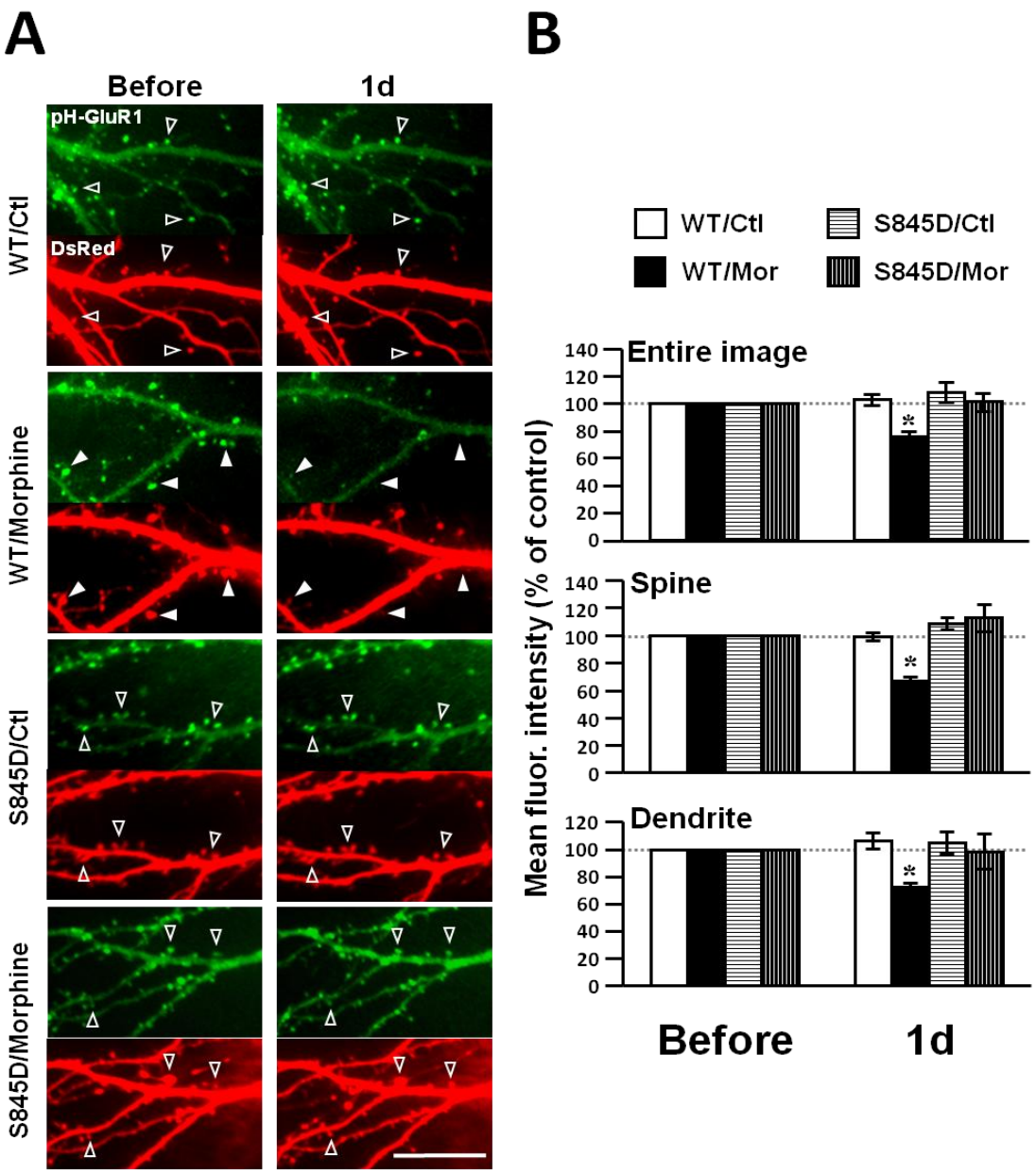

Figure 3.23. (con't)

Figure 3.23. The effect of GluR1-S845D phosphomutant on morphine-reduced surface AMPA receptors.

A, Neurons co-expressing DsRed and pHluorin-GluR1-WT (*top*) or pHluorin-GluR1-S845D (*bottom*) were imaged before (*left*) and after morphine (Mor) treatment (*right,* 10 mM for 1 day). Open arrowheads denote no change in pHluorin-GluR1 and spine morphology. Solid arrowheads denote loss of surface pHluorin-GluR1 (green fluorescence) and shrinkage of spines (DsRed fluorescence) by morphine. *Scale bar*, 10 mm. **B**, Averaged fluorescence (fluor.) of pHluorin-GluR1 from different regions of neurons (entire image, spines and dendritic shafts) were normalized to values before treatment in the four groups of experiments (WT/Ctl, overexpression of pHluorin-GluR1 WT with no drug; WT/Mor, pHluorin-GluR1 WT with morphine; S845D/Ctl, pHluorin-GluR1-S845D with no drug; S845D/Mor, pHluorin-GluR1-S845D with morphine). * $p < 0.05$, compared with data before treatment. At least 5 dendrites of single neurons were analyzed (n = 13 in each group). Error bars represent ± SEM.

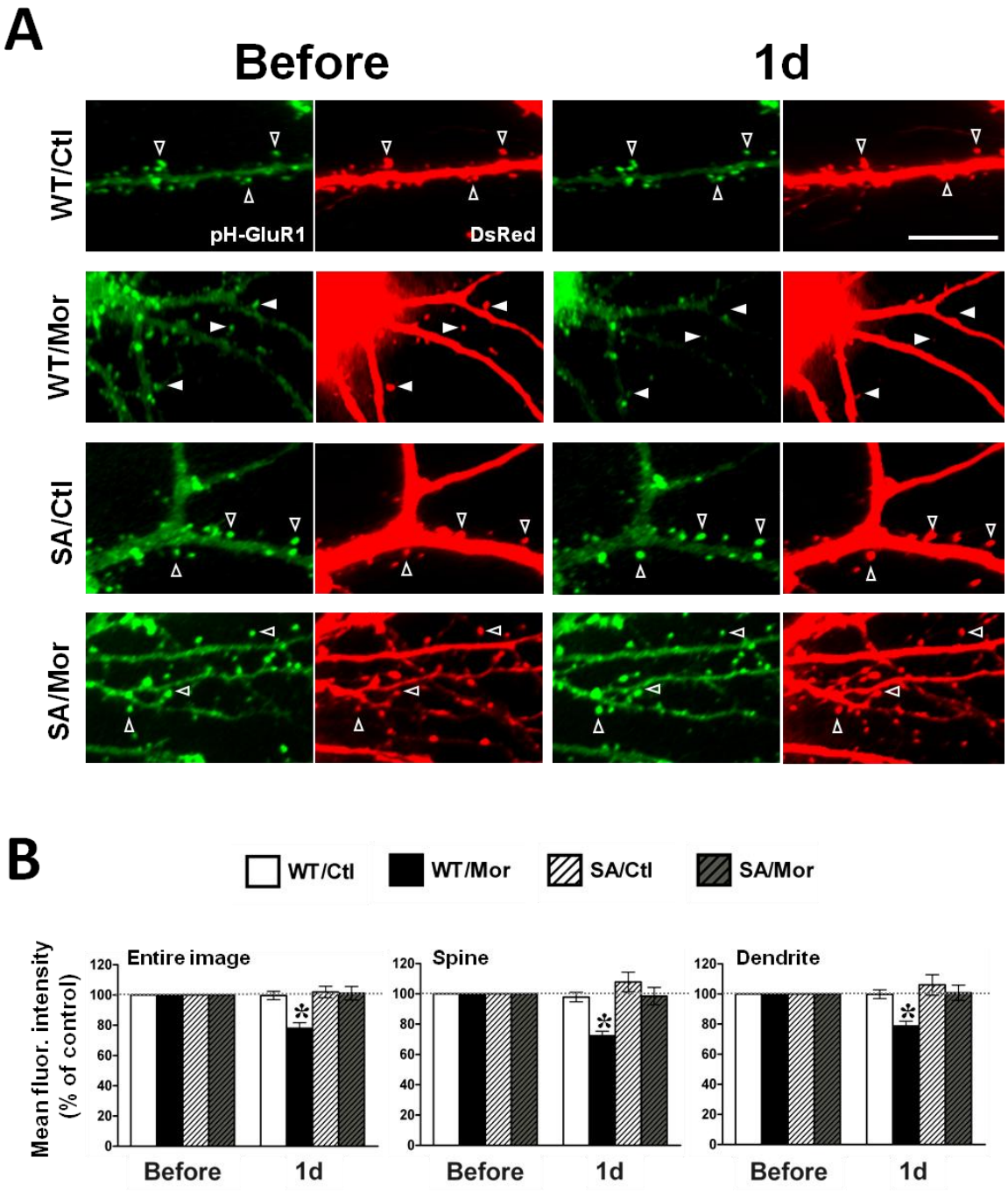

Figure 3.24. (con't)

Figure 3.24. Overexpression of pHluorin-GluR1-S845A mutant blocked the morphine-regulated AMPA receptor internalization. **A**, Neurons coexpressing DsRed and pHluorin-GluR1-WT (*top*) or pHluorin-GluR1-S845A (*bottom*) were imaged before (*left*) and after (*right*) morphine treatment (10 μM for 1 day). Open arrowheads denote no change in pHluorin-GluR1 and spine morphology. Solid arrowheads denote loss of surface pHluorin-GluR1 (green fluorescence) and shrinkage of spines (DsRed fluorescence) by morphine. *Scale bar*, 10 μm. **B**, Averaged fluorescence of pHluorin-GluR1 from different regions of neurons (entire image, spines and dendritic shafts) were normalized to values before treatment in the four groups of experiments (WT/Ctl, overexpression of pHluorin-GluR1-WT with no drug; WT/Mor, pHluorin-GluR1-WT with morphine; S845A/Ctl, pHluorin-GluR1-S845A with no drug; S845A/Mor, pHluorin-GluR1-S845A with morphine). ***** $p < 0.05$, comparing with data before treatment. At least five dendrites of single neurons were analyzed ($n = 10$ in each group). Error bars represent ± SEM.

3.3 Investigation of a functional role of GluR1 trafficking in morphine-induced addictive behaviors

Dynamic AMPA receptor trafficking contributes to synaptic plasticity including LTP and LTD, which in turn serve as a cellular model of learning and memory. Given that drug addiction occurs as a function of experience, its pathological form is closely related to these cognitive functions (Nestler, 2002; Kelley 2004). For example, a memory of drug experience is triggered when abusers are exposed to the environmental context previously associated with the drug availability. This context-dependent memory still exists even after long period of abstinence and is believed to motivate drug craving or drug-seeking behaviors, thereby increasing the risk of relapse (O'Brien et al., 1992; Childress et al., 1999; Hyman, 2005). In the last part of this study, we sought to investigate the functional role of the morphine-mediated GluR1 phosphorylation and endocytosis in the behavioral manifestation of opiate addiction, particularly the drug-induced contextual learning and memory. To do that, a line of homozygous mutant mouse in which the Ser^{845} on the GluR1 subunit is mutated to Ala (S845A) (Lee et al., 2010) was employed in a behavioral test for context preference, called conditioned place preference (CPP).

3.3.1 Morphine-regulated GluR1 phosphorylation and internalization was abolished in GluR1-S845A mutant mice

To determine the effect of morphine on the AMPA receptor trafficking in homozygous GluR1-S845A mutant mouse, internalization of AMPA receptors were

measured by the surface biotinylation assay in cultured hippocampal neurons from the wild-type (WT) and the mutant mice. The surface proteins in live cells were biotinylated before treatment with 3 μM or 10 μM morphine for 1 day (**Fig. 3.25**). In WT neurons, either 3 μM or 10 μM morphine for 1 d induced a significant increase in GluR1 endocytosis compared to control neurons without any drug treatment (**Fig. 3.25**). In contrast, morphine exposure had no influence on the receptor endocytosis in GluR1-S845A homozygous mutant neurons (**Fig. 3.25**). Moreover, phosphorylation of GluR1 at Ser^{845} and total amount of GluR1 from the whole-cell lysates were detected as well (**Fig. 3.25A**). Consistent with the above results obtained from rat hippocampal neurons (**Fig. 3.12**), dephosphorylation of GluR1 at Ser^{845} by morphine (3 μM and 10 μM for 1 d) was also observed in mouse WT cultures (**Fig. 3.25A**). As Ala residue was to substitute Ser^{845} on the GluR1 in mutant neurons, no protein signal could be detected with the antibody against phospho-GluR1-S845 by Western blotting (**Fig. 3.25A**). Altogether, these results confirm that the morphine's effects on GluR1 phosphorylation and endocytosis are attenuated in the GluR1-S845A homozygous mutant mice.

3.3.2 A decreased sensitivity to morphine-induced conditioned place preference in GluR1-S845A mutant mice

CPP paradigm involves pairing the effect of drugs with certain environmental cues provided by an experimental apparatus. CPP test hence measures the rewarding property of the drugs by assessing the acquisition of animals' preference for the drug-associated cues. The experimental apparatus comprises two main compartments and each of them gives different visual and tactile cues (**Fig. 2.1** in section 2.10.2, Material

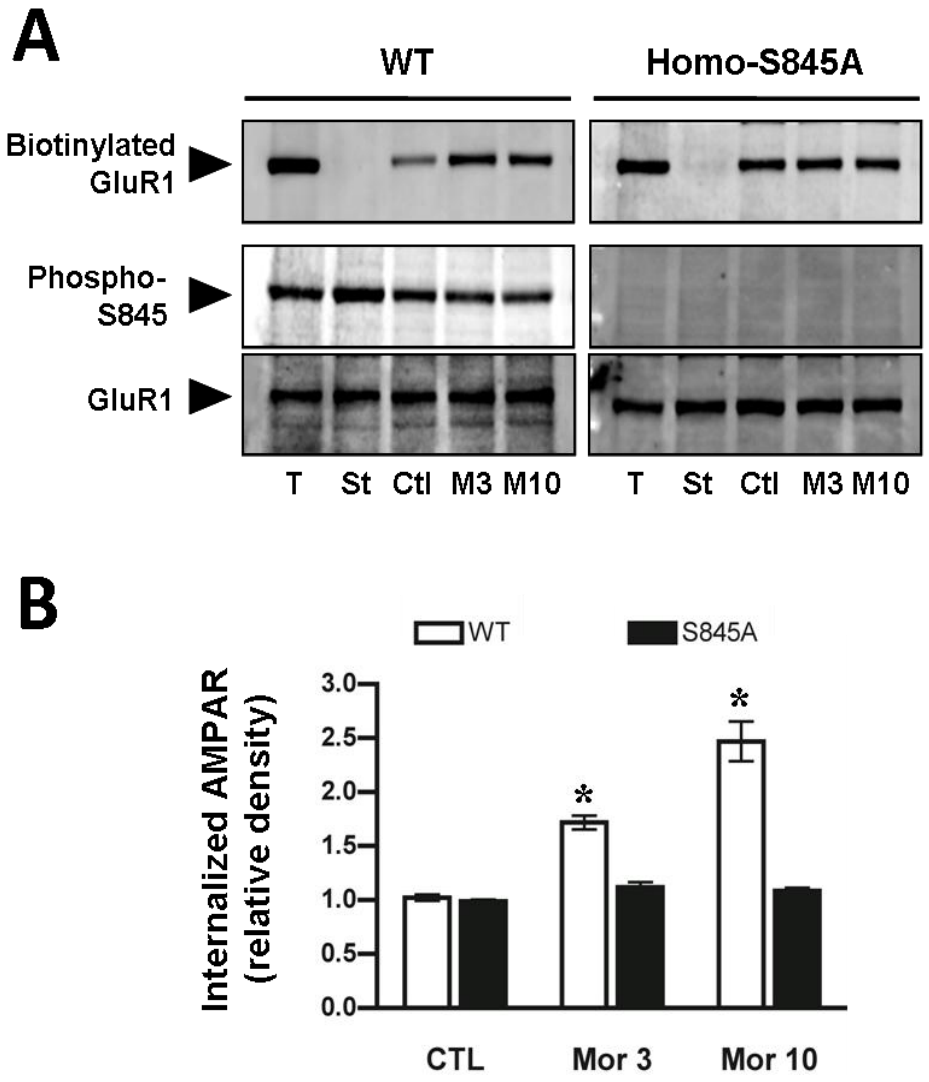

Figure 3.25. The effects of morphine on GluR1 phosphorylation and internalization were abolished in GluR1-S845A hippocampal cultures.

A, Dissociated hippocampal cultures were prepared from wild type mice (WT; left) or homozygous transgenic mice carrying GluR1-S845A mutation (Homo-S845A; right). Surface proteins were biotinylated before incubation of no drug media (control, Ctl) or 3 μM (M3) or 10 μM (M10) morphine for 1 day at 37°C to initiate receptor internalization. The residual biotin on surface proteins was stripped by glutathione. Cells were then lysed and the internalized receptors were isolated by streptavidin beads. Total biotinylated GluR1 on cell surface was detected in cells that held on ice without stripping incubation (T). Also, glutatione-stripped cells kept on ice was used to verify the efficiency of stripping process (St). The immunoblot (top row) shows total labeled surface GluR1 (T), strip control (St), and internalized GluR1 after no drug or morphine treatment. The phosphorylation of GluR1 at Ser^{845} and total GluR1 from whole cell extracts was also determined (bottom two rows of immunoblots). **B**, The immunoblots were quantified with densitometry and normalized to the untreated control (n = 4). * p < 0.05, comparing with the untreated control. Error bars represent ± SEM.

and Methods). **Figure 3.26A** shows timeline of the CPP experiment. During the training period, each of the mice would be given two 40-min conditioning sessions per day (at least 4h apart). In the first session, all mice were injected with saline subcutaneously (s.c.) and confined in the specified compartments. In the second session on the same day, one-half of them received morphine and the other half had saline, and they were placed in the other compartments. One day after conditioning period, the animals were tested in a drug-free state and were allowed with free access to the whole apparatus for 15 min. The amount of time the animals spending in the compartment paired with morphine serves as a measure of preference acquisition. First, we investigated the CPP responses of WT and GluR1-S845A mutant mice, which were conditioned with morphine at 5 mg/kg, 10 mg/kg or saline (s.c.) for two consecutive days (**Fig. 3.26B**). By comparing with the saline-injected control, both WT and GluR1-S845A mutant mice acquired a comparable CPP upon treatment of morphine at 5 mg/kg (CPP scores: WT, 109 $\pm$ 49 s; S845A, 109 $\pm$ 36 s; $P > 0.05$; n = 8) (**Fig. 3.26B**). Nevertheless, the injection of a higher dose of morphine (i.e. 10 mg/kg) for two days of conditioning caused a further increase of CPP only in the WT animals, but not in the mutant animals. The effect of the higher dose of morphine was significantly greater in the WT than that of GluR1-S845A mutants (WT, 197 $\pm$ 17 s; S845A, 121 $\pm$ 22 s; $P < 0.01$; n = 20) (**Fig. 3.26B**), suggesting a different sensitivity to morphine-induced CPP between genotypes. These results were further confirmed by using four consecutive days of morphine conditioning (**Fig. 3.26C**). After four days of conditioning in WT mice, 5 mg/kg morphine treatment was sufficient to induce CPP acquisition compared to that induced by 10 mg/kg morphine. However, 5 mg/kg morphine-induced CPP expression in GluR1-S845A mutants was significantly lower than that of the WT mice (S845A, 125 $\pm$ 24 s; WT, 202 $\pm$

20 s; $P < 0.05$; n = 15), although CPP responses to 10 mg/kg morphine in the mutant and WT mice were not significantly different (S845A, 200 ± 19 s; WT, 208 ± 22 s; $P > 0.05$; n = 12) (**Fig. 3.26C**). Therefore, GluR1-S845A mice exhibited a reduced sensitivity to CPP at a lower dose of morphine or shorter duration of morphine conditioning.

The decreased response to morphine CPP in GluR1-S845A mutants may be a result of their abnormal locomotor activity or deficit in contextual learning. We therefore compared locomotor activity between genotypes during the CPP training (section 2.10.2, Materials and Methods). Their locomotor activities are shown in **Figure 3.27.** by mean total distance they travelled (in 40 min) and their velocity of movement. Statistical analysis indicated that saline-injected WT and GluR1-S845A mutants did not significantly differ in locomotion activity (WT/distance, 30 ± 1.5 m; S845A/distance, 34 ± 1.6 m; $P > 0.05$) (WT/velocity, 2.5 ± 0.17 cm/s; S845A/velocity, 2.9 ± 0.17 cm/s; $P > 0.05$) (**Fig. 3.27**). Furthermore, upon administration with 10 mg/kg morphine both of them increased their distance travelled and velocity in similar magnitudes (WT/distance, 194 ± 12 m; S845A/distance, 176 ± 9.9 m; $P > 0.05$) (WT/velocity, 10 ± 0.7 cm/s; S845A/velocity, 9.3 ± 0.8 cm/s; $P > 0.05$) (**Fig. 3.27**). These results indicate that the mutation of S845A has no influence on animals' baseline and morphine-evoked locomotion. To evaluate animals' spatial learning and memory, a hippocampus-dependent task, Morris water maze, was used (Morris, 1984). In the test, rodents navigate in an open swimming tank by using visual cues to locate an escape platform, and the time taken to reach the platform (escape latency) is a measure of animals' spatial acquisition. During the first two days of training, WT and S845A mutant mice had comparable escape latencies, indicating that both genotypes started at the same level of performance to learn the location of the platform (**Fig. 3.28**). Furthermore, their escape

latencies across other successive days (Day 3 to Day 6) were decreasing at almost the same rates (**Fig. 3.28**). This similar improvement in performance between groups for searching the hidden platform suggests that the GluR1-S845A mutation did not affect regular contextual learning and memory behavior. Collectively, it appears that a decrease in morphine CPP by GluR1-S845A mutation is not related to abnormal locomotion or contextual learning deficits.

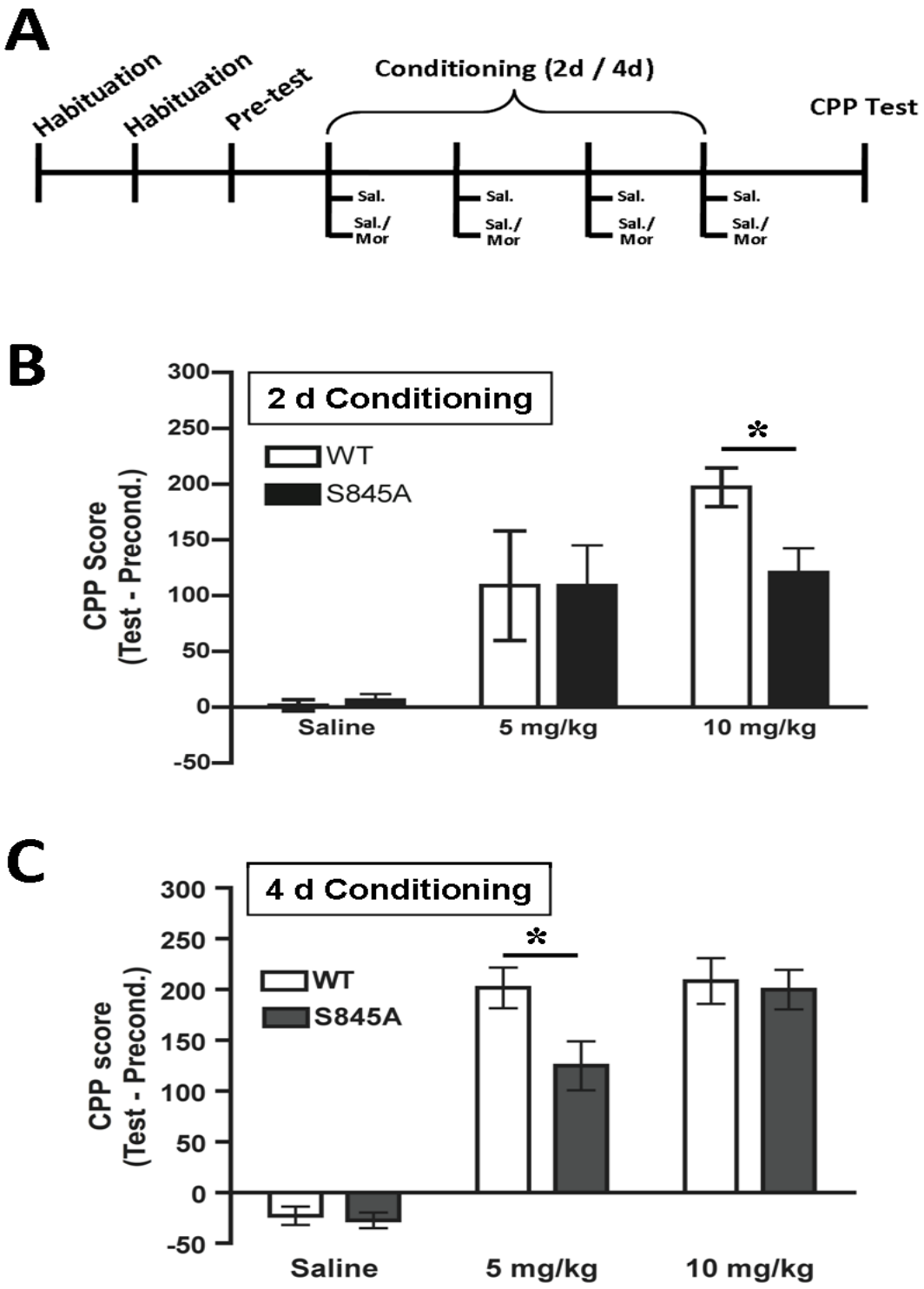
A
Habituation
Habituation
Pre-test
Conditioning (2d / 4d)
CPP Test
Sal.
Sal./ Mor
B
2 d Conditioning
WT
S845A
CPP Score (Test - Precond.)
300
250
200
150
100
50
0
-50
Saline
5 mg/kg
10 mg/kg
*
C
4 d Conditioning
WT
S845A
CPP score (Test - Precond.)
Saline
5 mg/kg
10 mg/kg
*

Fig. 3.26

Figure 3.26. A comparison of CPP acquisition between wild-type and GluR1-S845A homozygous mutant mice.

A, The experimental timeline for Conditioned Place Preference (CPP). CPP paradigm includes 4 phases: habituation, preconditioning test, saline or morphine conditioning and CPP test. It should be noted that the conditioning involves consecutive two or four days. **B** and **C,** GluR1-S845A mutation reduces the sensitivity to morphine-CPP. Wild type (WT) and GluR1-S845A mutant (S845A) mice were conditioned with either 5 mg/kg or 10 mg/kg morphine administration for consecutive two days (**B**) or four days (**C**). CPP score is calculated by subtracting the time mice spent in the morphine-paired chamber before conditioning from that after conditioning. *, Significant difference on CPP acquisition between WT and S845A mutants ($P < 0.05$). Error bars represent ± SEM.

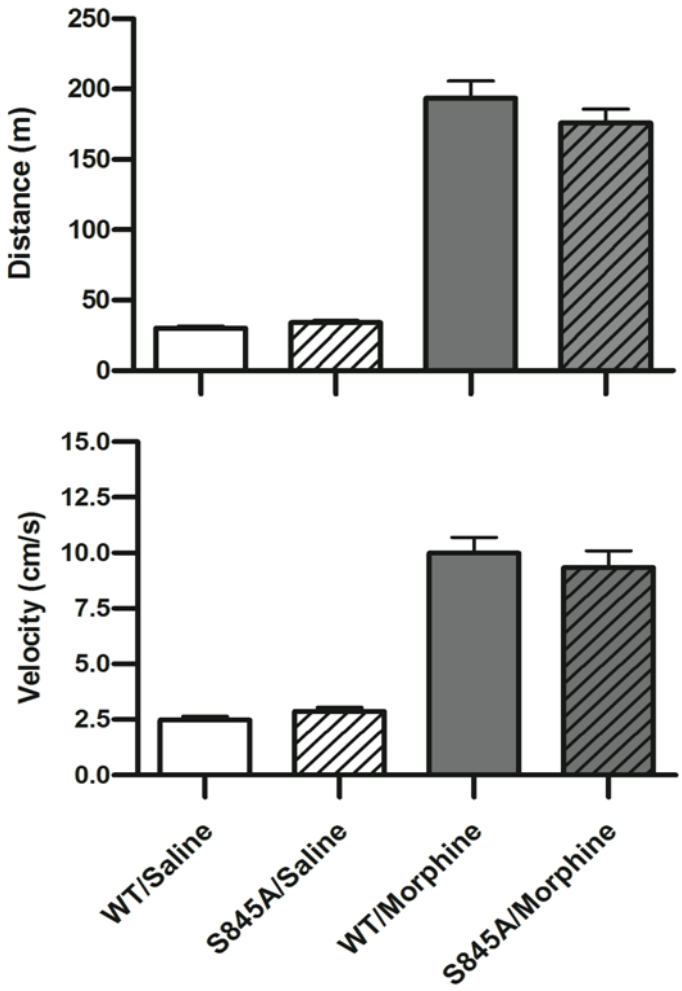

Figure 3.27. Basal and morphine-induced locomotion in wild-type and GluR1-S845A mutant mice.

Locomotor activity as measured by the mean total distance mice traveled (meter in 40 min) and velocity (centimeters per second) of their movement during CPP conditioning. All data are mean ± SEM (n = 21 in saline groups; n = 14 in morphine groups).

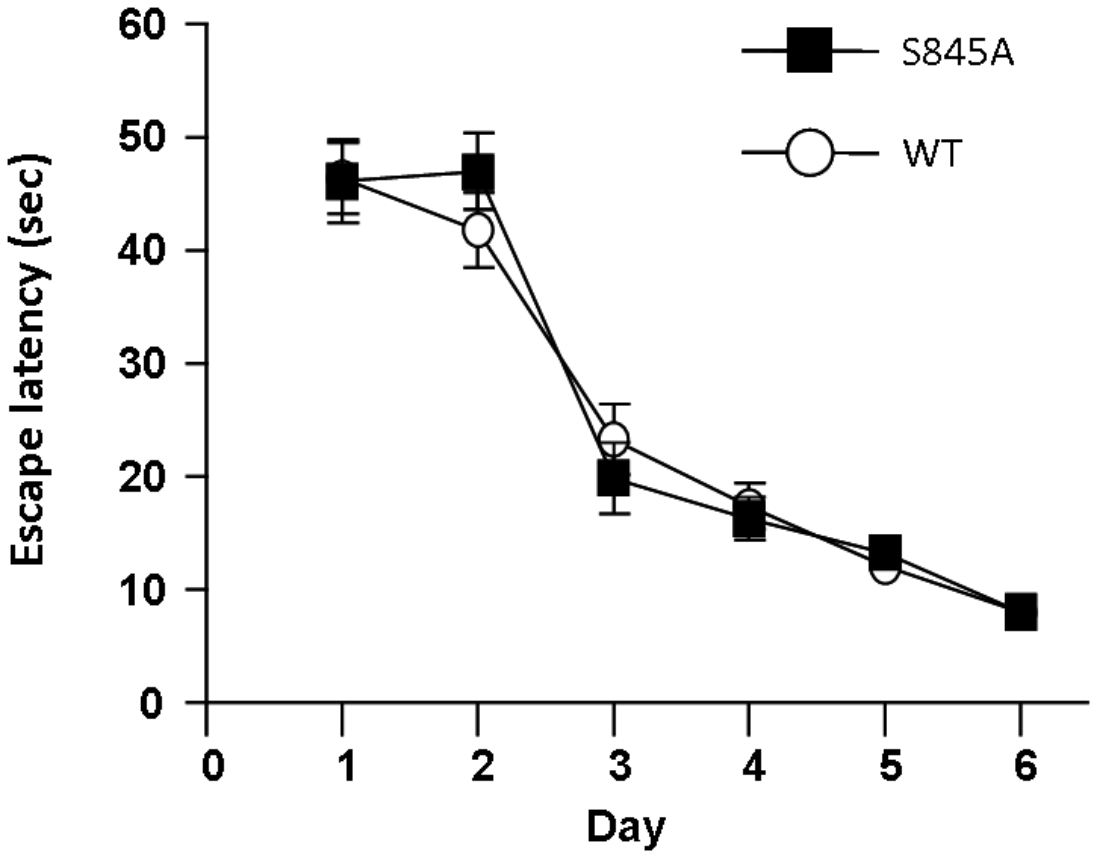

Figure 3.28. Performance of wild-type and GluR1-S845A mutant mice in the Morris water maze.

Mice were given four trials per day and they were trained to find the platform in a fixed position for consecutive six days. Escape latency is defined as time taken to reach the hidden platform. All data are shown as mean values of four trials from WT (n = 8) and S845A mutants (n = 7). Error bars represent ± SEM. It should be noted that GluR1-S845A mutants learned to locate the hidden platform as fast as that of WT.

3.3.3 GluR1-S845A mutation impaired extinction of morphine CPP

To examine the persistence of morphine-associated contextual memory in the GluR1-S845A mutant mice, we performed a series of extinction tests on mice conditioned with 10 mg/kg morphine for consecutive four days, in which both WT and mutants exhibited robust and similar CPP responses. Although both genotypes started at similar morphine CPP (WT, 200.7 ± 15 s; S845A, 186 ± 12.4 s; $P > 0.05$; n = 30) (**Fig. 3.29**), the CPP response in WT but not GluR1-S845A mutants was significantly reduced after 9 extinction tests (WT, 124.7 ± 21.3 s; S845A, 169.9 ± 19.5 s) (**Fig. 3.29**). During 11st test session, the reduction of CPP expression in WT was significantly greater than that of GluR1-S845A mutant mice (WT, 93.13 ± 18.4 s; S845A, 152.6 ± 19.5 s; $P = 0.03$; n = 28) (**Fig. 3.29**). Finally, CPP expression observed with the WT mice was completely extinguished after 15 test sessions, whereas the CPP response of GluR1-S845A mutants was extinguished after 23 sessions (**Fig. 3.29**). These findings suggest that the S845A mutation either impaired the learning of the new conditioning or prolonged the retention of the old conditioning with morphine.

Taken together, all of the above results suggest that an alteration in GluR1 phoshorylation at Ser^{845} and subsequent receptor endocytosis are involved in acquisition and extinction of morphine CPP, which might reflect the AMPA receptor's involvement in the mechanisms underlying opiate-seeking behaviors.

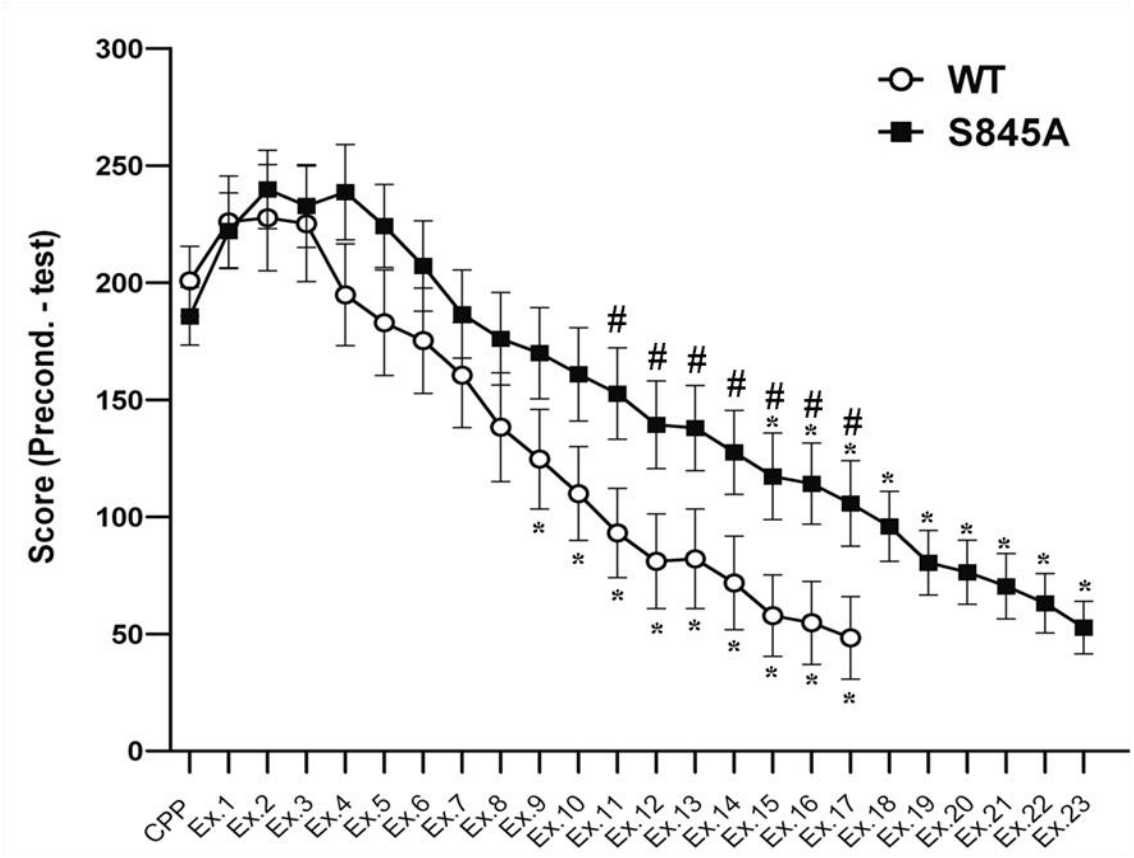

Figure 3.29. A prolonged extinction response in GluR1-S845A mutant mice.

Both wild-type and GluR1-S845A mutant animals were conditioned with 10 mg/kg morphine for consecutive four days to achieve similar expression of morphine-induced CPP. Every two days after the CPP test, animals in a drug-free state were repeatedly tested until their CPP response was completely extinct. Animals with the CPP scores higher than 60 sec were subjected for subsequent extinction tests. Data are mean ± SEM of test score in seconds (time spent in the morphine-paired chamber during CPP test or extinction test minus that spent during preconditioning test). * denotes the morphine preference was significantly reduced during extinction, while # represents a significant difference between wild-type and the mutant mice at different intervals.

CHAPTER 4

DISCUSSION

4.1 Morphine-induced internalization of AMPA receptors

Earlier electrophysiological studies on hippocampal cultures have demonstrated that chronic exposure to morphine decreases the amplitude of mEPSCs (Liao et al., 2005; Liao et al., 2007), which can be attributed to a removal of pre-existing AMPA receptor, an inhibition in synaptic delivery of the receptor, and/or a suppression of the receptor channel opening. In the current study, time-lapse imaging and biochemical experiments provided direct evidence that morphine treatment induced a time-dependent loss of pre-existing GluR1 at both spines and dendrites, likely through receptor internalization (**Figs. 3.3, 3.7**). However, the receptor internalization may not be the exclusive mechanism, as rats administrated with morphine have a marked reduction of LTP at hippocampi (Pu et al., 2002), which suggests a decrease in the re-insertion rate of synaptic AMPA receptors. Therefore, it is plausible that morphine-induced loss of postsynaptic GluR1 is a combination of increased internalization and decreased synaptic delivery (Ehlers, 2000; Man et al., 2007). Moreover, it should be noted that the loss of surface pHluorin-GluR1 could be detected by live-imaging 3 h after morphine treatment (**Fig. 3.3**), but an increase in endogenous internalized GluR1 appeared only after 6 h, as shown in the biochemical experiments (**Fig. 3.7**). This time discrepancy may be due to different sensitivity of the two analysis techniques. The live imaging is based on detection of overexpressed recombinant receptors in a single neuron, while the biochemical study measures endogenous receptors in a population of neurons. Hence, the imaging technique may have higher sensitivity to detect subtle changes in the receptor movement at an earlier time point.

Morphine is well known to inhibit the presynaptic release of GABA through activation of inwardly rectifying potassium channels and suppression of calcium channels in GABAergic neurons of hippocampus, leading to a disinhibition of neural circuits (Wimpey and Chavkin, 1991). Since TTX pretreatment, which prevents depolarization cannot attenuate morphine-induced GluR1 endocytsis and loss of surface-expressed GluR1 (**Fig. 3.11**), the morphine effect in cultured hippocampal neurons is not due to an alteration of the neural network. Notably, CTOP co-treatment can totally abrogate the morphine-induced AMPA receptor trafficking (**Figs. 3.9, 3.10**). In addition, previous studies have found that μ-opioid receptors predominantly express in postsynaptic membrane (Arvidsson et al., 1995; Liao et al., 2005) and mainly co-localized with postsynaptic AMPA receptors (Liao et al., 2005). All of these observations suggest that morphine likely acts on postsynaptic μ-opioid receptors to regulate AMPA receptor trafficking.

4.2 Morphine regulates dephosphorylation of GluR1 at Ser^{845} and GluR1 endocytosis in a calcineurin dependent manner

We found that prolonged application of morphine promotes the dephosphorylation of GluR1 at Ser^{845} and reduces the amount of PSD-95 in the immunoprecipitated GluR1 complex (**Figs. 3.12, 3.13**), indicating the detachment of GluR1 from the PSD. Importantly, the prevention of GluR1-S845 dephosphorylation by either GluR1-S845D or -S845A mutant clearly suppresses the morphine-induced GluR1 endocytosis (**Figs. 3.22, 3.25**). These observations are consistent with the prevalent view that the phosphorylation of AMPA receptors can regulate the receptor trafficking by

affecting the interactions between the receptors' cytoplasmic tails and postsynaptic scaffolding proteins, especially PDZ-domain containing proteins such as SAP97, PSD-95, GRIP/ABP and PICK (Dong et al., 1997; Leonard et al., 1998; Xia et al., 1999; Shepherd and Huganir, 2007). As our results suggest that an alteration of phosphorylation status of GluR1-S845 by calcineurin-induced dephosphorylation is important for morphine-regulated GluR1 trafficking (**Figs. 3.22, 3.23, 3.24**), this implies that the induction of dephosphorylation can facilitate the dissociation of the GluR1 cytoplasmic tails and postsynaptic scaffolding proteins. Furthermore, since AMPA receptors are believed to cluster in PSD of synapses via the binding of stargazin or related transmembrane AMPAR binding proteins (TARPs) to PSD-95 (Nicoll et al., 2006), it will be of interest to determine whether GluR1-S845 dephosphorylation by morphine affects the interaction between AMPA receptors and TARPs or TARPs and PSD-95, and how the dephosphorylation suppresses this interaction.

The net level of GluR1-S845 phosphorylation depends on the opposing activities of PKA and phosphatases such as calcineurin (Barria et al., 1997; Beattie et al., 2000). Since postsynaptic protein A kinase-anchoring protein 150 (AKAP150) can scaffold PKA and calcineurin at different binding sites and is recruited to the complexes of SAP-97/PSD-95 and GluR1, AKAP150 acts as a link to position these intracellular enzymes adjacent to the surface receptors. The physical proximity of these proteins in turn allows PKA and calcineurin to regulate GluR1-S845 phosphorylation in a highly coordinated manner (Colledge et al., 2000, Dell'Acqua et al., 2006). In this study, 3 days of morphine treatment only elicits a transient reduction on GluR1-S845 phosphorylation by db-cAMP (**Fig. 3.14**), suggesting that morphine-induced PKA inhibition alone is insufficient to reduce GluR1-S845 phosphorylation level. Conversely, FK506 pretreatment completely

reverses the morphine-induced GluR1-S845 dephosphorylation and morphine is able to increase calcineurin activity (**Figs. 3.15, 3.16**), indicating that activated calcineurin appears to be the dominant regulator of GluR1-S845 phosphorylation when the primary hippocampal neurons were treated with morphine.

Recently, several *in vivo* studies have found that discontinuous treatment of animals with morphine increases GluR1-S845 phosphorylation, in contrast to our findings (Billa et al., 2009; Billa et al., 2010). This difference may be related to different experimental models, particularly the method of morphine application. They used a 12-hr period without morphine injections before animal dissection, potentially leading to a decrease in morphine level by metabolism and elimination. The decreased morphine level may cause drug withdrawal that in turn increases adenylate cyclase activity, cAMP level and PKA activity (Sharma et al., 1975). Once PKA activity overwhelms calcineurin activity, GluR1-S845 phosphorylation level could then be increased. In contrast, our study employed a continuous incubation of hippocampal cultures with morphine, in which PKA was inhibited, thus favoring the action of activated calcineurin (**Figs. 3.14, 3.15, 3.16**). As a result, there was dephosphorylation of GluR1-S845. Furthermore, our *in vitro* primary culture studies were also not affected by the circuitry synaptic activities as shown in our TTX and APV studies, which might not be case in the *in vivo* studies if the animals treated with morphine were undergoing withdrawal. Hence, cultured hippocampal neurons can provide an experimental model to directly study any neuro-modulation induced by morphine itself or μ-opioid receptors.

Calcineurin is a Ca^{2+}-dependent protein phosphatase (Klee et al., 1979), and it plays a pivotal role in morphine-regulated GluR1-S845 dephosphorylation at Ser^{845} and receptor endocytosis (**Figs. 3.15, 3.19, 3.20**). The key issue is how calcineurin is

stimulated or where Ca^{2+} comes from upon morphine treatment. Although the precise mechanism underlying morphine activated calcineurin in our study is still unclear, at least we narrow down the pathway that NMDA receptors are not involved, as DL-APV has no effect on morphine-increased calcineurin activity (**Fig. 3.17**). Apart from NMDA receptors, other glutamate receptors such as Gq-coupled metabotropic glutamate receptors (mGluRs) and the related intracellular messengers such as phospholipids-Ca^{2+}-PKC are believed to regulate morphine-induced signal transduction *in vitro* and tolerance development *in vivo* (Chu et al., 2010; Narita et al., 2005; Fundytus and Coderre, 1996). Therefore, mGluRs or/and phospholipid-Ca^{2+}-PKC may be the potential signal pathways mediating the calcineurin activation. Considering a recent report that Ca^{2+}-permeable AMPA receptor is absent from perisynaptic sites in GluR1-S845A mutant mice (He et al., 2009), and our data that overexpression of pHluorin-GluR1-S845A causes the attenuation of morphine-regulated GluR1 trafficking (**Figs. 3.24, 3.25**), Ca^{2+}-permeable AMPA receptor may be another potential source of Ca^{2+} activating calcineurin.

4.3 Implications of morphine-regulated GluR1-containing AMPA receptors trafficking

The present study directly demonstrates that chronic treatment with morphine induces GluR1 endocytosis, resulting in a loss of GluR1 at excitatory synapses of hippocampi (**Figs. 3.3, 3.7**). This morphine effect may represent a key step in an addiction model proposed by Lüsher and Bellone (2008). In this model, chronic exposure to addictive drugs such as cocaine will induce an initial synaptic plasticity, in which the

amount of synaptic AMPA receptors in nucleus accumbens initially decreases (Thomas et al., 2001). However, later withdrawal of the drug increases synaptic insertion of the receptors, even exceeding the baseline. Intriguingly, Ca^{2+}-impermeable-AMPA receptors are gradually replaced by Ca^{2+}-permeable ones during the late withdrawal (Conrad et al., 2008). Such exchange for Ca^{2+}-permeable AMPA receptors is considered to conduct synaptic currents more readily and to contribute long-lasting alterations in synaptic strength that implies the relapse of addiction. This multiple-step addiction model emphasizes that the addictive drugs-evoked synaptic plasticity indeed is a hierarchical organization: an initial induction of synaptic plasticity is important for developing subsequent plasticity (Lüsher and Bellone, 2008). Therefore, chronic exposure to morphine-induced removal of synaptic GluR1 is probably the initial induction of plasticity that may underlies the drug addiction. This speculation provoked us to examine the physiological significance of morphine-regulated AMPA receptor trafficking in the hippocampus for opioid addictive behaviors, which will be discussed below. Since the hippocampus is a vital part of the brain responsible for learning and memory, our work emphasized on the formation of the memory for the environmental context of the drug experience, like CPP paradigm that contributes to drug seeking and relapse behaviors (Hyman et al., 2006).

4.4 Potential involvement of synaptic plasticity in the alterations of acquisition and extinction of morphine CPP by impaired change in GluR1 phosphorylation at Ser^{845}

The phenotype of homozygotes of GluR1-S845A mutant mice used in the current behavioral study has been well examined (He et al., 2009; Lee et al., 2010). They not only express normal levels of total GluR1 proteins and cell surface GluR1 (He et al., 2009), but also have no deficit in constitutive receptor internalization under basal conditions, the basal synaptic transmission and presynaptic function (Lee et al., 2003; Lee et al., 2010), therefore implying that no dramatic functional compensation occur in this transgenic model to mask the specific role of GluR1 phosphorylation at Ser^{845}. Although the phosphorylation of GluR1-S845 is critical for extra-synaptic insertion of GluR1-containing AMPA receptor, these mutant mice still have no abnormalities in induction, magnitude and stability of LTP (Lee et al., 2010), suggesting other phosphorylation sites such as S831 can support LTP. Interestingly, they display significant impairment on NMDA receptor activation-induced AMPA receptor endocytosis and LTD (Lee et al., 2010; He et al., 2009). Given that morphine-induced GluR1 endocytosis was attenuated in cultured hippocampal neurons from GluR1-S845A mutants (**Fig. 3.25**) and the evidence for the role of dynamic GluR1 trafficking in mediating strength in hippocampal glutamatergic synapses is compelling, it is plausible that the GluR1-S845A mutation may alter synaptic plasticity evoked by morphine and the drug-related contextual experience, such as hippocampus-dependent CPP paradigm.

Previous reports showed that contextual learning such as inhibitory avoidance learning requires synaptic insertion of GluR1-containing AMPA receptors and synaptic potentiation in hippocampus (Whitock et al., 2006; Kessels and Malinow, 2009; Mitsushima et al., 2011). Consistent to these observations, synaptic potentiation by GluR1 trafficking has been suggested to play an important role in addictive drugs-associated learning and memory (Kauer and Malenka, 2007). For instance, CPP and

conditioned locomotor responses to cocaine, but not behavioral sensitization, were impaired in adult GluR1 knockout mice, in which LTP is essentially abolished (Dong et al., 2004; Zamanillo et al., 1999; Mack et al., 2001). As mentioned before, the GluR1-S845A mutant mice exhibited normal LTP in comparison to WT, suggesting no deficit in synaptic GluR1 delivery. This may explain why the GluR1-S845A mutant mice displayed acquisition of morphine CPP comparable to WT after undergoing the maximum amount of training in our study (i.e. 4 days of conditioning with 10 mg/kg morphine) (Fig. 3.26). Nevertheless, our results showing decreased sensitivity to acquire morphine CPP in GluR1-S845A mutant mice (**Fig. 3.26**) may be related to the alterations of neural plasticity driven by morphine and/or the drug-associated contextual experience in the mutants. As the GluR1-S845A mutation abolished morphine-regulated GluR1-containing AMPA receptor endocytosis (**Fig. 3.25**), the size of an intracellular receptor pool available for modifying synaptic strength may be smaller and/or the refilling may occur at a slower rate compared with that of WT. Hence, it is proposed that the GluR1-S845A mutants may show lower propensity to trigger reinsertion of AMPA receptors and/or initiate morphine-evoked synaptic plasticity such as LTP, resulting in different sensitivity in morphine CPP acquisition between the mutants and WTs. Further studies are needed to clarify whether the association between morphine and contextual stimuli can affect the levels of synaptic or intracellular GluR1-containing AMPA receptors and synaptic plasticity in hippocampus and compare the changing pattern of AMPA receptor expression between WT and the GluR1-S845A mutants. Apart from AMPA receptor trafficking, it should be noted that the long-lasting synaptic plasticity can also be caused by the drugs of abuse-evoked gene transcription and protein synthesis (Luscher and Malenka, 2011), which may be an alternative explanation why the GluR1-S845A

mutation could not completely impair the acquisition of morphine CPP (**Figs. 3.26 and 3.29**).

Previous genetic studies have demonstrated that the GluR1 knockout mice exhibited deficit in the extinction of cocaine CPP, revealing a prominent role of GluR1 in mediating the persistence of seeking behavior (Stephens and Mead, 2003; Engblom et al., 2008). Similarly, we observed a prolonged extinction of morphine CPP in the GluR1-S845A mutants (**Fig. 3.29**). Thus, it provides direct evidence on the specific involvement of GluR1 phosphorylation and trafficking in the CPP extinction. The paradigm of CPP extinction, in which the environmental cue/conditioned stimulus was repeatedly presented in the drug-free state, results in progressive reduction in the CPP expression. In fact, the existing memory of drug reward-associated cue cannot be modified directly by extinction, instead it is suppressed by new learning of non-reward presentation that can compete with the original learning (Pavlov, 1924; Rescorla, 1996; Monfils et al., 2009). Therefore, the impaired morphine extinction in GluR1-S845A mutants suggests that the S845A mutation may impair the learning of the new conditioning. Apart from the mechanism of extinction, the retrieval of the conditioned stimulus in the tests also engages an opposite mechanism called reconsolidation (Nader et al., 2000; Eisenberg et al., 2003, Lee et al., 2006). In the process of reconsolidation, the existing CPP memory upon retrieval transiently becomes labile and prone to modification, resulting in either enhancement or disruption of the existing memory (Tronson et al., 2006; Monfils et al., 2009; Schiller et al., 2010). A recent study has demonstrated that retrieval of conditioned stimulus leads to a transient endocytosis of AMPA receptors. Importantly, the blockade of the regulated AMPA receptor endocytosis prolonged the contextual fear response. These findings thus suggest that endocytosis of AMPA receptors triggers

synaptic changes for constraining the memory strength and so facilitating the loss of conditioned response (Rao-Ruiz et al., 2011). In our study, the GluR1-S845A mutation possibly attenuated the regulated endocytosis of AMPA receptors, which in turn may represent an alternative mechanism to induce prolonged extinction of morphine CPP by preventing the constraint on memory strength.

4.5 Conclusion

Incubation of cultured hippocampal neurons with morphine triggered calcineurin-mediated dephosphorylation of GluR1 at Ser^{845}, resulting in loss of both synaptic and extrasynaptic AMPA receptors through internalization. Importantly, this alteration in GluR1 phosphorylation at Ser^{845} and subsequent receptor endocytosis by morphine treatment are involved in the acquisition and extinction of morphine CPP, which suggests the involvement of AMPA receptor trafficking in the mechanisms underlying opiate-seeking behaviors.

References

Andrasfalvy BK, Smith MA, Borchardt T, Sprengel R and Magee JC (2003) Impaired regulation of synaptic strength in hippocampal neurons from GluR1-deficient mice. J. Physiol. **552**:35-45.

Arvidsson U, Dado RJ, Riedl M, Lee JH, Law PY, Loh HH, Elde R and Wessendorf MW (1995) Delta-Opioid receptor immunoreactivity: distribution in brainstem and spinal cord, and relationship to biogenic amines and enkephalin. J. Neurosci. **15**:1215-1235.

Asai A, Qiu J, Narita Y, Chi S, Saito N, Shinoura N, Hamada H, Kuchino Y and Kirino T (1999) High level calcineurin activity predisposes neuronal cells to apoptosis. J. Biol. Chem. **274**: 34450-34458.

Ashby MC, Ibaraki K and Henley JM (2004) It's green outside: tracking cell surface proteins with pH-sensitive GFP. Trends Neurosci. **27**:257-261.

Barria A, Muller D, Derkach V, Griffith LC and Soderling TR (1997) Regulatory phosphorylation of AMPA-type glutamate receptors by CaM-KII during long-term potentiation. Science **276**:2042-2045.

Beattie EC, Carroll RC, Yu X, Morishita W, Yasuda H, von Zastrow M and Malenka RC (2000) Regulation of AMPA receptor endocytosis by a signaling mechanism shared with LTD. Nat. Neurosci. **12**:1291-1300.

Bhargava HN (1991) Multiple opiate receptors of brain and spinal cord in opiate addiction. Gen. Pharmacol. P767-772.

Billa SK, Liu J, Bjorklund NL, Sinha N, Fu Y, Shinnick-Gallagher P and Morón JA(2010) Increased insertion of glutamate receptor 2-lacking alpha-amino-3-hydroxy-5-methyl-4-isoxazole propionic acid (AMPA) receptors at hippocampal synapses upon repeated morphine administration. Mol. Pharmacol. **77**:874-883.

Billa SK, Sinha N, Rudrabhatla SR and Morón JA (2009) Extinction of morphine-dependent conditioned behavior is associated with increased phosphorylation of the GluR1 subunit of AMPA receptors at hippocampal synapses. Eur. J. Neurosci. **29**:55-64.

Bliss TV and Collingridge GL (1993) A synaptic model of memory: long-term potentiation in the hippocampus. Nature **361**:31-39.

Bodnar RJ (2011) Endogenous opiates and behavior: 2010. Peptides **32**:2522-2552.

Boehm J, Kang MG, Johnson RC, Esteban J, Huganir RL and Malinow R (2006) Synaptic incorporation of AMPA receptors during LTP is controlled by a PKC phosphorylation site on GluR1. Neuron **51**:213-225.

Borgdorff AJ and Choquet D (2002) Regulation of AMPA receptor lateral movements Nature **417**:649-653.

Borgdorff AJ and Choquet D (2002) Regulation of AMPA receptor lateral movements Nature **417**:649-653.

Carr AS, Holtby HM, Hartley EJ and Cox P (1994) Anesthesiology 81, A1348.

Chakrabarti S and Gintzler AR (2003) Phosphorylation of Gβγ is augmented by chronic morphine and enhances Gβγ stimulation of adenylyl cyclase activity. Brain Res. Mol. Brain Res. **119**:144-151.

Chen L, Chetkovich DM, Petralia RS, Sweeney NT, Kawasaki Y, Wenthold RJ, Bredt DS and Nicoll RA (2000) Stargazin regulates synaptic targeting of AMPA receptors by two distinct mechanisms. Nature **408**:936-943.

Chen Y, Mestek A, Liu J and Yu L (1993) Molecular cloning of a rat kappa opioid receptor reveals sequence similaries to the mu and delta opioid receptors. Biochem. J. **295**:625-628.

Childress AR, Mozley PD, McElgin W, Fitzgerald J, Reivich M and O'Brien CP (1999) Limbic activation during cue-induced cocaine craving. Am. J. Psychiatry **156**:11-18.

Cho KO, Hunt CA and Kennedy MB (1992) The rat brain postsynaptic density fraction contains a homolog of the Drosophila discs-large tumor suppressor protein. Neuron **9**:929-942.

Chu J, Zheng H, Zhang Y, Loh HH and Law PY (2010) Agonist-dependent mu-opioid receptor signaling can lead to heterologous desensitization. Cell Signal. **22**:684-696.

Chung HJ, Steinberg JP, Huganir RL and Linden DJ (2003) Requirment of AMPA receptor GluR2 phosphorylation for cerebellar long-term depression. Science **300**:1751-1755.

Colledge M, Dean RA, Scott GK, Langeberg LK, Huganir RL and Scott JD (2000) Targeting of PKA to glutamate receptors through a MAGUK-AKAP complex. Neuron **27**:107-119.

Collier HO and Francis DL (1975) Morphine abstinence is associated with increased brain cyclic AMP. Nature **255**:159-162.

Conrad KL, Tseng KY, Uejima JL, Reimers JM, Heng LJ, Shaham Y, Marinelli M and Wolf ME (2008) Formation of accumbens GluR2-lacking AMPA receptors mediates incubation of cocaine craving. Nature **454**:118-121.

Craig AM, Blackstone CD, Huganir RL and Banker G (1993) The distribution of glutamate receptors in cultured rat hippocampal neurons-postynaptic clustering of AMPA-selective subunits. Neuron **10**:1055-1068.

Crombag HS, Sutton JM, Takamiya K, Holland PC, Gallagher M and Huganir RL (2008) A role for alpha-amino-3-hydroxy-5-methylisoxazole-4-propionic acid GluR1 phosphorylation in the modulatory effects of appetitive reward cues on goal-directed behavior. Eur. J. Neurosci. **27**:3284-3291.

de Jong CA, Gongora VC, Engelhard P and Breteler MH (2006) Effects of craving self-report measurement on desire for heroin in opioid dependent individuals. Subst. Use Misuse. **41**:1695-1704.

Delfs JM, Kong H, Mestek A, Chen Y, Yu L, Reisine T and Chesselet MF (1994) Expression of mu opioid receptor mRNA in rat brain: an in situ hybridization study at the single cell level. J. Comp. Neurol. **345**:46-68.

Dell'Acqua ML, Smith KE, Gorski JA, Horne EA, Gibson ES and Gomez LL (2006) Regulation of neuronal PKA signaling through AKAP targeting dynamics. Eur. J. Cell Biol. **85**:627-633.

Derkach VA, Oh MC, Guire ES and Soderling TR (2007) Regulatory mechanisms of AMPA receptors in synaptic plasticity. Nat. Rev. Neurosci. **8**:101-113.

Dhawan BN, Cesselin R, Raghubir R, et al. (1996) International Union of Pharmacology. XII. Classificiation of opioid receptors. Pharmacol. Rev. **48**:567-592.

Di Chiara G and Imperato A (1988) Drugs abused by humans preferentially increase synaptic dopamine concentrations in the mesolimbic system of freely moving rats. Proc. Natl. Acad. Sci. USA **85**:5274-5278.

Dong H, O'Brien RJ, Fung ET, Lanahan AA, Worley PF and Huganir RL (1997) GRIP: a synaptic PDZ-containing protein that interacts with AMPA receptors. Nature **386**:279-284.

Dong Y, Saal D, Thomas M, Faust R, Bonci A, Robinson T and Malenka RC (2004) Cocaine-induced potentiation of synaptic strength in dopamine neurons: behavioral correlates in GluR1A(-/-) mice. Proc. Natl. Acad. Sci. USA **101**:14282-14287.

Duman RS, Tallman JF and Nestler EJ (1988) Acute and chronic opiate-regulation of adenylate cyclase in brain: specificeffects in locus coeruleus. J. Pharmacol. Exp. Ther. **246**:1033-1039.

Eddy NB, Friebel H, Hahn KJ and Halbach H (1968) Codeine and its alternates for pain and cough relief. I. Codeine, exclusive of its antitussive action. Bull. World Health Organ. **38**:673-741.

Ehlers MD (2000) Reinsertion or degradation of AMPA receptors determined by activity-dependent endocytic sorting. Neuron **28**:511-525.

Eisenberg M, Kobilo T, Berman DE and Dudai Y (2003) Stability of retrieved memory: inverse correlation with trace dominance. Science **301**:1102-1104.

Engblom D, Bilbao A, Sanchis-Segura C, Dahan L, Perreau-Lenz S, Balland B, Parkitna JR, Lujan R, Halbout B, Mameli M, Parlato R, Sprengel R, Lusher C, Schutz G and Spanagel R (2008) Glutamate receptors on dopamine neurons control the persistence of cocaine seeking. Neuron **59**:497-508.

Esteban JA, Shi SH, Wilson C, Nuriya M, Huganir RI and Malinow R (2003) PKA phosphorylation of AMPA receptor subunits controls synaptic trafficking underlying plasticity. Nat. Neurosci. **6**:136-143.

Everitt BJ, Dickinson A and Robbins TW (2001) The neuropsychological basis of addictive behavior. Brain Res. Brain Res. Rev. **36**:129-138.

Fan GH, Wang LZ, Qiu HC, Ma L and Pei G (1999) Inhibition of calcium/calmodulin-dependent protein kinase II in rat hippocampus attenuates morphine tolerance and dependence. Mol. Pharmacol. **56**:39-45.

Floresco SB, Blaha CD, Yang CR and Phillips AG (2001) Modulation of hippocampal and amygdalar-evoked activity of nucleus accumbens neurons by dopamine: cellular mechanisms of input selection. J. Neurosci **21**:2851-2860.

Foye WO. Principles of Medicinal Chemistry, 3 rd Ed.; Lea and Febiger: Philadelphia, 1989 p. 624.

Fruman DA, Pai SY, Klee CB, Burakoff SJ and Bierer BE (1996) Measurement of calcineurin phosphatase activity in cell extracts. Methods **9**:146-54.

Fundytus ME and Coderre TJ (1996) Chronic inhibition of intracellular Ca2+ release or protein kinase C activation significantly reduces the development of morphine dependence. Eur. J. Pharmacol. **300**:173-181.

Gabra BH, Bailey CP, Kelly E, Sanders AV, Henderson G, Smith FL and Dewey WL (2007) Evidence for an important role of protein phosphatases in the mechanism of morphine tolerance. Brain Res. **1159**:86-93.

Garner CC and Kindler S (1996) Synaptic proteins and the assembly of synaptic junctions. Trends Cell Biol. **6**:429-433.

Ghosh A and Greenberg ME (1995) Distinct roles for bFGF and NT-3 in the regulation of cortical neurogenesis. Neuron **15**:89-103.

Goldfrank LR, ed. (2006) Goldfrank's Toxicologic Emergencies. 8th ed. New York, NY: McGraw Hill.

Haefely W (1986) Biological basis of drug-induced tolerance, rebound, and dependence. Contribution of recent research on benzodiazepines. Pharmacopsychiatry **19**:353-361.

Harrison LM, Kastin AJ and Zadina JE (1998) Opiate tolerance and dependence: receptors, G protein, and antiopiates. Peptides **19**:1603-1630.

Hassen AH, Feuerstein G and Faden AI (1984) Selective cardiorespiratory effects mediated by mu opioid receptors in the nucleus ambiguous. Neuropharmacology **23**:407-415.

Hayashi T and Huganir RL (2004) Tyrosine phosphorylation and regulation of the AMPA receptor by SRC family tyrosine kinases. J. Neurosci. **24**:6152-6160.

Hayashi Y, Shi SH, Esteban JA, Piccini A, Poncer JC and Malinow R (2000) Driving AMPA receptors into synapses by LTP and CaMKII: requirement for GluR1 and PDZ domain interaction. Science **287**:2262-2267.

He K, Song L, Cummings LW, Goldman J, Huganir RL and Lee HK (2009) Stabilization of Ca^{2+}-permeable AMPA receptors at perisynaptic sites by GluR1-S845 phosphorylation. Proc. Natl. Acad. Sci. USA **106**:20033-20038.

Hepler JR and Gilman AG (1992) G proteins. Trends Biochem. Sci. **17**:383-387.

Hescheler J, Rosenthal W, Trautwein W and Schultz G (1987) The GTP-binding protein, G_o, regulates neuronal calcium channels. Nature **325**:445-447.

Holman D, Feligioni M and Henley JM (2007) Differential redistribution of native AMPA receptor complexes following LTD induction in acute hippocampal slices. Neuropharmacology **52**:92-99.

Holzer P (2009) Opioid receptors in the gastrointestinal tract. Regul. Pept. **155**:11-17.

Hyman SE (2005) Addiction: a disease of learning and memory. Am. J. Psychiatry **162**: 1414-1422.

Hyman SE, Malenka RC and Nestler EJ (2006) Neural mechanisms of addiction: The role of reward-related learning and memory. Annu. Rev. Neurosci. **29**: 565-598.

Inoue M, Mishina M and Ueda H (2003) Locus-specific rescue of GluRepsilon1 NMDA receptors in mutant mice identifies the brain regions important for morphine tolerance and dependence. J. Neurosci. **23**:6529-6536.

Isaac JT, Nicoll RA and Malenka RC (1995) Evidence for silent synapse: implications for the expression of LTP. Neuron **15**:427-434.

Johnson SW and North RA (1992) Opioids excite dopamine neurons by hperpolarization of local interneurons. J. Neurosci. **12**:483-488.

Joiner ML, Lisé MF, Yuen EY, Kam AYF, Zhang M, Hall DD, Malik ZA, Qian H, Chen Y, Ulrich JD, Burette AC, Weinberg RJ, Law PY, El-Husseini A, Yan Z and Hell JW (2009) Assembly of a beta(2)-adrenergic receptor-GluR1 signalling complex for localized cAMP signalling. EMBO. J. **29**: 482-495.

Kam AY, Chan AS and Wong YH (2004) Phosphatidylinositol-3 kinase is distinctively required for mu-, but not kappa-opioid receptor-induced activation of c-Jun N-terminal kinase. J. Neurochem. **89**:391-402.

Kandel ER and O'Dell TJ (1992) Are adult learning mechanisms also used for development? Science **258**:243-245.

Kauer JA and Malenka RC (2007) Synaptic plasticity and addiction. Nat. Rev. Neurosci. **8**:844-858.

Kelley AE (2004) Memory and addiction: shared neural circuitry and memory mechanisms. Neuron **44**:161-179.

Kessels HW and Malinow R (2009) Synaptic AMPA receptor plasticity and behavior. Neuron **61**:340-350.

Kim DY, Kim SH, Choi HB, Min C and Gwag BJ (2001) High abundance of GluR1 mRNA and reduced Q/R editing of GluR2 mRNA in individual NADPH-diaphorase neurons. Mol. Cell. Neurosci. **17**:1025-1033.

Kirby GW (1967) Biosynthesis of the morphine alkaloids. Science **155**:170-173.

Klee CB, Crouch TH and Krinks MH (1979) Calcineurin: a calcium- and calmodulin-binding protein of the nervous system. Proc. Natl. Acad. Sci. U S A **76**:6270-6273

Kohler M, Kornau HC and Seeburg PH (1994) The organization of the gene for the functionally dominant α-amino-3-hydroxy-5-methylisoxazole-4-propionic acid receptor subunit GluR-B. J. Biol. Chem. **269**:17367-17370.

Komatsu T, Sakurada S, Kohno K, Shiohira H, Katsuyama S, Sakurada C, Tsuzuki M and Sakurada T (2009) Spinal ERK activation via NO-cGMP pathway contributes to nociceptive behavior induced by morphine-3-glucuronide. Biochem. Pharmacol. **78**:1026-1034.

Kondo I, Marvizon JC, Song B, Salgado F, Codeluppi S, Hua XY and Yaksh TL (2005) Inhibition by spinal mu- and delta-opioid agonists of afferent-evoked substance P release. J. Neurosci. **25**:3651-3600.

Koob GF and Bloom FE (1988) Cellular and molecular mechanisms of drug dependence. Science **242**:715-723.

Koob GF, Maldonado R and Stinus L (1992) Neural substrates of opiate withdrawal. Trends. Neurosci. **15**:186-191.

Koob GF, Volkow ND (2010) Neurocircuitry of addiction. Neuropsychopharmacology **35**: 217-238.

Kopec CD, Real E, Kessels HW and Malinow R (2007) GluR1 links structural and functional plasticity at excitatory synapses. J. Neurosci. **27**:13706-13718.

Lane-Ladd SB, Pineda J, Boundy VA, Pfeuffer T, Krupinski J, Aghajanian GK and Nestler EJ (1997) CREB (cAMP response element-binding protein) in the locus coeruleus: biochemical, physiological, and behavioral evidence for a role in opiate dependence. J. Neurosci. **20**:7890-7901.

Lee HK, Takamiya K, Han JS, Man H, Kim CH, Rumbaugh G, Yu S, Ding L, He C, Petralia RS, Wenthold RJ, Gallagher M and Huganir RL (2003) Phosphorylation of the

AMPA receptor GluR1 subunit is required for synaptic plasticity and retention of spatial memory. Cell **112**:631-643.

Lee HK, Takamiya K, He K, Song L and Huganir RL (2010) Specific roles of AMPA receptor subunit GluR1 (GluA1) phosphorylation sites in regulating synaptic plasticity in the CA1 region of hippocampus. J. Neurophysiol. **103**: 479-489.

Lee JL, Milton AL and Everitt BJ (2006) Reconsolidation and extinction of conditioned fear: inhibition and potentiation. J. Neurosci. **26**:10051-10056.

Lee SH, Simonetta A and Sheng M (2004) Subunit rules governing the sorting of internalized AMPA receptors in hippocampal neurons. Neuron **43**:221-236.

Legault M, Rompré PP and Wise RA (2000) Chemical stimulation of the ventral hippocampus elevates nucleus accumbens dopamine by activating dopaminergic neurons of the ventral tegmental area. J. Neurosci **20**: 1635-1642.

Leonard AS, Davare MA, Horne MC, Garner CC and Hell JW (1998) SAP97 is associated with the amino-amino-3-hydroxy-5-methylisoxazole-4-propionic acid receptor GluR1 subunit. J. Biol. Chem. **273**:19518-19524.

Li ST, Kato K, Tomizawa K, Matsushita M, Moriwaki A, Matsui H and Mikoshiba K (2002) Calcineurin plays different roles in group II metabotropic glutamate receptor- and NMDA receptor-dependent long-term depression. J. Neurosci. **22**:5034-5041.

Liao D, Grigoriants OO, Loh HH and Law PY (2007) Agonist-dependent postsynaptic effects of opioids on miniature excitatory postsynaptic currents in cultured hippocampal neurons. J. Neurophysiol. **97**:1485-1494.

Liao D, Hessler NA and Malinow R (1995) Activation of postsynaptically silent synapses during pairing-induced LTP in CA1 region of hippocampal slice. Nature **375**:400-404.

Liao D, Lin H, Law PY and Loh HH (2005) Mu-opioid receptors modulate the stability of dendritic spines. Proc. Natl. Acad. Sci. USA **102**:1725-1730.

Liao D, Zhang X, O'Brien R, Ehlers MD and Huganir RL (1999) Regulation of morphological postsynaptic silent synapses in developing hippocampal neurons. Nat. Neurosci. **2**:37-43.

Lieberman DN and Mody I (1994) Regulation of NMDA channel function by endogenous Ca^{2+}-dependent phosphatase. Nature **369**:235-9.

Lin H, Huganir R and Liao D (2004) Temporal dynamics of NMDA receptor-induced changes in spine morphology and AMPA receptor recruitment to spines. Biochem. Biophys. Res. Commun. **316**:501-511.

Lin JW, Ju W, Foster K, Lee SH, Ahmadian G, Wyszynski M, Wang YT and Sheng M (2000) Distinct molecular mechanisms and divergent endocytotic pathways of AMPA receptor internalization. Nat. Neurosci. **3**:1282-90.

Lin LH, Sahr KE and Chishti AH (1997) Identification of the mouse homolgous of human disc large and rat SAP97 genes. Biochim. Biophys. Acta. Mol. Basis Dis. **1362**:1-5.

Lisman JE and Zhabotinsky AM (2001) A model of synaptic memory: a CaMKII/PP1 switch that potentiates transmission by organizing an AMPA receptor anchoring assembly. Neuron. **31**:191-201.

Lissin DV, Carroll RC, Nicoll RA, Malenka RC and von Zastrow M (1999) Rapid, activation-induced redistribution of ionotropic glutamate receptors in cultured hippocampal neurons. J. Neurosci. **19**:1263-1272.

Liu Q, Wang X, Liu Y, Lu R, Yuan Q, Yang B, Zhou J, Wang Y and Wang Z (2011) RACK1 inhibits morphine re-exposure via inhibition of Src. Neurol. Res. **33**:56-62.

Luch A (2009) Molecular, clinical and environmental toxicology. Springer. P20.

Luscher C, Bellone C (2008) Cocaine-evoked synaptic plasticity: a key to addiction? Nat. Neurosci **11**:737-738.

Luscher C and Malenka RC (2011) Drug-evoked synaptic plasticity in addiction: from molecular changes to circuit remodeling. Neuron **69**:650-663.

Luscher C, Xia H, Beattie EC, Carroll RC, von Zastrow M, Malenka RC and Nicoll RA (1999) Role of AMPA receptor cycling in synaptic transmission and plasticity. Neuron **24**:649-658.

Ma YY, Chu NN, Guo CY, Han JS and Cui CL (2007) NR2B-containing NMDA receptor is required for morphine-but not stress-induced reinstatement. Exp. Neurol. **203**:309-319.

Mack V, Burnashev N, Kaiser KMM, Rozov A, Jensen V, Hvalby O, Seeburg PH, Sakmann B and Sprengel R (2001) Conditional restoration of hippocampal synaptic potentiation in GluR1-A-deficient mice. Science **292**:2501-2504.

Malinow R and Malenka RC (2002) AMPA receptor trafficking and synaptic plasticity. Annu. Rev. Neurosci. **25**:103-126.

Mammen AL, Kameyame K, Roche KW and Huganir RL (1997) Phosphorylation of the α-amino-3-hydroxy-5-methylisoxazole-4-propionic acid receptor GluR1 subunit by calcium/calmodulin-dependent kinase II. J. Biol. Chem. **272**:32528-32533.

Man HY, Sekine-Aizawa Y and Huganir R (2007) Regulation of alpha-amino-3-hydroxy-5-methyl-4-isoxazolepropionic acid receptor trafficking through PKA phosphorylation of the GluR1 subunit. Proc. Natl. Acad. Sci. USA **104**:3579-3584.

Mansour A, Fox CA, Burke S, Akil A and Watson SJ (1995) Immunohistochemical localization of the cloned μ opioid receptor in the rat CNS. J Chem. Neuroanat. **8**:283-305.

Mansour A, Fox CA, Thompson RC, Akil H and Watson SJ (1994) μ-opioid receptor mRNA expression in the rat CNS: comparison to μ-opioid binding. Brain Res. **643**:245-265.

Mao J, Price DD, Phillips LL, Lu J and Mayer DJ (1995) Increase in protein kinase Cγ immunoreactivity in the spinal cord of rats associated with tolerance to the analgesic effects of morphine. Brain Res. **677**:257-267.

Matthes HW, Maldonado R, Simonin F, Valverde O, Slowe S, Kitchen I, Befort K, Dierich A, Le Meur M, Dolle P, Tzavara E, Hanoune J, Roques BP and Kieffer BL (1996) Loss of morphine-induced analgesia, reward effect and withdrawal symptoms in mice lacking the μ-opioid-receptor gene. Nature **383**:819-823.

Mayer ML, Westbrook GL and Guthrie PB (1984) Voltage-dependent block by Mg^{2+} of NMDA responses in spinal cord neurons. Nature **309**:262-263.

Mei B, Niu L, Cao B, Huang D and Zhou Y (2009) Prenatal morphine exposure alters the layer II/III pyramidal neurons morphology in lateral secondary visual cortex of juvenile rat. Synapse **63**:1154-1151.

Mircea S and Rodolfo L (1988) The functional states of the thalamus and the associated neuronal interplay. Physiological Reviews **68**:649-742.

Mitsushima D, Ishihara K, Sano A, Kessels HW and Takahashi T (2011) Contextual learning requires synaptic AMPA receptor delivery in the hippocampus. Proc. Natl. Acad. Sci. USA **108**:12503-12508.

Moncada A, Cendán CM, Baeyens JM and Del Pozo E (2003) Effects of serine/threonine protein phosphatase inhibitors on morphine-induced antinociception in the tail flick test in mice. Eur. J. Pharmacol. **465**:53-60.

Monfils MH, Cowansage KK, Klann E and LeDoux JE (2009) Extinction-reconsolidation boundaries: key to persistent attenuation of fear memories. Science **324**:951-955.

Morón JA and Green TA (2010) Exploring the molecular basis of addiction: drug-induced neuroadaptations. Neuropsychopharmacology **35**:337-338.

Morris R (1984) Developments of a water-maze procedure for studying spatial learning in the rat. J. Neurosci. Methods **11**:47-60.

Murai KK, Nguyen LN, Irie F, Yamaguchi Y and Pasquale EB (2003) Control of hippocampal dendritic spine morphology through ephrin-A3/EphA4 signaling. Nat. Neurosci. **6**:153-160.

Nader K, Schafe GE and Le Doux JE (2000) Fear memories require protein synthesis in the amygdala for reconsolidation after retrieval. Nature **406**:722-76.

Narita M, Suzuki M, Narita M, Niikura K, Nakamura A, Miyatake M, Aoki T, Yajima Y and Suzuki T (2005) Involvement of spinal metabotropic glutamate receptor 5 in the development of tolerance to morphine-induced antinociception. J. Neurochem. **94**:1297-1305.

Nestler EJ (2002) Common molecular and cellular substrates of addiction and memory. Neurobiol. Learn. Mem. **78**:637-647.

Nestler EJ, Hope BT and Widnell KL (1993) Drug addiction: a model for the molecular basis of neural plasticity. Neuron **11**: 995-1006.

Nicoll RA, Tomita S and Bredt DS (2006) Auxiliary subunits assist AMPA-type glutamate receptors. Science **311**:1253-6.

North RA, Williams JT, Surprenant A and Christie MJ (1987) Mu and delta receptors belong to a family of receptors that couple to potassium channels. Proc. Natl. Acad. Sci. USA **84**:5487-5491.

Novak BH, Hudlicky T, Reed JW, Mulzer J and Trauner D (2000) Morphine synthesis and biosynthesis-an update. Current Organic Chemistry P343-362.

O'Brien CP, Childress AR, Ehrman R and Robbins SJ (1998) Conditioning factors in drug abuse: can they explain compulsion? J. Psychopharmacol. **12**:15-22.

O'Brien CP, Childress AR, McLellan AT and Ehrman R (1992) Classical conditioning in drug-dependent humans. Ann. NY Acad. Sci. **654**: 400-415.

Oh MC and Derkach VA (2005) Dominant role of the GluR2 subunit in regulation of AMPA receptors by CaMKII. Nat. Neurosci. **8**:853-854.

Oh MC, Derkach VA, Guire ES and Soderling TR (2006) Extrasynaptic membrane trafficking regulated by GluR1 serine 845 phosphorylation primes AMPA receptors for long-term potentiation. J. Biol. Chem. **281**:752-758.

Ortiz J, Harris HW, Guitart X, Terwilliger RZ, Haycock JW and Nestler EJ (1995) Extracellular signal-regulated protein kinases (ERKs) and ERK kinase (MEK) in brain: regional distribution and regulation by chronic morphine. J.Neurosci. **15**:1285-1297.

Passafaro M, Nakagawa T, Sala C and Sheng M (2003) Induction of dendritic spines by an extracellular domain of AMPA receptor subunit GluR2. Nature **424**:677-681.

Pavlov IP. Conditioned Reflexes. Oxford: Oxford University Press; (1927).

Pellegrini-Giampietro DE, Cherici G and Moroni F (1988) Studies on the role of calcium and phospholipase C in the morphine withdrawal syndrome. Pharmacol. Res. Commun. **20**:413-414.

Pickard L, Noel J, Duckworth JK, Fitzjohn SM, Henley JM, Collingridge GL and Molnar E (2001) Transient synaptic activation of NMDA receptors lead to the insertion of native AMPA receptors at hippocampal neuronal plasma membranes. Neuropharmacology **41**: 700-713.

Piercey MF, Einspahr FJ, Dorby PJK, Schroeder LA and Hollister RP (1979) Morphine does not antagonize the substance P mediated excitation of dorsal horn neurons. Brain Res. **186**:421-434.

Pu L, Bao GB, Xu NJ, Ma L and Pei G (2002) Hippocampal long-term potentiation is reduced by chronic opiate treatment and can be restored by reexposure to opiates. J. Neurosci. **22**:1914-1921.

Rao-Ruiz Priyanka, Rotaru DC, van der Loo RJ, Mansvelder HD, Stiedl O, Smit AB and Spijker S (2011) Retrieval-specific endocytosis of GluA2-AMPARs underlies adaptive reconsolidation of contextual fear. Nat. Neurosci. **14**:1302-1308.

Raynor K, Kong H, Chen Y, Yasuda K, Yu L, Bell GI and Reisine T (1994) Pharmacological characterization of the cloned κ-, δ- and μ-opioid receptors. Mol. Pharmacol. **45**:330-334.

Reisel D, Bannerman DM, Schmitt WB, Deacon RM, Flint J, Borchardt T, Seeburg PH ad Rawlins JN (2002) Spatial memory dissociations in mice lacking GluR1. Nat. Neurosci. **5:**868-873.

Rehni AK and Singh N (2011) Modulation of src-kinase attenuates naloxone-precipitated opioid withdrawal syndrome in mice. Behav. Pharmacol. **22**:182-190.

Rescorla RA (1996) Preservation of Pavlovian associations through extinction. J. Exp. Psychol. **49B**:245-258.

Robinson TE and Kolb B (1999) Morphine alters the structure of neurons in the nucleus accumbens and neocortex of rats. Synapse **33**:160-162.

Robinson TE, Gorny G, Savage VR and Kolb B (2002) Widespread but regionally specific effects of experimenter-versus self-administered morphine on dendritic spines in

the nucleus accumbens, hippocampus, and neocortex of adult rats. Synapse **46**:271-279.

Roche KW, O'Brien RJ, Mammen AL, Bernhardt J and Huganir RL (1996) Characterization of multiple phosphorylation sites on the AMPA receptor GluR1 subunit. Neuron **16**:1179-1188.

Rouach N, Byrd K, Petralia RS, Elias GM, Adesnik H, Tomita S, Karimzadegan S, Kealey C, Bredt DS and Nicoll RA (2005) TARP gamma-8 controls hippocampal AMPA receptor number, distribution and synaptic plasticity. Nat. Neurosci. **8**:1525-1533.

Roy S, Liu HC, and Loh HH (1998) Mu-opioid receptor-knockout mice: the role of mu-opioid receptor in gastrointestinal transit. Brain Res. Mol. Brain Res. **56**:281-283.

Saglietti L, Dequidt C, Kamieniarz, Rousset MC, Valnegri P, Thoumine O, Beretta F, Fagni L, Choquet D, Sala C, Sheng M and Passafaro M (2007) Extracellular interactions between GluR2 and N-cadherin in spine regulation. Neuron **54**:461-477.

Sanderson DJ, Gray A, Simon A, Taylor AM, Deacon RM, Seeburg PH, Sprengel R, Good MA, Rawlins JN and Bannerman DM (2007) Deletion of gluamate receptor-A (GluR-A) AMPA receptor subunits impairs one-trial spatial memory. Behav. Neurosci. **121**:559-569.

Sánchez-Blázquez P, Rodríguez-Muñoz M and Garzón J (2010) Mu-opioid receptors transiently activate the Akt-nNOS pathway to produce sustained potentiation of PKC-mediated NMDAR-CaMKII signaling. PLoS One **5**:e11278.

Schmitt WB, Deacon RM, Seeburg PH, Rawlins JN and Bannerman DM (2003) A within-subjects, within-task demonstration of intact spatial reference memory and impaired spatial working memory in glutamate receptor-A-deficient mice. J. Neurosci. **23**:3953-3959.

Schiller D et al. (2010) Preventing the return of fear in humans using reconsolidation update mechanisms. Nature **463**:49-53.

Schuller AG, King MA, Zhang J, Bolan E, Pan YX, Morgan DJ, Chang A, Czick ME, Unterwald EM, Pasternak GW and Pintar JE (1999) Retention of heroin and morphine-6 beta-glucuronide analgesia in a new line of mice lacking exon 1 of MOR-1. Nat. Neurosci. **2**:151-6.

Seidenman KJ, Steinberg JP, Huganir RL and Malinow R (2003) Glutamate receptor subunit 2 serine 880 phosphorylation modulates synaptic transmission and mediates plasticity in CA1 pyramidal cells. J. Neurosci. **23**:9220-9228.

Sharma SK, Klee WA and Niremberg M (1977) Opiate dependent modulation of adenylate cyclase activity. Pro. Natl. Acad. Sci. USA **74**:3365-3369.

Sharma SK, Klee WA and Nirenberg M (1975) Dual regulation of adenylyl cyclase accounts for narcotic dependence and tolerance. Proc. Natl. Acad. Sci. USA **72**:3092-3096.

Shen L, Liang F, Walensky LD and Huganir RL (2000) Regulation of AMPA receptor GluR1 subunit surface expression by a 4.1N-linked actin cytoskeletal association. J. Neurosci. **20**:7932-7940.

Shepherd JD and Huganir RL (2007) The cell biology of synaptic plasticity: AMPA receptor trafficking. Annu. Rev. Cell Dev. Biol. **23**:613-643.

Shi S, Hayashi Y, Esteban JA and Malinow R (2001) Subunit-specific governing AMPA receptor trafficking to synapses in hippocampal pyramidal neurons. Cell **105**:331-343.

Shi SH, Hayashi Y, Petralia RS, Zaman SH, Wenthold RJ, Svoboda K and Malinow R (1999) Rapid spine delivery and redistribution of AMPA receptors after synaptic NMDA receptor activation. Science **284**:1811-1816.

Shy M, Chakrabarti S and Gintzler AR (2007) Plasticity of adenylyl cyclase-related signaling sequelae after long-term morphine treatment. Mol. Pharm. **73**:868-879.

Sommer B, Kohler M, Sprengel R and Seeburg PH (1991) RNA editing in brain controls a determinant of ion flow in glutamate-gated channels. Cell **67**:11-19.

Song I and Huganir RL (2002) Regulation of AMPA receptors during synaptic plasticity. Trends Neurosci. **25**:578-588.

Songyang Z, Fanning AS, Fu C, Xu J, Marfatia SM, Cgishti AH, Crompton A, Chan AC, Anderson JM and Cantley LC (1997) Recognition of unique carboxyl-terminal motifs by distinct PDZ domains. Science **275**:73-77.

Sora I, Takahashi M, Funada M, Ujike H, Revay RS, Donovan DM, Miner LL and Uhl GR (1997) Opiate receptor knockout mice define mu receptor roles in endogenous nociceptive responses and morphine-induced analgesia. Proc. Natl. Acad. Sci. USA **94**: 1544-1549.

Stephens DN and Mead AN (2003) What role do GluR1 subunits play in drug abuse? Trends Neurosci. **26**:181-182.

Srivastava S, Osten P, Vilim FS, Khatri L, Inman G, States B, Daly C, DeSouza S, Abagyan R, Valtschanoff JG, Weinberg RJ and Ziff EB (1998) Novel anchorage of GluR2/3 to the postsynaptic density by the AMPA receptor-binding protein ABP. Neuron **21**:581-91.

Swanson GT, Kamboj SK and Cull-Candy SG (1997) Single-channel properties of recombinant AMPA receptors depend on RNA editing, splice variation, and subunit composition. J. Neurosci. **17**:58-69.

Terashima A, Cotton L, Dev KK, Meyer G, Zaman S, Duprat F, Henley JM, Collingridge GL and Isaac JT (2004) Regulation of synaptic strength and AMPA receptor subunit composition by PICK1. J. Neurosi. **24**:5381-5390.

Thomas MJ, Beurrier C, Bonci A and Malenka RC (2001) Long-term depression in the nucleus accumbens: a neural correlate of behavioral sensitization to cocaine. Nat. Neurosci **4**:1217-1223.

Tronson NC, Wiseman SL, Olausson P and Taylor JR (2006) Bidirectional behavioral plasticity of memory reconsolidation depends on amygdalar protein kinase A. Nat. Neurosci. **9**:167-169.

Tu H, Rondard P, Xu C, Bertaso F, Cao F, Zhang X, Pin JP and Liu J (2007) Dominant role of GABAB2 abd Gbetagamma for GABAB receptor-mediated ERK1/2/CREB pathway in cerebellar neurons. Cell Signal. **19**:1996-2002.

Ueda H, Harada H, Nozaki M, Katada T, Ui M, Satoh M and Takagi H (1988) Reconstitution of rat brain mu opioid receptors with purified guanine nucleotide-binding regulatory proteins, Gi and Go. Proc. Natl. Acad. Sci. USA **85**:7013-7017.

Ueda H and Ueda M (2009) Mechanisms underlying morphine analgesic tolerance and dependence. Front. Biosci. **14**:5260-5272.

Valtschanoff JG, Burette A, Davare MA, Leonard AS, Hell JW and Weinberg RJ (2000) SAP97 concentrates at the postsynaptic density in cerebral cortex, Eur. J. Neurosci. **12**:3605-3614.

Vaughan CW and Christie MJ (1997) Presynaptic inhibitory action of opioids on synaptic transmission in the rat periaqueductal gray in vitro. J. Physiol. (Lond) **498**:463-472.

Vorel SR, Liu X, Hayes RJ, Spector JA, Gardner EL (2001) Relapse to cocaine seeking after hippocampal theta burst stimulation. Science **292**:1175-1178.

Walensky LD, Blackshaw S, Liao D, Watkins CC, Weier HU, Parra M, Huganir RL, Conboy JG, Mohandas N and Snyder SH (1999) A novel neuron-enriched homolog of the erythrocyte membrane cytoskeletal protein 4.1. J. Neurosci. **19**:6457-6467.

Wenthold RJ, Petralis RS, Blahos J II and Niedzielski AS (1996) Evidence for multiple AMPA receptor complexes in hippocampal CA1/CA2 neurons. J. Neurosci. **16**:1982-1989.

Wick MJ, Minnergh SR, Lin X, Elder R, Law PY and Loh HH (1994) cDNA encoding a putative membrane receptor with high homology to the cloned μ, δ and κ opioid receptors. Mol. Brain Res. **27**:37–44.

Williams JT, Christie MJ and Manzoni O (2001) Cellular and synaptic adaptations mediating opioid dependence. Physiol. Rev. **81**:299-343.

Whitlock JR, Heynen AJ, Shuler MG and Bear MF (2006) Learning induces long-term potentiation in the hippocampus. Science **313**:1093-1097.

Xia J, Zhang X, Staudinger J and Huganir RL (1999) Clustering of AMPA receptors by the synaptic PDZ domain-containing protein PICK1. Neuron **22**:179-187.

Xie W, Samoriski GM, McLaughlin JP, Romoser VA, Smrcka A, Hinkle PM, Bidlack JM, Gross RA, Jiang H and Wu D (1999) Genetic alteration of phospholipase C beta3 expression modulates behavioral and cellular responses to mu opioids. Proc. Natl. Acad. Sci. U S A. **96**:10385-10390.

Xing J, Ginty DD and Greenberg ME (1996) Coupling of the Ras-MAPK pathway to gene activation by RSK, a growth factor-regulated CREB kinase. Science **273**:959-963.

Yang SN, Yang JM, Wu JN, Kao YH, Hsieh WY, Chao CC and Tao PL (2000) Prenatal exposure to morphine alters kinetic properties of NMDA receptor-mediated synaptic currents in the hippocampus of rat offspring. Hippocampus **10**:654-662.

Zamanillo D, Sprengel R, Hvalby O, Jensen V, Burnashev N, Rozov A, Kaiser KM, Koster HJ, Borchardt T, Worley P et al. (1999) Importance of AMPA receptors for hippocampal synaptic plasticity but not for spatial learning. Science **284**:1805-1811.

Zastawny RL, George SR, Nguyen T, Cheng R, Tsatsos J, Briones-Urbina R and O'Dowd BF (1994) Cloning, characterization, and distribution of a mu-opioid receptor in rat brain. J. Neurochem. **62**:2099-2105.

Zhang G, Chen W and Marvizon JCG (2010) Src family kinases mediate the inhibition of substance P release in the rat spinal cord by μ-opioid receptors and $GABA_B$ receptors, but not α_2 adrenergic receptors. Eur. J. Neurosci. **32**:963-973.

Zhang L, Zhao H, Qiu Y, Loh HH and Law PY (2009) Src phosphorylation of micro-receptor is responsible for the receptor switching from an inhibitory to a stimulatory signal. J. Biol. Chem. **284**:1990-2000.

Zhu JJ, Esteban JA, Hayashi Y and Malinow R (2000) Postnatal synaptic potentiation: delivery of GluR4-containing AMPA receptors by spontaneous activity. Nat. Neurosci. **3**:1098-1106.

Zieglgansberger W, French ED, Siggins GR and Bloom FE (1979) Opioid peptides may excite hippocampal pyramidal neurons by inhibiting adjacent inhibitory interneurons. Science **205**:415-417.